PhD degree in Molecular Medicine

European School of Molecular Medicine (SEMM),

University of Milan

Faculty of Medicine

Settore disciplinare: BIO/10

FUNCTIONAL DISSECTION OF HISTONE LYSINE METHYLATION IN B CELL SPECIFICATION

Agnieszka Chronowska

The Department of Experimental Oncology,

European Institute of Oncology (IEO),

IFOM-IEO-Campus, Milan, Italy

Matricola n. R06824

Supervisor: Dr. Giuseppe Testa Ph.D M.D.

IFOM-IEO Campus, Milan, Italy

Added co-Supervisor: Dr. Pier Giuseppe Pelicci Ph.D M.D.

IFOM-IEO Campus, Milan, Italy

Anno accademico 2009-2010

Acknowledgments

Some people say the acknowledgments are be the most read pages of a thesis. I am glad about that as there are many people to whom I wish to thank for great help, knowledge and wisdom they have shared with me.

I wish to thank and express my deepest gratitude to Dr. Giuseppe Testa Ph.D M.D. for his outstanding scientific supervision and support during my Ph.D study. It has been a pleasure to work in such inspiring atmosphere. Also I would like to thank him for so patient proofreading the thesis, rainbow of colours of track changes and for all advices and invaluable help.

I would like to thank Dr. Stefano Casola Ph.D. M.D. I am truly grateful for his collaboration, excellent scientific advices, discussions and ideas, and shared reagents, as well as for being live version of the newest edition of "Fundamental Immunology".

I would like to thank my external co-supervisor Dr. Francis Stewart Ph.D. for discussion, suggestions and criticism about my work. Also I would like to thank him for reagents he shared with me.

I would like to thank my co-supervisor Dr. Pier Giuseppe Pelicci Ph.D. M.D for his scientific supervision.

I would like to kindly thank my egzaminators Anne Corcoran Ph.D and Maria Rescigno, Ph.D. for their time and excellent suggestions about my thesis and work. I would like to thank them particularly for an outstanding discussion that they shared with me during my Ph.D. exam.

Very special acknowledgements are for all the facilities of IFOM-IEO Campus for their priceless technical support.

I wish to thank to all members of my group, Thomas Burgold, Elena Schiffer Signaroldi, Serena Buontempo, Giulia Fragola, Elisabetta Incorvaia, Prem Tripathi and Fabio

Spreafico for wonderful work atmosphere you have created, and friendship and help you have offered. In particular I want to thank Thomas Burgold for all the entertainment he constantly provided during those 5 years and Signora Schiffer-Oldi for all the coffee breaks and breakfasts she took with me.

I wish to thank all my institute colleagues for your advices, support and so friendly and international atmosphere you have created. In particular I wish to thank Marieta Caganova for all her invaluable help with the experiments and Federica Mainoldi for all her time she spent explaining me the secrets of ELISA.

There are no words that could express my gratitude to all my friends – you made this entire time truly awesome, without you it would not be the same. In particular I want to express my deepest appreciation to Sigrun Murr that despite the differences and distance, has shown me what friendship is.

I must express my deepest gratitude to my parents and brothers for emotional support.

Chciałabym szczeże podziękować moim rodzicom i braciom za ich wsparcie. Dziękuję Wam za czas jaki mi poświęciliście i za to, że nadal jestem Waszą małą córeczką i siostrą. Dziękuję mojej Mamie za niesamowitą zdolność rozwiązywania wszystkich moich problemów na odległość i mojemu Tacie za zakrzywianie czasoprzestrzeni tak, że gdziekolwiek by nie był, mój dom jest zawsze *dans chemin*.

Nadal pamiętam mój pierwszy mikroskop, który dostałam od Was - to kim jestem dzisiaj, zawdzięczam Wam.

And finally and very specially I would like to thank Matteo D'Antonio – PdPD'A, for all the small things that make it different and for being always in the right place at the right time. Thanks to you the time I was writing my thesis was possibly most relaxing ever.

Abstract

Methylation on lysine 4 of histone H3 (H3K4) by the histone methyltransferases (HMTs) of the trithorax group is associated with the activation and maintenance of transcriptional programs, but virtually nothing is known about the function of these key epigenetic regulators in differentiating cell compartments of adult animals. Here I present the first characterization of the role of the H3K4 HMT Mll2 (Mixed lineage leukemia), also known as Mll4 or Wbp7 in adult tissues focusing on the ontogeny of B cells as the best characterized system for the dissection of lineage commitment and terminal specification. Expression analysis in sorted populations revealed that both Mll2 and its closest homolog Mll1 are expressed throughout B cell maturation, and the hypothesis I set out to test was whether they form a redundant regulatory circuit or whether their selective ablation would uncover functional requirements for specific B cell subsets.

To this end I used a conditional knock out mouse line in which the Mll2 gene is ablated according to the 'knock-out-first' approach, (Glaser et al., 2006; Testa et al., 2004; Testa et al., 2003), an innovative engineering strategy that allows to knock out the gene by transcription trapping, restore it using FLP-mediated recombination and knock it out again using Cre-mediated recombination. In order to knock out Mll2 specifically in mature B cells I selected the CD21-Cre3A mouse line that expresses Cre recombinase under the CD21 promoter (Kraus et al., 2004). In this line Cre-mediated deletion follows the expression of CD21, which takes place at the immature B to mature B cell transition (Kraus et al., 2004) (Takahashi et al., 1997). Flow cytometric analysis of B cell subsets in compound mutants performed on over 50 pairs of mice (homozygous versus heterozygous Mll2 flox mice carrying the CD21-Cre transgene) revealed that upon Mll2 deletion, size of marginal zone (MZ) ($CD19^{high}$ - $CD21^{high}$ - $CD38^{high}$ - $CD1d^{high}$ - $CD23^{low}$) B cell compartment on average was reduced by about 50% with respect to the control animals.

This was confirmed by histological analysis of the spleen of control and mutant mice. Other B mature cell compartments, including follicular, B1 and germinal center B cells from different lymphopoietic organs were not affected in mutant animals, indicating a specific requirement for Mll2 in the establishment and/or maintenance of the MZ B cell lineage. A gene expression profiling did not reveal aberrant expression of key regulators of the homeostasis of MZ B cell compartment, nor remarkable differences between transcriptomes of Mll2 deficient and proficient cells. However *in vitro* analysis of the dynamics demonstrated higher, by about 75%, rate of proliferation of mutant MZ B cell compartment. Similarly significant increase in the proliferating fraction was also observed in mutant follicular and immature/transitional B cells. This higher turnover of splenic B cell populations upon loss of Mll2 may reflect the presence of a stimulus promoting cell proliferation as part of a feed back loop triggered by the decrease in MZ B cells. Moreover functional analysis of MZ B cells revealed that upon loss of Mll2 cells are not capable to switch class of immunoglobulin in a response to NP-Ficoll immunization indicating a crucial role of Mll2 in the establishment of a new transcriptional program. These findings are in agreement with previously published results demonstrating requirement of Mll2 for the activation and timing of lineage-specific transcriptional programs in both sperm and oocyte germ layers (Andreu-Vieyra et al., 2010; Glaser et al., 2009). Together, present results could suggest that Mll2 plays a role also in B lymphophoiesis and therefore we consider a candidacy of Mll2 as a putative lymphopoietic regulating factor.

Table of Contents

Acknowledgements

Abstract

1. Introduction

Epigenetic information is is sequence independent information about the status of DNA rather than its content (Berger et al., 2009) and it is the modification of epigenetic information that changes the outcome of the information encoded in the DNA and leads to so enormous cell variability. If we accept this concept of epigenetics, we must admit that development is, by definition, epigenetic. Despite the vast amount of work conducted with a purpose of better understanding role of epigenetics, our knowledge about it is still fragmentary. Until now it was demonstrated that various epigenetic modifications are involved not only in the regulation of gene expression but also in the maintenance of genome stability (Peters et al., 2001), transposon suppression (Lippman et al., 2004; Slotkin and Martienssen, 2007), dosage compensation (Plath et al., 2003) and genomic imprinting (Li et al., 1993). Moreover different patterns of epigenetic modifications have been associated with a variety of disorders, including syndromes caused by chromosomal instability, mental retardation (Iwase et al., 2007), but also schizophrenia (Roth et al., 2009), obesity (Okamura et al., 2010) and finally – cancer (Cameron et al., 1999; Eden et al., 2003; Feinberg and Tycko, 2004). Particularly interesting is the line of research addressing epigenetic modifications in the context of differentiation (Arney and Fisher, 2004). Present work has as a goal a better understanding of the role of Mll2 histone methyltransferase (FitzGerald and Diaz, 1999), which catalyses one of the most intensively studied epigenetic modification – H3K4 methylation.

1.1 Chromatin is a subject of epigenetic information

Chromatin refers to the packaging of DNA together with histones, histone associated proteins and transcription factors in the nucleus of eukaryotic cells. Appearance of chromatin in evolution was parallel with the prokaryotic to eukaryotic transition and was a consequence of an increased genome complexity (Struhl, 1999). The increase of genome complexity was in turn associated with an increase in its size. Hence also the number of potential binding sites for transcription factors dramatically increased while their physical accessibility dropped. In addition, the relative position of other regulatory elements changed. A great amount of non-coding DNA could have become a source of a number of random binding sites for transcription factors. Here, it is important to remember about the C-value paradox - the genome size is not proportional to the complexity of an organism. For example we can compare the genomes of *Caenorhabditis elegans* and human. The genome of *C.elegans* is about 30 times smaller than human (around 10^8 bp versus 3×10^9 bp) and substantially less complex in terms of cell lineages, both however contain approximately the same number of genes – around 20,000 (Gregory, 2001). Together, evolution of a genome structure challenged its special organisation in the nucleus. In consequence it became a necessary selective advantage to partition and rearrange the genome, in order to direct transcription factors to their appropriate targets and to avoid aberrant transcription factors-DNA binding. Genome organization into chromatin allows compaction of the DNA $1 - 5\times10^4$ times and therefore is considered a huge step in the evolution as ensured both (Workman and Kingston, 1998). Chromatin is present in a nucleus in three forms depending on the transcriptional state of regions forming it. Transcriptionaly inactive constitutive chromatin is highly condensed and often contains repetitive DNA and is considered as being gene poor (Dillon and Festenstein, 2002). Constitutive heterochromatin was shown to be localized at the periphery of a nucleus

and as being enriched for late firing origins of replication (Ferreira et al., 1997; Sadoni et al., 1999). The best examples of a constitutive heterochromatin are regions comprised of satellite sequences surrounding centromeres (Pardue and Gall, 1970). Facultative heterochromatin is also transcriptionally inactive but its precise nature is not yet fully defined. It is known however, that beside silenced cell type-specific transcription factors. It contains active genes like Xist (Lee et al., 1996; Lyon, 1961; Penny et al., 1996). Facultative chromatin can be localized in proximity of constitutive heterochromatin forming silent domains, therefore may be difficult to distinguish. Inactivation of one of the X chromosomes in females and Barr body formation (Barr and Bertram, 1949) is the best known example of the facultative chromatinization. Euchromatin on the other hand, contains transcriptionally active genes or genes prone for transcription. Euchromatin is assembled loosely with nucleosomes. This open conformation renders it in principle accessible for transcriptional complexes (Weintraub and Groudine, 1976). Euchromatin is associated with transcriptional factors, chromatin remodelling factors (Havas et al., 2001) and histone associated remodelling complexes as in example of β-globin locus (Cook, 2003; Gribnau et al., 2000). The main unit of chromatin is a nucleosome. A single nucleosome is composed of a 205 bp long DNA fragment, out of which 147 bp fragment is wrapped around a histone core (Kornberg, 1974). The core of the nucleosome consists of a histone octamer made out of two copies each of the histones from classes H2A, H2B, H3 and H4. (Kornberg, 1974; Kornberg and Thomas, 1974). Linker histone H1 stabilizes linking fragment of DNA between two octamers and nucleosomes aggregated together (Kornberg and Lorch, 1999) - reviewed).

Histones are one of the most highly conserved proteins in eukaryotic cells, to the extent that H3 of plants and mammals differ by 2 out of 102 amino acids and within the animal kingdom by 1. They are rich in positively charged alkaline amino acids, which results in their high affinity for negatively charged DNA. Histones were discovered by Albrecht Kossel in 1884

(Kornberg and Lorch, 1999) but the pioneering hints about their structure only come from 1984 (Bentley et al., 1984). Further details about histones and histone octamer were revealed in 1997, thanks to the progress in the X-ray diffraction technique. All histones were found to be small globular proteins (102 – 135 amino acids (Jenuwein and Allis, 2001) with N-terminal extensions known as histone "tails" (Bentley et al., 1984; Luger et al., 1997). Histone tails undergo diverse post-translational modifications including acetylation, methylation, phosphorylation, ubiquitination, glycosylation, ADP- ribosylation and sumoylation (Shiio and Eisenman, 2003; Strahl and Allis, 2000; Wolffe and Hayes, 1999) that have been shown to be essential in chromatin organisation, and further in the regulation of gene expression.

Acetylation of histones is a modification that neutralizes the positive charge of the target lysine of a histone tail decreasing histone affinity to DNA. Hence it leads to a more open chromatin architecture and in consequence to an increased access of transcription factors to DNA (Shahbazian and Grunstein, 2007). Placement of the acetylation mark is catalyzed by histone acetyltransferases (HATs) and is associated with the transcriptional activation of a given locus. Acetylation is a plastic modification - the mark can be removed by histone deacetylases (HDACs), which is correlated with transcriptional repression, and indeed transcriptionaly active and non-active loci can be distinguished by their acetylation level. Histone phosphorylation has also emerged as an important modification having structural consequences comparable with acetylation. Phosphorylated Serine 10 (S10) was found on all histones, including H1 (Bhaumik et al., 2007; Hendzel et al., 1997; Sweet et al., 1996; Wei et al., 1998). Phosphorylation of H3S10 has been associated both with transcriptional activation and in chromosome condensation during mitosis. Ubiquitination has been reported to occur on histones H2A, H2B and H3 and was associated with transcriptional activity (Zhang, 2003). Enrichment in ubiquitinated H2A is an epigenetic mark of transcriptional activation and was found to be particularly high at the C-terminus of active genes, however monoubiquitination

of H2AK119 correlates with transcription silencing (Cao et al., 2005). Since the C-terminus of histone H2A contacts nucleosomal DNA, ubiquitination is considered to prevent higher order of chromatin structures (Usachenko et al., 1994). Another two histone modifications that still require to be better understood are ADP-ribosylation and sumoylation. ADP-ribosylation deserves a particular interest as it has been demonstrated to play a particularly important role in DNA repair. The ADP-ribosytation mark was colocalized with histone acetylation, therefore it is believed that it may also lead to localized unfolding of the chromatin fiber (Golderer and Grobner, 1991). ADP-ribosytation has been also associated with DNA replication and transcription (Wolffe and Hayes, 1999). In contrast to previously described histone modifications that were shown to be associated with transcriptional activity, sumoylation was linked to histone repression. It was shown to mediate the recruitment of histone deacetylases and heterochromatin protein 1 (HP1) and in consequence transcriptional repression (Shiio and Eisenman, 2003). Very little is known about histone glycosylation. Clear evidences that core histones H2A, H2B, H3 and linker histone H1 contain mannose and fucose residues was reported in 1983 (Levy-Wilson, 1983). Later the glycosylation of H1 was confirmed linking glycosylation mark with the cell cycle (Kim, 1994). Based on the fact that presence of glucose residues in histone core increases its negative charge (Jobst et al., 1991) it is possible that histone glycosylation leads to more open chromatin conformation.

Among all known histone modifications the greatest interest is focused on acetylation and on histone methylation. Methylation mark can be placed on lysine, arginine or both residues of H3 and H4 (Kouzarides, 2007). Arginine can be mono- and dimethlated. Monomethylated arginine can be deaminated by converting arginine into citruline (Wang et al., 2004). Arginine methylation has been linked to transcriptional activation (Bauer et al., 2002). Histone methylation of lysine residues can occur on lysine 4 (K4), K9, K27, K36 and K79 of H3 and on K20 of H4. Those modification are linked with both transcriptional activation and

repression (Klose and Zhang, 2007; Zhang and Reinberg, 2001). Methylation of H3K4, H3K36 and H3K79 (Bannister et al., 2005; Feng et al., 2002; Nakayama et al., 2001; Santos-Rosa et al., 2002) is associated with active gene expression, whereas methylated H3K9, H3K27 and H4K20 were found on silenced loci (Muller et al., 2002; Nakayama et al., 2001; Plath et al., 2003; Schotta et al., 2008). Histone methylation was considered to be a stable histone modification until 2004 when the first histone lysine demethylase Lysine Specific Demethylase 1 -LSD1 (KDM1) was identified (Shi et al., 2004). Currently 17 histone lysine demethylases are known (Lan et al., 2008). In addition each of the lysine residues can be mono-, di- or trimethylated and depending on the number of methyl groups added the outcome is different. Final transcriptional state of a gene is dictated by the sum of different marks contemporary placed at its locus (Jenuwein and Allis, 2001; Strahl and Allis, 2000). Since identification of bivalent domains in 2006 it become obvious that the histone code is much more complex than previously was thought (Bernstein et al., 2006; Mikkelsen et al., 2007). The simultaneous presence of "active" trimetylated H3K4 (H3K4me3) and "repressive" trimetylated histone 3 (H3) at lysine9 (H3K9me3) and lysine20 (H3K20me3) marks at the gene promoters was found to maintain genes poised for activation. Until the repressive mark is removed the gene remains silent. During development and differentiation of embryonic stem cells (ESC) to a cell of a given lineage bivalent domains become resolved in a lineage specific manner. Transcriptional factors of the given lineage loose the repressive mark at their promoters and become activated, in contrast genes that are not involved in the differentiation of a pluripotent cell into that lineage remain repressed (Burgold et al., 2008; Cui et al., 2009).

It became obvious that epigenetics and in particular histone modifications play crucial role throughout development. The same regions of DNA at different cell states or in different cell types form different chromatin structures (Cairns, 2005). If one compares within the same organism the chromatin of an ES with that of a differentiated cell, the difference becomes

evident. If take on account chromatin from an epigenetic point of view its three conformation states are very distinct. Each chromatin conformation is characterised by different histone modification. The most important epigenetic characteristics of chromatin types are briefly described below. Constitutive chromatin is characterized by high DNA methylation profile and enrichment for H3K9me3 and H3K20me3. Additionally histidine4 (H4) of H3 lacks acetylation (Kourmouli et al., 2004; Lachner et al., 2003; Schotta et al., 2004). Facultative chromatin carries similar epigenetic mark, and in addition lysine27 (K27) of H3 is trimetylated (H3K27me3). Very distinct from them is euchromatin. The hallmark of transcriptionally active and transcription poised regions of euchromatin are tri- and dimetylated H3K4 (H3K4me3 and H3K4me2) (Kouzarides, 2007; Sims and Reinberg, 2006). Methylation of active regions is also present at lysine79 of (H3K79) (Im et al., 2003), arginine2 (R2), R17, R26 of H3 and R4 of H4 (Bauer et al., 2002; Lachner et al., 2003). Simultaneously euchromatic active genes are rich in phosphorylated H3 (Nowak and Corces, 2000) and acetylated residues of H3 and and H4 (Bauer et al., 2002).

1.2 Commitment, differentiation and epigenetics

The strictly controlled gene expression regulating the balance between pluripotency and lineage commitment is the key to understand cell specification of a multicellular organism. And the same is a key to understand processes that permits cells to escape this control, namely the long list of disorders, including cancer. The knowledge that covers that is as fascinating as still incomplete. It is clear however that the balance between stability and plasticity of transcriptional programs is a main challenge for a developing multicellular organism (Reik, 2007). This challenge seems to be the most obvious in mammalian ESCs with their potential to differentiate into every cell type of an adult organism. This potential decreases during

differentiation, and is eventually lost in a fully differentiated cell of a given line. This progressive restriction of developmental potency can be not only forced but also inverted upon an appropriate in vitro stimulation. Differentiation and dedifferentiation imply the switch between different transcriptional programs – silencing one and establishment and maintenance of another. Regulation of this reprograming takes place at two different levels. First consists of an on – off expression regulation of cell line specific genes by transcription factors. During the last few years, several genes were identified as key regulatory factors controlling pluripotency – differentiation equilibrium. It was demonstrated that Nanog, Oct3/4, Sox2, c-Myc, Klf4, Notch1 play a role of switches between those two states (Cartwright et al., 2005; Hochedlinger and Jaenisch, 2006; Li et al., 2005; Loh et al., 2006; Mitsui et al., 2003; Nichols et al., 1998; Niwa et al., 2000; Schroeder et al., 2006) and (Hochedlinger and Jaenisch, 2006; Takahashi and Yamanaka, 2006). The other level of the regulation is epigenetic (Bernstein et al., 2007) and consist of DNA methylation, chromatin remodelling and posttranslational histone modifications. The tight interplay of all levels of regulation drives cell specification (Jaenisch and Bird, 2003).

Every cell contains the macromolecule of deoxyribonucleic acid encoding exactly the same information. The outcome however of this encoded sequence is enormously different if compare different cell types of the same organism. Epigenetic information is sequence independent information about the status of DNA rather than its content. And it is the modification of epigenetic information that changes the outcome of the information encoded in the DNA and leads to such enormous cell type variability. What is more, the cell type variability is not the only result of the changes in the epigenetic information. Huge difference can be tracked within the same cell during its differentiation from an ES into a fully committed cell. If exclude mutations, DNA sequence remains the same during the passage from the cell “starting point” (an ESC state), to the baseline (a differentiated cell of a given

lineage). Hence the differences in the DNA status at two states of a cell development are exclusively epigenetic. As mentioned previously epigenetic regulation of a level of cell pluripotency takes place through chromatin remodelling, DNA methylation at the CpG islands of gene promoters, and covalent posttranslational modifications of histone core. The mammalian nucleus organisation is not random. Chromosomes occupy discrete positions (Cremer et al., 1982; Parada and Misteli, 2002) and the genome is arranged in a tissue specific manner (Parada et al., 2004). Special organization of nucleus was demonstrated as being tissue and cell type specific and changing during development (Bolzer et al., 2005; Kim et al., 2004; Misteli, 2004; Parada et al., 2004). Moreover, chromatin remodeling complexes were shown as essential for the maintenance of pluripotency (Gao et al., 2008; Ho et al., 2009a; Ho et al., 2009b). Number of evidences allow for a conclusion that nuclear positioning must influence gene expression (Marshall, 2003; Meshorer and Misteli, 2006).

Methylation of the DNA at CpG islands is known as an efficient epigenetic regulation pathway as affects the transcription of genes in two ways. First, the methylation of DNA physically impede the binding of transcriptional proteins to the gene. Second, to methylated DNA are recruited methyl-CpG-binding domain proteins (MBDs) that then recruit additional proteins to the locus, such as histone deacetylases and other chromatin remodelling proteins that modifying histones lead to heterochromatinization (Bird, 1986); (Cross et al., 1997; Hendrich and Bird, 1998; Millar et al., 2002; Nan et al., 1997; Nan et al., 1993). Moreover DNA methyltransferases were demonstrated as essential for a correct mouse development. Knock out of Dnmt1 or Dnmt3b leads to embryonic lethality (Goll and Bestor, 2005). Genome wide studies revealed very low level of CpG methylation in stem cells (Fouse et al., 2008; Meissner et al., 2008) and its progressive accumulation during cell specification at the promoters and regions surrounding them (Farthing et al., 2008; Illingworth et al., 2008). What is more, different targets of differentiation associated *de novo* methylation were identified at

promoters of stem cells or germline specific genes (Mohn et al., 2008). DNA methylation may be considered as a repressor of pluripotency and in conclusion a hallmark of differentiated cells. In support of this theory are experiments demonstrating enhancement of induced pluripotent (iPS) cells reprogramming upon DNA methyltransferase inhibitor treatment (Mikkelsen et al., 2008). A striking example of global epigenetic changes is coming from the example of preimplantational embryogenesis in mouse. The first differences are already visible in a newly fertilized zygote. Later, during the formation of a blastocyst, inner cell mass DNA is enriched in methylated regions in comparison with DNA of trophoectoderm cells. It is important however to highlight that changes in the level of the DNA methylation are accompanied by simultaneous changes in histone modifications (Reik et al., 2003; Santos et al., 2002). Covalent posttranslational modification of histones is a main epigenetic mode of the pluripotency regulation (Bhaumik et al., 2007). The most extensively studied histone modifications are mentioned previously histone acetylation and methylation.

Histone acetylation as well as histone acetylases and deacetylases were linked with the control of ES cell identity and differentiation (Keohane et al., 1996; Lee et al., 2004). Histone deacetylation occurs after initiation of ESC differentiation and it was shown that its pharmacological block inhibits embroid body formation and the same differentiation (Lee et al., 2004).

As it was demonstrated in an outstanding work, pluripotent and differentiated cells are very distinct if their histone lysine methylation profile is taken into account (Mikkelsen et al., 2007). Loci simultaneously methylated at H3K4 and H3K27 are often found in ESC or precursor cells on loci of different transcription factors like HOX genes that are essential for development and differentiation (Bernstein et al., 2006). Consequently, Burgold demonstrated the necessitate of removal of H3K27 by Jmjd3, and resolving the same bivalent domain of Nestin locus, in order to ensure differentiation into neural lineage (Burgold et al., 2008). While

DNA methylation is still considered to be a stable mark, methylation of histones is very plastic. An example coming from work described by Su and colleagues demonstrates not only the importance of histone modifications during differentiation but also high dynamics of this process. Dntt gene becomes silenced during the T lymphopoiesis in thymus (Guidos, 1996). 2 – 6 hours after the initiation of T cell maturation the promoter of Dntt is deacetylated at H3K9. After 4 – 12 hours H3K4 methylation mark is removed with a simultaneous placement methylation mark at H3K9. This modification spread from the promoter with an estimated speed 2kb/hour ensuring permanent, heritable silencing of the gene. Interestingly CpG methylation at this locus can be detected much later in the mature T cells in spleen (Su et al., 2004).

1.3 H3K4 methylation regulates development including lymphopoiesis

The transcriptionally active euchromatic state is established by the presence of a combination of covalent histone modifications among which methylation of H3K4 seems to play a central role. Not only the presence of the methylation mark at the H3K4 residue is important. The final output is determined by the degree of methylation. Monomethylated H3K4 (H3K4me1) was found on the silenced euchromatic loci (van Dijk et al., 2005) while di- and trimethylation of H3K4 (H3K4me2 and H3K4me3) are associated with transcriptionally active loci. Genes poised for transcription are characterized by enrichment of H3K4me2 that is considered to prevent large-scale silencing (Ng et al., 2003; Nishioka et al., 2002). Genes that are actively transcribed carry trimetylated mark H3K4me3 (Santos-Rosa et al., 2002). Additionally it was observed that H3K4me2 seems to be distributed along the active gene while H3K4me3 is localized specifically on the 5' end of transcribed genes (Araki et al., 2009; Pokholok et al., 2005). H3K4me3 present in bivalent domains holds genes poised for transcription and

prevents their constitutive repression - after removal of the repressive metylation mark from H3K9 or H3K27 the gene is transcribed (Cui et al., 2009).

H3K4 methylation was demonstrated to regulate development and differentiation (Bernstein et al., 2006; Bhaumik et al., 2007; Su et al., 2004). On the example of hematopoiesis in a genome-wide scale analysis of pluripotent, multipotent, and unipotent cell types, H3K4me2 and H3K4me3 marks were associated with genes expressed at different stage of erythroid development proving the same lineage-specific pattern of H3K4 methylation (Orford et al., 2008). H3K4 methylation has also been shown to play a key role in B lymphopoiesis. Clusters of di- and trimethylated H3K4 were colocalized at Pax5 target genes (Hagman and Lukin, 2007; Schebesta et al., 2007). Pax5 is the key transcription factor of B lymphopoiesis and its mutation leads to a developmental arrest at the early Pro B cell stage in the bone marrow (Nutt et al., 1997). Pax5-dependent enrichment of active H3K4me2 and H3K4me3 was found at the promoters and immediate downstream sequences of the nine Pax5 target genes. It was noted that enrichment of the three active marks is an effective predictor of the locations of promoters as H3K4 me3 was exclusively detected at 5′ ends of genes coinciding with promoter elements (Araki et al., 2009; Schebesta et al., 2007). During assembly of D and J segments of Ig heavy chain, peaks of H3K4me2 are observed at the locus prior to rearrangement (Morshead et al., 2003). As H3K4me2 is known to prevent large-scale silencing therefore it is plausible that this pattern of methylation ensures accessibility of the locus for BRG1 - mediated V(D)J reorganization in Pro B cells. Similarly, Perkins found a very strong correlation between presence and the degree of H3K4 methylation and the activation of several loci required for the Pre B to immature B cell transition. He observed that during V(D)J recombination at the Igκ locus levels of H3K4me3 and H3K4me2 become enriched up to 12 times and H3K4me2 up to 6 times, respectively. Peaks of H3K4 methylation were specifically localized at the 5' end (Perkins et al., 2004). This observation was confirmed also by others, suggesting the same

that epigenetic patterns, detected as early as at the Pro B cell stage, prime the chromatin for allelic exclusion (Corcoran, 2005; Goldmit et al., 2005). Allelic exclusion is a process in which one copy of Ig heavy and light chains become repressed ensuring expression of only one type of an Ig molecule by a B cell. Decrease of the H3K4me3 as well as a mutation that impairs recognition of H3K4me3 mark by RAG2, a V(D)J recombinase, severely impairs V(D)J recombination in vivo (Matthews et al., 2007). It is worth noticing that patients with inherited immunodeficiency syndrome carry similar mutation of RAG2 at W453 - a structural component of the binding surface that is essential for recognition of H3K4me3 by RAG2. The importance of H3K4 methylation in lymphopoiesis and in development in general was demonstrated in an outstanding work in which modulating the expression of Oct4, Sox2, Klf4, and c-Myc, mature mouse B lymphocytes were dedifferentiated to a fully pluripotent state. Hanna and colleagues proven enrichment of H3K4me3 at several bivalent loci in ES cells that was parallel to the acquisition of pluripotency (Hanna et al., 2008). There are no doubts about the importance of H3K4 methytlation in B cell development. It is important however to point out that similar observation were also proven for T lymphopoiesis as well as the role of other epigenetic marks in lymphopoiesis (Corcoran, 2005, 2010; Morshead et al., 2003; Perkins et al., 2004).

1.4 H3K4 methylation mark is posed by Mll2

The H3K4 methylation mark is conserved in evolution to a remarkable degree. It is found in yeast (Miller et al., 2001), plants (Tariq and Paszkowski, 2004) and higher eukaryotes, including mammals (Bernstein et al., 2005). Similarly striking is the evolutionary age of the SET – domain superfamily of proteins, to which among others, H3K4 methyltransferases (HMTs) belong. SET – domain proteins were first identified in *Drosophila melanogaster*

(Tschiersch et al., 1994) and further in other species (Kouzarides, 2002; Miller et al., 2001; Rea et al., 2000). Members of SET superfamily belong to two groups Polycomb (PcG) and Trithorax (TrxG). While TrxG group of proteins activate, PcG proteins are involved in the transcriptional silencing of lineage specific genes. Their reciprocal counteraction enables development by stabilizing cell identity through setting and maintaining transcriptional programs during differentiation (Pirrotta, 1998). The majority of H3K4 HMTs belongs to the SET domain superfamily of proteins, and were identified in two groups, related to the SET domain of yeast Set1 and *Drosophila* Trx (MLL family - Mixed Lineage Leukemia) (Dillon et al., 2005; Martin and Zhang, 2005). Their common feature is presence of 130 amino acids long evolutionary conserved motif, SET domain, that was demonstrated to catalyse methylation of histone tails (Milne et al., 2002). Yeast Set1 was the first identified H3K4 methyltransferase (Briggs et al., 2001). Both yeasts H3K4 HMTs Set1 and Set2 catalyze mono-, di- and trimethylation (Miller et al., 2001). In mammals there are 6[1] enzymes catalysing methylation of H3K4, yeast homologs Set1A and Set1B and 5 members of Trx (Mll) family Mll1 through 5 (Emerling et al., 2002; Shilatifard, 2006). None of mammalian enzymes is capable to place all three methyl groups on H3K4 residue nor their role in the embryonic development is redundant. It was demonstrated that knock out of Mll1, Mll2 or Mll3 leads to embryonic lethality (Glaser et al., 2006; Lee et al., 2006; Yu et al., 1995). It has been found however that they share common components within multiprotein complexes, such as WDR5, RbBP5, and ASH2 regulating their activity (Dou et al., 2006; Lee et al., 2006). Despite their similarity, proteins from MLL family are not, at least completely, redundant in their function. Mll1 and Mll2 have been demonstrated to be essential for the long-term maintenance of Hox gene expression patterns during development, however both have their own specific target genes. In addition, apart from the number of fusion proteins with which

[1] MLL5 was demonstrated to lack HMT activity (Madan et al., 2009; Sebastian et al., 2009)

mutated MLL1 has been colocalized in various types of leukaemia, MLL1 fused to Hox genes causes abnormal hematopoiesis (Yokoyama et al., 2004). The crucial role of MLL1 in hematopoiesis has been also demonstrated in mice in which Mll1 deletion resulted in a total HSC failure (McMahon et al., 2007).

Mll2 called also Trx2, Mll4 or Wbp7 is the closest homolog of Mll1 that arose from it through gene duplication (FitzGerald and Diaz, 1999). It is ubiquitously expressed in human (FitzGerald and Diaz, 1999) and as I demonstrated in a scrupulous analysis, mouse tissues (Fig. 1).

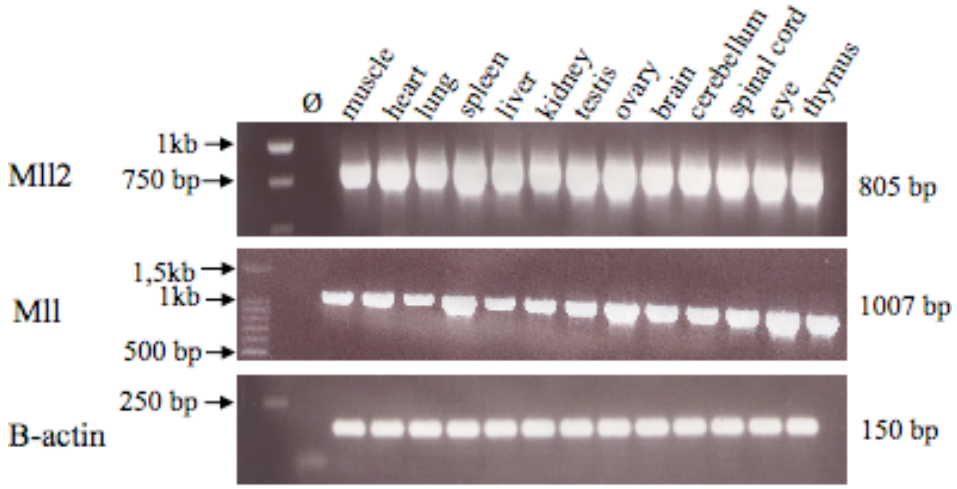

Figure 1. RT PCR expression analysis of Mll2 and Mll1 in different wild type mouse tissues.

RT-PCR and qPCR analysis demonstrated that Mll2 is also expressed throughout B cell development and in all mature B cell types (Pre/Pro B, IgM+, MZ, Fo, B1a and B1b cells, GC and Non-GC cells) and T lymphocyte subpopulations: thymic double positive CD4+CD8+ T cells (DP), T CD4+ - (Th) and T CD8+ (Tc) from thymus (T) and spleen (SP)) (Fig. 2). Moreover, subsequent quantification of both Mll1 and Mll2, closest homologs, shown their similar expression in all analyzed cell types (Fig. 2). Constant expression of both Mll2 and Mll1 during the B cell maturation and in all mature B and T cell subpopulations, as well as in all analyzed mouse tissues, points to the continuous requirement of both genes throughout the life of the animal (Fig. 1 and 2). High level of Mll1 expression may implicate its role in the germinal center B cells biology (Fig. 2B).

RT-PCR and qPCR Mll2 and Ml1 expression analysis was performed on the cDNA synthesized from total RNA obtained from pooled cells from 3 C57BL/6 animals.

A.

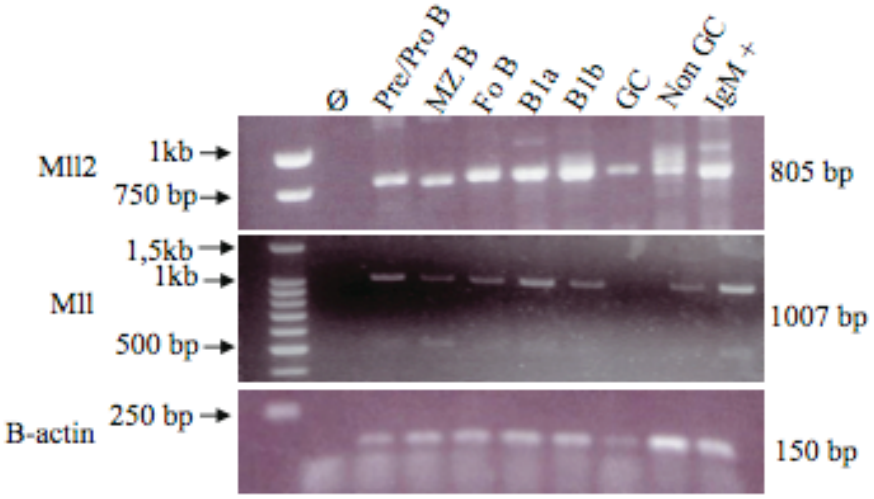

B.

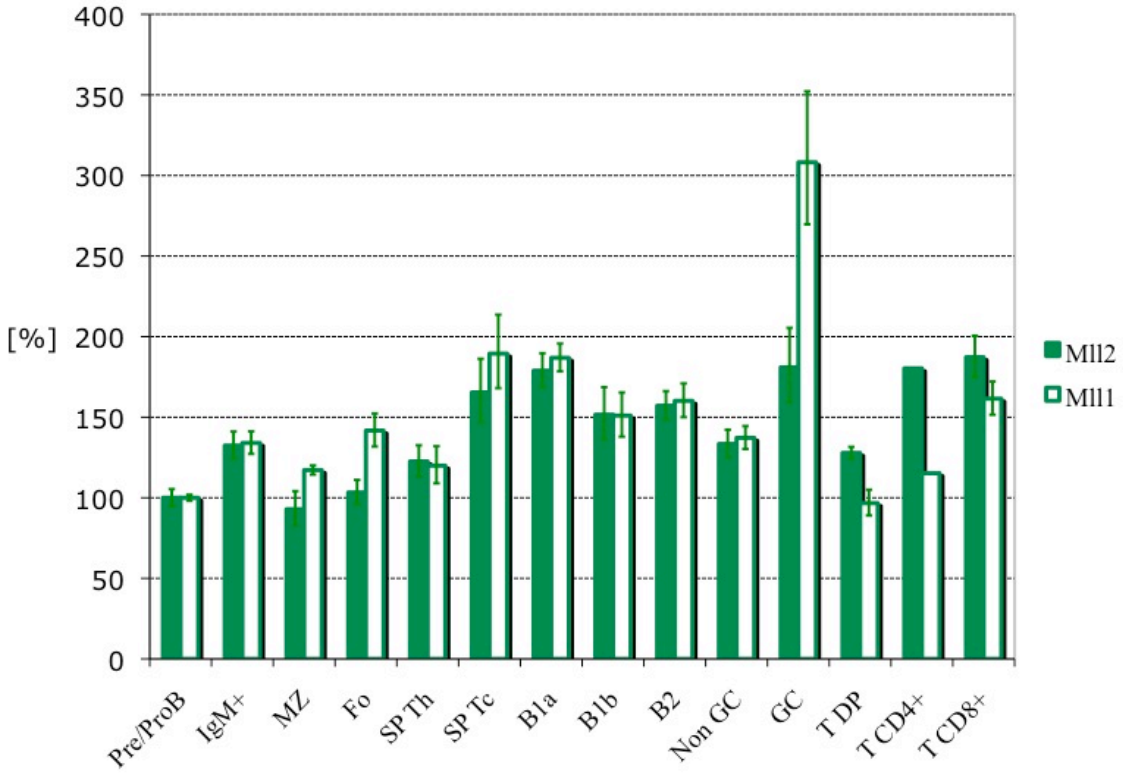

Figure 2. Expression analysis of Mll2 and Mll in different wild type subpopulations of B and T lymphocytes. A. RT-PCR analysis of the expression of Mll2 and Mll1 in different B cell subpopulations; Mll2 - 805bp, Mll1 – 1007 bp, β – actin – 150 bp., **B.** RT PCR analysis of the expression of Mll2 and Mll1 in mouse tissues; **Ø** – negative control, **Pre/Pro B** – Pre/Pro B cell, **IgM+** - IgM positive B cell from bone marrow, **MZ** – marginal zone B cell, **Fo** – follicular B cell, **SP CD4+** – spleenic T CD4+ cells, **SP CD4+** – spleenic T CD8+ cells **B1a** – B1a B cell, **B1b** – B1b B cell, **Non GC** – non germinal center B cell, **GC** – germinal center B cell, **T DP** – thymic CD4+CD8+ T cells, **T CD4+** – thymic CD4+ T cells, **T CD4+** – thymic CD8+ T cells.

Despite high similarity to Mll1 (95% of similarity between the SET domain of both genes) MLL2, in contrast to MLL1, has never been associated with leukemia, confirming further that there are likely differences in the function between both genes. Similarly, while Mll1 has been associated with the maintenance of the expression (in mouse and human) of HoxA7, Hoxa9, Hoxc6, Hoxc8, Hoxc9, Hoxc10 and Hoxd4 (Milne et al., 2005; Terranova et al., 2006; Yokoyama et al., 2004), Mll2 was associated with Hocb2 and Hoxb5 but not with Hoxa2, Hoca3, Hoxa4 (Glaser et al., 2006). Recently MLL2 and MLL1 were demonstrated to differ minimally at the CXXC and post-CXXC domains and in the consequence are guided to nonoverlapping target genes repertoire. That in consequence excludes role of MLL2 in the leukemogenesis (Bach et al., 2009) and further supports the hypothesis of the lack of complete redundancy between different members of the Mll family .

Yet, despite these evident differences Mll2 shows high structural similarity to Mll1 in terms of domain organization, proving that they are parologues (FitzGerald and Diaz, 1999) (Fig. 3). They both share the central Plant Homeo Domain (PHD) though which protein – DNA and protein – protein interactions are possible. C-terminal SET domain ensures catalytic activity as a histone methyltransferase, and a methyltransferase (MT) domain that allows discrimination of DNA with unmethylated CpG sequences (Birke et al., 2002). Similarly to Mll1 and its ortholog Trx, Mll2 is encoded by a very large gene and is located on chromosome 7 (in mouse) and 19 (in human).

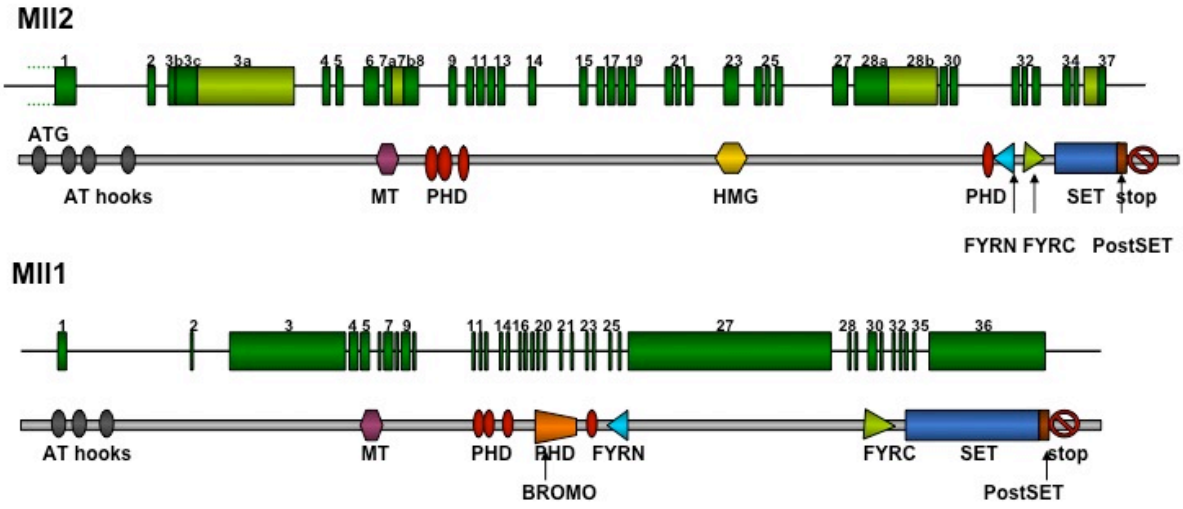

Figure 3. Schematic representation of gene structure and protein of Mll2 and Mll1 (Glaser et al. 2006 - modified); **AT hook** – DNA binding motif, **MT** – 100aa domain shared with DNA methyltransferase1, **PHD** - Plant Homeo Domain, **HMG** - High Mobility Group box involved in DNA binding, **FYRN** and **FYRC** – domains of unknown function occuring frequently in chromatin-associated proteins, **BROMO** – domain involved in recognition of acetylated lysine residues, **SET** - methyl group transferase; Schemes are out of scale.

Mll2 knock out leads to embryonic lethality around the day 8.5 - 9.5 (Glaser et al., 2006), which however can be overcome by a conditional deletion. Indeed Mll2 seems to be dispensable after day 11,5 of embryogenesis (Glaser et al., 2009). Mll2 was observed to be required only at a certain timepoints, during gastrulation, spermatogenesis, and postnatal oogenesis (Andreu-Vieyra et al., 2010; Glaser et al., 2009). Mll2 deficient ESC are viable and maintain their pluripotency (Glaser et al., 2006) however their proliferative potential is strongly decreased and the differentiation into cells of all three layers is delayed. This growth impairment is caused by increased rate of apoptosis enhanced by lack of H3K4me3 mark on Bcl2 (Lubitz et al., 2007). Upon conditional loss of Mll2 in an adult organism both spermatogenesis and oogenesis fail leading to sterility of both males and females (Andreu-

Vieyra et al., 2010; Glaser et al., 2009). Previously Mll2 was considered to be involved only in early embryogenesis and in gametogenesis, and its role in the homeostasis of other cellular compartments in the adult animal has been questioned (Glaser et al., 2004, 2009). Yet currently we can conclude that Mll2 is involved in the tightly timed establishment of lineage specific transcriptional programs (Andreu-Vieyra et al., 2010). Moreover, this opinion is strongly supported by example coming from *in vitro* studies. In 2007 Mll2 was found to be localized to the β-globin locus in erythroid lineage during terminal erythroid differentiation. In a NF-E2 (erythroid transcription factor) dependent manner Mll2-containing methyltransferase complex is recruited to the β-globin gene. Additionally, presence of Mll2 along the locus was reported also later during erythroid differentiation (Demers et al., 2007). Interestingly, the fact that Mll2 is not only recruited to, but also continuously present at the β-globin locus during erythropoiesis, suggests a role of Mll2 also in lineage maintenance.

1.5 Conditional knocking out of Mll2 in mature B lymphocytes

In the light of the findings discussed above, we decided to focus our attention on Mll2. Its role has been studied extensively, however all the work is focused at the early stages of development and virtually nothing is known about its function in differentiated cell compartments of adult animals. Due to the embryonic lethality of Mll2 (Glaser et al., 2006) it is only possible to study the effect of Mll2 loss in adult tissues through conditional mutagenesis approaches. Applying "knock-out first" strategy (Testa et al., 2004; Testa et al., 2003) a Mll2 conditional knock out mouse line was generated (Glaser et al., 2006).

The Mll2 locus was targeted with a cassette consisting of a splice acceptor sequence from the second exon of the engrailed 2 gene, Encephalomyocarditis virus (EMCV), internal ribosome entry site (IRES), a LacZ-neo fusion and SV40 early polyadenylation signal. FRT sites flank

the cassette, while loxP sites flank exon 2 of Mll2. The design of the alleles of Mll2 knock out (Glaser et al., 2006) is presented in the Figure 4. Such design of this multipurpose allele allows to knock out the gene (Mll2 KO allele – straight knock out allele), restore it using Flp-mediated recombination (Mll2F allele – Mll2 KO allele after Flp-mediated recombination of Mll2 KO allele) and knock it out again using Cre-mediated recombination (Mll2FC allele – Mll2F allele after Cre-mediated recombination) (Fig. 4). This strategy enables Mll2 ablation not only ubiquitously but also in time-and-space specific manner using inducible or tissue specific Cre recombinases. In the present work the gene trap cassette of Mll2 KO straight knock out allele was removed by crossing mice heterozygous for Mll2 KO allele with PGK-Cre line (Lallemand et al., 1998) obtaining mice heterozygous for Mll2F conditional knock out allele (Glaser et al., 2006).

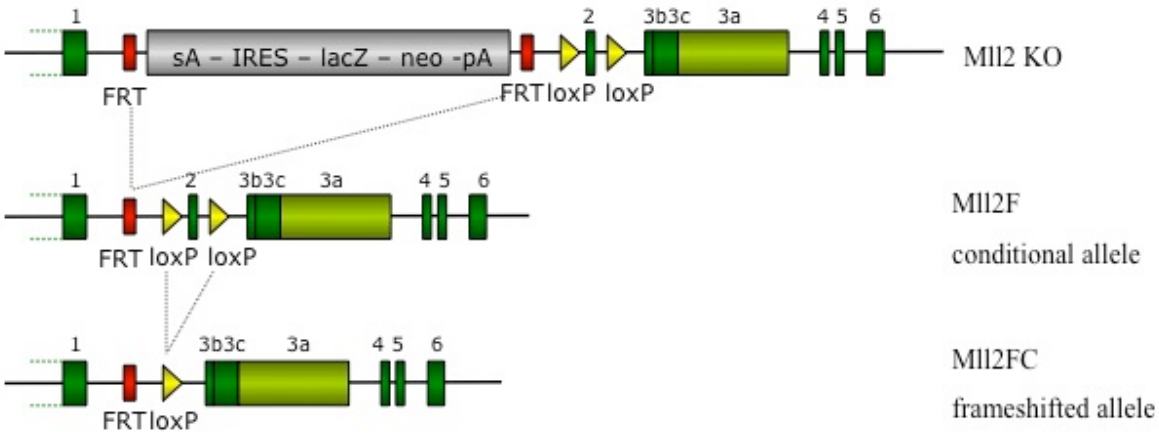

Figure 4. Scheme of the Mll2 conditional knock out strategy. (Glaser et al., 2006; Testa et al., 2004). **1-6** – numbers of exons**, FRT** – FRT sites, **loxP** – lox P sites, **sA** – splice acceptor, **IRES** – internal ribosomal entry site, **lacZ** – LacZ cassette, **neo** – neomycin cassette, **pA** – polyadenylation signal, Mll2 null allele - **Mll2 KO** knock out allele, **Mll2F** – conditional allele, **Mll2FC** – frameshifted allele.

In order to investigate the role of Mll2 in differentiated cell lineages, I have chosen one of the best known systems of cellular differentiation - the maturation of B cells. The choice of B cell development as a model system is due to several reasons. The main advantage of lymphoid development for the study of lineage commitment is due to the fact that stages of maturation are precisely defined and cells at these various stages can be easily accessed, and analyzed for functional abnormalities, for example at the level of immunological response raised against bacterial/viral antigens. Moreover, using powerful tools, in the form of stage specific Cre-expressing mouse lines, it is possible to ablate gene function at defined stages of B cell maturation. In order to knock out Mll2 specifically in mature B cells I selected the CD21-Cre3A mouse line that expresses Cre recombinase under the CD21 promoter. The line was established by inserting Cre gene into CD21/35 locus on a transgenic artificial chromosome (Kraus et al., 2004) (Fig. 5) and results in Cre expression at the moment of the transition from immature B into long-lived mature B cell (Kraus et al., 2004; Takahashi et al., 1997).

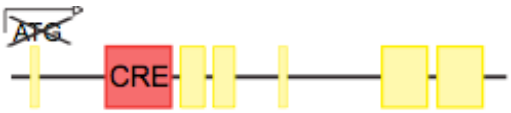

Figure 5. Scheme of CD21-Cre transgene. (Kraus et al., 2004)

1.6 B cell specification, B cells and marginal zone B cells

Lymphopoiesis takes place during the entire lifespan of mammals. Primitive hematopoietic cells first appear within blood islands of the yolk sac (Lux et al., 2008; Palis and Yoder, 2001). Hematopoiesis starts during embryogenesis in the fetal liver (Yokota et al., 2003) and shortly before the birth is continued in the spleen. Around birth the definitive hematopoiesis starts in the bone marrow where it is carried on for whole the life of the organism (Nunez et al., 1996). Hematopoietic stem cells (HSCs), through several different developmental stages, differentiate into all types of mature B cells including splenic follicular B cells (Fo; also called B2), marginal zone B cells (MZ) and B1 cells, which reside in peritoneal and pleural cavities. Multipotent HSC differentiate into common lymphoid progenitors (CLP) that can give rise to B and T lymphocytes, natural killer cells (NK) and dendritic cells. CLP are characterized by the lack of B and T cell-specific markers, intermediate levels of c-KIT, and the expression of the IL-7R ($CD45/B220^{neg}$ - $CD19^{neg}$ - $c\text{-}KIT^{interm}$ - $Il\text{-}7R^{+}$). Further down in lineage commitment, the expression of the CD45/B220 marker correlates with a decrease in progenitors multipotency, as documented by the observation that CD45/B220 positive fraction ($CD45/B220^{+}$ - $CD19^{neg}$) gives poor results in reconstructing T cell lineage (Rumfelt et al., 2006). As a further commitment step, the expression of the CD19 marker defines the Pro B cell ($CD45/B220^{+}$ - $CD19^{+}$) which is irreversibly committed to the B cell lineage due to the expression of Pax5, which represses all lineage-inappropriate genes simultaneously activating B cell specific transcription program. Pax5 is a key transcriptional regulator of B lymphopoiesis. Pax5 ablation leads to lymphopoiesis arrest at the Pro B uncommitted stage (Cobaleda et al., 2007). Further stages of developing B cells are defined on the basis of their capacity for growth under different culture conditions such as presence of IL-7 stimulus and independence from contact of stromal microenvironment in the bone marrow niche (Hayashi

et al., 1990; Sudo et al., 1989). Later stages do not require cell/stroma contact, however are dependent on cytokine stimulation (Era et al., 1991). Application of multiparameter flow cytometry facilitated classification of B cells into different subpopulations. Thus, bone marrow fractions can be further divided according to the expression of CD43 into Pro B cells expressing CD43 ($CD45/220^{+}$ - $CD19^{+}$ - $CD43^{high}$) which give rise to the Pre B subpopulation of CD43 negative cells ($CD45/220^{+}$ - $CD19^{+}$ - $CD43^{neg}$). Niche independent B cells retain requirement for IL-7 that promotes survival and proliferation both *in vivo* and *in vitro,* as shown by the fact that block of Il-7 or IL-7R arrests B cell development (Hardy et al., 1991). A further critical step in B cell development is the rearrangement and expression of the proteins that define B cell identity and function – immunoglobulins (Ig). The role of Ig is to recognize and bind to an epitope of an antigen (ag) (Cohn, 2002). Immunoglobulins are heterodimers consisting of 2 heavy (H) and 2 light (L) chains (Edelman and Poulik, 1961). Each of the chains contains an N-terminal variable domain (V) and C-terminal constant domain (C). There are 5 types of constant domains that define Ig heavy chains: α ε, δ, γ, and μ and in turn different classes (isotypes) of Ig: Ig A, E , D, G, and M respectively. Different Ig classes differ in their biological properties, functional locations and ability to respond to different antigens. In mammals the constant domain of light chains is present in two forms: λ and κ. In mice, immunoglobulin V region assembly begins with the joining of one of 13 diversity gene segments (D_H) to one of four joining gene segments (J_H) – DJ join. Next one of 110 variable gene segments (V_H) is joined (Johnston et al., 2006). After the functional H chain creation, L chain from the rearranged clusters of loci λ and κ is assembled. The λ locus contains 3 V λ, 3 J λ and 2-3 C λ, while locus κ contains 5 J κ, 140 V κ and one C κ region (Paul, 2003). The first stages of immunoglobulin heavy chain rearrangements process take place in the HSC. Further in development, about 30 – 50% of CLP and 80% of $CD45/B220^{+}$ - $CD19^{neg}$ cells rearrange DJ segments on at least one chromosome (Rumfelt et al., 2006). D-J

and V-D junctions are regulated by Rag1 and Rag2 that activate recombination and promote double strand breaks of DNA required for Ig rearrangements (Oettinger et al., 1990). The extent of heavy or light chain rearrangement varies between subpopulations. At the heavy chain locus, D-J rearrangements occur before the V-DJ junction and those cells are distinguishable as early Pro B cell ($CD45/B220^{+}$ - $CD19^{neg}$ - $CD43^{high}$) while V-DJ rearrangements take place in cells of Pre B cell ($CD45/B220^{+}$ - $CD19^{+}$ - $CD43^{neg}$). First light chain rearrangements are detectable already in Fr. B ($CD45/B220^{+}$ - $CD19^{+}$ - $CD43^{high}$), although extensive rearrangements take place only at the stage of Pre B cell.

Immunoglobulins are present either in a soluble form or bound to the membrane of a B cell as B cell antigen receptor (BCR). Pre BCR receptor containing μ chain is expressed on the surface of Pre B cells. After the full assembly of both heavy and light chain of the immunoglobulin, functional IgM is present in the cytoplasm and on the surface as a BCR receptor, of an immature B cell ($CD45/220^{+}$ - $CD19^{+}$ - $CD43^{neg}$ - IgM^{+} - IgD^{neg}). Immature B cells leave the bone marrow and continue their maturation in the spleen. Newly formed immature B cells can be distinguished from mature B lymphocytes on the basis of their inability to proliferate in response to BCR cross linking. Recent studies demonstrated that immature from mature cells can be distinguished by the presence of CD93 (AA4.1) on their surface ($CD45/220^{+}$ - $CD19^{+}$ - $CD43^{neg}$ - IgM^{+} - IgD^{neg} - $CD93^{high}$) (Allman et al., 2001), however the distinction of immature cells that are going to give rise to different mature B cell types is still unclear. After the migration from bone marrow to the spleen newly formed B cells undergo negative selection (Lang et al., 1997). If instead an immature B cell is positively selected it undergoes further maturation to a mature B cell state. Those maturing cells can be subdivided on the basis of their surface markers. Splenic transitional cells are currently identified by a panel of markers: $CD93^{interm}$ - $CD23^{+}$ - $CD21^{+}$ - IgM^{+}. They mature then into all mature B cells of all subsets: B1 cells ($CD93^{neg}$ – $CD23^{neg}$ - $CD21^{neg}$ – $CD43^{+}$ - $CD5^{low-high}$-

IgM^{+} - IgD^{neg}), follicular B cells (Fo) (B2 cells) ($CD43^{neg}$ - $CD93^{neg}$ – $CD23^{high}$ - $CD21^{interm}$ – IgM^{low} - IgD+) and marginal zone B cells (MZ) ($CD43^{neg}$ - $CD93^{neg}$ – $CD23^{neg\text{-}low}$ - $CD21^{high}$ – IgM^{+} - IgD^{+}) (Amano et al., 1998; Cariappa et al., 2001; Paul, 2003). Fraction of the mature bone marrow B cell pool consists on recirculating mature follicular B cells. B cell maturation stages are presented in a schematic way in Figure 6.

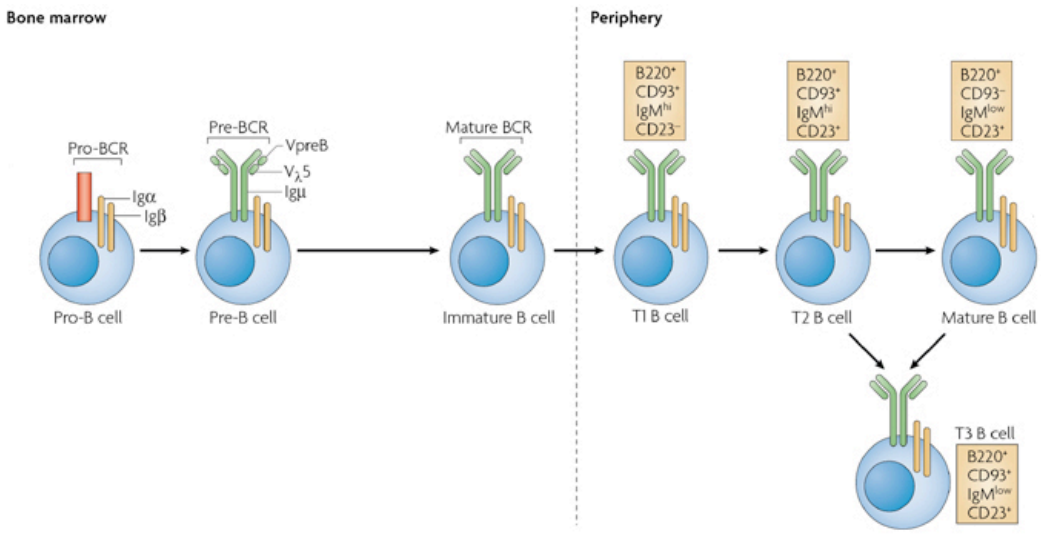

Figure 6. Schematic representation of B cell developmental stages (Cambier et al., 2007); **BCR** - B cell receptor, **Ig** – immunoglobulin chain (clusters: α, β, δ, μ, λ), **Pro-BCR** and **Pre-BCR** – immature forms of BCR that present on the B cell surface before complete V(D)J rearrangement and assemblement of functional BCR. The Pro-BCR includes **Igα** and **Igβ** while the Pre-BCR is composed from **Igμ** and surrogate light chains (**VpreB**,**Vλ5**) **T1 – T3** – transitional B cells

It is no surprise that such a complex system of cell differentiation is strictly controlled. At the earliest the stage of hematopoiesis Notch1 signaling is essential for generation of HSC, however its role seems to be dispensable for later stages of embryonic hematopoiesis (Kumano et al., 2003). In vivo studies demonstrated that Notch1 increases self-renewal potential of HSC *in vivo*, favoring lymphoid lineage (Stier et al., 2002). Later Notch1 is rather involved in T than B lymphopoiesis. Activation of Notch1 enriches CD4+ - CD8+ T cells in the BM and simultaneous blocks B lymphopoiesis at its early stage. This suggests that Notch1 provides a key regulatory signal in determining T lymphoid vs. B lymphoid lineage decisions, probably by influencing lineage commitment in CLP cells (Pui et al., 1999). Another key regulator of B cell development is Notch2. Its expression increases during B cell maturation and is most prominent in splenic B cells. Moreover Notch2 has been proven to be indispensable specifically for marginal zone B cell development (Saito et al., 2003). Already its haploinsufficiency leads to a dramatic reduction of MZ B cell compartment (Witt et al., 2003). Furthermore, several genes involved in Notch2 signaling were also shown to play a fundamental role in MZ development. Knock out of a Notch2 ligand - Delta-like1 (Dll1) or Notch 2 coactivators - Mastermind-like (Maml1) Lunatic and Manic Fringe (Lfng and Mfng) and RBP-J[2] led to marginal zone specification failure (Hozumi et al., 2004; Tan et al., 2009; Wu et al., 2007). Previously mentioned Pax5 - key transcriptional regulator of B lymphopoyesis, activating the expression of B cell lineage signaling molecules restricts the pluripotency of a CLP cell, pushing it into B lymphoid differentiation. BSAP (B cell specific activator protein), the product of the Pax5 gene, is expressed throughout B cell development. Moreover Pax5 expression is critical for maintenance of B cell identity and functionality (Cobaleda et al., 2007; Horcher et al., 2001). Pax5 activates CD19 and BLNK and upregulate V-DJ heavy chain rearrangements (Nutt et al., 1998; Nutt et al., 1997; Schebesta et al., 2002;

[2] RBP-J - Recombination signal binding protein for immunoglobulin kappa J region

Thevenin et al., 1998). The B lymphopoiesis arrest at the Pro B cell stage upon Pax5 ablation is due to the lack of complete heavy chain rearrangement, as the presence of fully rearranged and functional Ig heavy chain determines cell independence from the contact with the stroma of a bone marrow niche. Correct recombination and assembly of V(D)J regions into a functional Ig chains is controlled by Rag1 and Rag 2, two recombination activating proteins (Oettinger et al., 1990). As in case of Pax5 knock out, deletion of any of two Rag1 or 2 genes results in a block of B cell development at the early developmental stage due to the lack of functional Ig chains (Mombaerts et al., 1992; Shinkai et al., 1992). Furthermore, fully assembled and functional BCR provides a survival signal for a mature cell (Kraus et al., 2004) and the strength of BCR signaling itself determines B cell fate, pushing maturation into direction of follicular (if signal is strong), or marginal zone B cell and B1 (if signal is weak) (Casola et al., 2004).

As discussed (1.2 – 1.3) regulation of cell specification takes place at two different levels, by transcription regulators and via epigenetic modification. Number of publications demonstrate that also in case of B lymphopoiesis, epigenetic regulation is crucial for B cell development. Peaks of H3K4me2 and H3K4me3 found on the promoters of the Pax5 target genes (Hagman and Lukin, 2007; Schebesta et al., 2007) ensure the activation and maintenance of the B lineage transcriptional program. Similarly fundamental for B cell development and function, Ig rearrangement is possible thanks to the similar marks found on the D and J segments during V(D)J recombination that maintain the active state of the chromatin of Ig loci and thus guarantee its accessibility (Corcoran, 2005; Goldmit et al., 2005; Matthews et al., 2007; Morshead et al., 2003; Perkins et al., 2004).

For these reasons, the functional dissection of mammalian H3K4 histone methyltransferases in B cell specification appears like a most worthwhile project with the aim of understanding the contribution of this chromatin mark to this exemplary system of cell differentiation.

Considering role of Mll2 in the tightly timed establishment of lineage specific transcriptional programs (Andreu-Vieyra et al., 2010; Glaser et al., 2009) lymphopoiesis seems to be the best system to study its role in commitment and maintenance. Following well defined developmental stages of B cell maturation we will be able to pinpoint requirement for Mll2 during lymphopoiesis and understand its role in the regulation of a transcriptional program. With the aim of shedding light on the role of Mll2 in the homeostasis of a mature cell compartment, we employed conditional knock out strategy (Glaser et al., 2006; Takahashi et al., 1997; Testa et al., 2004; Testa et al., 2003) to dissect the role of Mll2 in lymphopoiesis.

2. Materials and Methods

2.1. Materials

2.1.1 Solutions, buffers and media

2.1.1.1 DNA electrophoresis in agarose gel

50X TAE buffer	2M Tris base
	500mM Glacial acetic acid
	500mM EDTA
Loading buffer	37% Glycerol
	0,37% Bromophenol blue
	0,37% Xylene cyanol
	4,5 mM EDTA pH=8,0

2.1.1.2 Genomic DNA isolation

Lysis buffer	100 mM Tris-HCl pH=8.5
	5 mM EDTA
	200 mM NaCl
	0,2% SDS
	Proteinase K

2.1.1.3 Enzyme-linked immunosorbent assay

Blocking buffer	50 mM Tris buffered saline pH 8.0 1% BSA
Coating buffer	0,5M Carbonate-bicarbonate buffer pH 9,6
Enzyme Substrate	TMB Peroxidase Substrate Peroxidase Solution B Prepared freshly in a ratio 1:1
Sample/Conjugate Diluent	Blocking buffer 0,05% Tween 20
Washing solution	50 mM Tris buffered Saline pH 8,0 0,05% Tween 20

2.1.1.4 Immunostaining

2.1.1.4.1 Immunostaining of cells for flow cytometry and fluorescence-activated cell sorting (FACS)

FACS buffer	1x PBS 1% BSA 0,05% NaN3

Fixing solution	FACS buffer 1% Formaldehyde
Gey's solution	H_2O, Solution A, B and C mixed in the ratio: 7: 2: 0,5 : 0,5. Prepared freshly.
Solution A	650 mM NH_4Cl 25 mM KCl 40 mM Na_2HPO_4 280 mM Glucose 0,15 mM Phenol red
Solution B	2 mM $MgCl_2$ 0.55mM $MgSO_4$ 3 mM $CaCl_2$
Solution C	25 mM NaHCO

2.1.1.4.2 Immunostaining of cells for magnetic-activated cell sorting (MACS®)

MACS® buffer	1x PBS 0,5% BSA 2 mM EDTA

2.1.1.4.3 Immunofluorescence

Fixing solution	1x PBS
	4% PFA
Blocking solution	1x PBS
	2% BSA
	2% goat serum

2.1.1.5 Protein isolation

Lysis buffer	8M Urea
	Protease inhibitors

2.1.1.6 Southern blot

Denaturation buffer	1,5 M NaCl
	0,5 M NaOH
Transfer buffer	20x SSC
Washing buffer I	2x SSC
Washing buffer II	0,2x SSC
	0,1% SDS

Washing buffer III	0,2% SSC

2.1.1.7 Western blot

2.1.1.7.1 Protein electrophoresis in SDS-PAGE gel

Coomasie staining solution	0,25% Coomassie Brilliant Blue G-250 10% Glacial Acetic Acid 50% Methanol
Destaining solution	5% Glacial Acetic acid 20% Methanol
Ponceau S	0,2% Ponceau S 1% Glacial Acetic acid
10x Running buffer	250 mM Tris base 2 M Glycine 1% SDS
Separating gel – 5%	5% Arlylamide/Bisarylamide 1x Separatig gel buffer 0,1% APS 0,08% TEMED

4x Separating gel buffer pH 8,8	1,5 M Tris-HCl pH 8,8 0,4% SDS
Stacking gel	5% Arlylamide/Bisarylamide 1x Stacking gel buffer 0,1% APS 0,1% TEMED
4x Stacking gel buffer pH 6,8	500 mM Tris-HCl pH 6,8 0,4% SDS
10x Transfer buffer	250 mM Tris base 2 M Glycine Add 20% of Methanol to 1x Transfer buffer

2.1.1.7.2 Incubation of protein – bound membranes with antibodies

Blocking buffer	5% Milk powder solvent: TBST buffer
TBST buffer	1x TBS buffer 0,2% Tween 20

2.1.1.8 Cell culture media

DPBS	Sigma
DMEM	Gibco
GlutaMAX™	Gibco
Penicillin – Streptomycin	Sigma
Trypsin/EDTA (0,05/0,02% in PBS)	Gibco

B cell medium	GlutaMAX™
	5% FBS North America
	Glutamine
	$C_3H_3NaO_3$
	NEAA
	Penicillin – Streptomycin
	β – Mercaptoethanol

2.1.2 Antibodies

2.1.2.1 Antibodies used in flow cytometry and fluorescence-activated cell sorting (FACS)

antibody	clone	company
Monoclonal Mouse-anti BrdU (FITC)	PRB-1	eBioscience
Monoclonal Mouse-anti BrdU (APC)	-	eBioscience
Monoclonal Rat-anti mouse CD1d (FITC)	1B1	eBioscience
Monoclonal Rat-anti mouse CD4 (PE)	RM4-5	eBioscience
Monoclonal Rat-anti mouse CD5 (PE)	53-7.3	eBioscience
Monoclonal Rat-anti mouse CD8 (FITC)	KT15	Beckman Coulter
Monoclonal Rat-anti mouse CD19 (Cy7 PE)	eBio1D3	eBioscience
Monoclonal Rat-anti mouse CD21/CD35 (FITC)	7G6	BD Pharmingen

antibody	clone	company
Monoclonal Rat-anti mouse CD23 (PE)	B3B4	eBioscience
Monoclonal Rat-anti mouse CD38 (APC)	90	eBioscience
Monoclonal Rat-anti mouse CD38 (FITC)	90	eBioscience
Monoclonal Rat-anti mouse CD43 (PE)	S7	BD Pharmingen
Monoclonal Rat-anti mouse/human CD45R(B220) (FITC)	RA3-6B2	eBioscience
Monoclonal Rat-anti mouse/human CD45R(B220) (Cy7PE)	RA3-6B2	eBioscience
Monoclonal Mouse-anti mouse CD45.1 (Ly5.1) (FITC)	A20	eBioscience
Monoclonal Mouse-anti mouse CD45.2 (Ly5.2) (APC)	104	eBioscience
Monoclonal Rat-anti mouse CD93 (AA4.1) (PE)	AA4.1	eBioscience
Monoclonal Mouse-anti mouse CD95 (Fas)	15A7	eBioscience
IgM Alexa 488	-	homemade
Monoclonal Rat-anti mouse IgD (PE)	11-26c	eBioscience
Streptavidin (APC)	-	eBioscience
Streptavidin (FITC)	-	eBioscience

2.1.2.2 Antibodies used in magnetic-activated cell sorting (MACS®)

antibody	Kit no.	company
Monoclonal Rat anti-mouse CD19 (MicroBeads)	130-052-201	Miltenyi Biotech
Monoclonal Rat anti-mouse CD11b (biotin)	130-090-861	Miltenyi Biotech
Monoclonal Rat anti-mouse CD45R (biotin)		
Monoclonal Rat anti-mouse DX5 (biotin)		
Monoclonal Rat anti-mouse Ter-119 (biotin)		
Anti-biotin MicroBeads		
Monoclonal Armenian Hamster anti-mouse CD3 (biotin)	145-2C11	eBioscience
Monoclonal Rat anti-mouse CD4 (biotin)	GK1.5	eBioscience
Monoclonal Rat anti-mouse CD8 (biotin)	53-6.7	eBioscience

2.1.2.3 Antibodies used in immunofluorescence

antibody	clone	company
Monoclonal Rat-anti mouse/human CD45R (B220) (FITC)	RA3-6B2	eBioscience
Monoclonal Rat-anti mouse Macrophages MOMA-1(biotin)	CL89149B	Cedarlane
IgM Alexa 488	-	homemade
Streptavidin (Cy3)	-	Jackson ImmunoResearch

2.1.2.4 Antibodies used in enzyme-linked immunosorbent assay (ELISA)

antibody	Lot	company
Goat-anti Mouse IgG3	A90-11A-9	Bethyl
Goat-anti Mouse IgM	A90-11A-9	Bethyl
Goat-anti Mouse IgG3 HRP conjugated	A90-101P-23	Bethyl
Goat-anti Mouse IgM HRP conjugated	A90-111O17	Bethyl

2.1.2.5 Antibodies used in Western blot

antibody	company
Polyclonal Rabbit-anti Mouse Mll2	Sigma
Monoclonal Mouse Anti-Vinculin	Sigma
Goat-anti Rabbit	Biorad
Goat-anti Mouse	Biorad

2.1.3 Enzymes

Deoxyribonuclease I, Amplification Grade	Invitrogen
GoTaq® DNA Polymerase	Promega
Phusion™ High-Fidelity DNA Polymerase	Finnzymes
Proteinase K	Sigma
Restriction enzymes (with supplied buffers)	New England Biolabs and Promega
Ribonuclease H	Invitrogen
RnaseOUT™ Recombinant Ribonuclease Inhibitor	Invitrogen
SuperScript™ III Reverse Transcriptase	Invitrogen

2.1.4 Kits

APC BrdU Flow Kit	BD Pharmingen
FITC BrdU Flow Kit	BD Pharmingen
Ladderman™ labeling Kit	TakaRa
Mouse IgG3 ELISA Quantification Kit	Bethyl
Mouse IgM ELISA Quantification Kit	Bethyl
CD19MicroBeads	Miltenyi Biotec
Pan T Cell Isolation Kit	Miltenyi Biotec
ProbeQuant™ G-50 Micro Columns	GE Healthcare
QIAGEN® Plasmid Maxi Kit	QIAGEN®
Rediprime™II Random Prime Labelling System	Amersham Pharmacia
RNeasy® Plus Micro Kit	QIAGEN®
SuperScript™ III Reverse Transcriptase Kit	Invitrogen
SYBR®Green PCR Master Mix	Applied Biosystems
Wizard® Plus SV Minipreps DNA Purification System	Promega
Wizard® SV gel and PCR Clean Up System	Promega

2.1.5 Vectors

TOPO® Vector	Invitrogen

2.1.6 Laboratory materials

0,2ml Thermo-Tubes	AB Gene
Cell culture flask	BD Falcon™
Cell Strainer 70µm Nylon	BD Falcon™
Electroporation cuvetts (0.2cm gap)	Bio-rad
Extra thick blot paper Protean®	Bio-Rad
Filtered tips	Grelner Blo-One GmbH
Filter Stericups	Stericup
Hyperfilm™ ECL	GE Healthcare
Hybond – N+	BD Falcon™
Microcentrifuge tubes	Eppendorf
Microscope Slides Superfrost ultra Plus®	Thermo Scientific
MICROTEST™ Tissue Culture Plate, 6 Well	BD Falcon™
MICROTEST™ Tissue Culture Plate, 96 Well	BD Falcon™
O.C.T™ Compound	Tissue-Tek®
Petri dishes	Sterilin
Pipette tips	Grelner Blo-One GmbH
Protran®	Whatman®
Serological pipettes	BD Falcon™
Whatman® blotting paper GB 002	Whatman®

2.1.7 Instruments

3730XL DNA Analyzer	Applied Biosystems
ABI PRISM 3100 genetic Analyzer	Applied Biosystems
ABI PRISM® 7900 Fast Real Time PCR System	Applied Biosystems
ABI PRISM® 7900HT Sequence Detection System	Applied Biosystems
Allegra™ X-12R Centrifuge	Beckman Coulter
Biofue fresco	Heraeus
Biofuge pico	Heraeus
Confocal Microscope TCS SP2 AOBS	Leica
Electroporator	Bio-rad
FACSAria	BD Biosciences
FACSCalibur	BD Biosciences
Horizontal Electrophoresis Systems	EuroClone
DU® 730 Spectrophotometer	Beckman Coulter®
Mini PROTEAN® 3 System	Bio-rad
NanoDrop® 1000	Thermo Scientific
Storage phosphor screen	Amersham Bioscience
T3000 Thermocycler	Biometra
Typhoon TRIO Variable Mode Imager	GE Healthcare
Thermomixer compact	Eppendorf
Transblot® SD Semi-dry transfer cell	Bio-rad
Water bath sonicator Bioruptor™ UCD-200	Diagenode

Victor$^{3}_{TM}$ 1420 Multilabeled Couner Perkin-Elmer™

2.1.8 Sterilization of solutions and equipments

All solution and plastic wares that are not heat sensitive were sterilized at 121˚C, 10^5 Pa for 60 min in an autoclave (Fedegari FM02 1M, Fedegari FVA). Heat sensitive solutions were filtered through disposable sterile filter (0,2μm pore size). Glassware were sterilised overnight in an oven at 220˚C.

2.1.9 Bacterial strains

E.coli DH5α Sigma

2.1.10 Mouse strains

Mouse strains initially brought from Biotechnology Center TU Dresden (Germany) and further bred in animal facility of IFOM – IEO Campus Milan, Italy.

2.1.11 cDNA probes

Probe C

(Glaser et al., 2006)

ACGGGGTGAGGAGGGCACAGAACGGATGGTGCAGGCACTGACTGAACTTCTCCG
GCGGTCCCAAGCACCCCAACCCCCCCGGAGCCGGGCACGGGCACGTGAACCCTCT
ACTCCCCGACGGTCTCGGGGAAGGCCCCCAGGACGGCCAGCCGGTCCCTGCCGGA
AAAAGCAGCAAGCAGTAGTGTTAGCAGAAGCGGCTGTGACAATCCCTAAACCCG
AGCCTCCGCCCCCTGTGGTTCCAGTAAAGAACAAAGCTGGCAGTTGGAAATGCAA
GGAGGGACCTGGTCCAGGACCTGGAACCCCCAAACGTGGAGGACAGCCTGGGAG
AGGAGGCCGTGGAGGCAGGGGCAGAGGCCGAGGCGGACTTCCCCTTATGATCAA
GTTTGTTTCCAAGGCCAAGAAAGTGAAGATGGGACAATTGTCCCAGGAACTAGAA
TCAGGTCAGGG

2.1.12 Synthetic oligonucleotide primers

The synthetic oligonucleotides primers were obtained either from Sigma Genosys or from Eurogentec and dissolved in water to a final concentration of 100 pmol/µl, and stored at -20˚C.

19	5’	G C C T G C A T T A C C G G T C G A T G C A A C G A	3’
20	5’	G T G G C A G A T G G C G C G G C A A C A C C A T T	3’
34	5’	G G G C T G A C C G C T T C C T C G T G C T T T A C	3’
36	5’	G G A G A A C A G T T G T G G G G A G A T G G G T C	3’
145	5’	C G G A G G A A G A G A G C A G T G A C G	3’
147	5’	G G A C A G G A G T C A C A T C T G C T A G G	3’
A1LoxP R	5’	T C C T A A G C A A T A G A A T C C A C A C C C	3’
B1LoxP F	5’	A G G T A G A G T G G T G G A G G C T T C T T A	3’
Ex2-3 F	5’	A G A T G A A G A T G T G G C C C C C A G T	3’
Ex2-3 R	5’	A G A A G T T C A G T C A G T G C C T G C A	3’
mβ-actin F	5’	C T T T G C A G C T C C T T C G T T G	3’
mβ-actin R	5’	A C G A T G G A G G G G A A T T A C A G C	3’
Mll F	5’	G G A T C A G A G T G G A C T T T A A G G A A G	3’
Mll R	5’	C T T C A C A A T A T C A T C G C T G A A C T C	3’
Mll2 F	5’	A C A C C C G C G T G A A A A G G G G G C C T G C T	3’
Mll2 R	5’	C T G T C T G G C T C A C C G G G T T C T G G G C T	3’
Mll3 F	5’	A C C C C C C T A A G A C C T A C A C C C A G G A	3’
Mll3 R	5’	G C T C A G G A C T G A G G A T C C C A T C T A G C	3’
M-Neo F	5’	C C A T C A T G G C T G A T G C A A T G C G	3’
M-Neo R	5’	G A T G C G C T G C G A A T C G G G A G C G	3’

2.2. Methods

2.2.1 Isolation of nucleic acids

2.2.1.1 Isolation of plasmid DNA

(Sambrook, 1989)

2.2.1.1.1 Small – scale isolation of plasmid DNA

A single *E.coli* colony was inoculated in 5 ml LB medium with the appropriate antibiotic and incubated in a shaker overnight at 37˚C with a speed of 240 rpm. 500 µl of this saturated culture were used for making glycerol stock and the rest of the culture was centrifuged at 3273 g for 15 min. Plasmid DNA preparation was performed according to Promega Plasmid DNA Isolation and Purification Protocol supplied with the Wizard® Plus SV Minipreps DNA Purification System.

2.2.1.1.2 Large – scale preparation of plasmid DNA

A single colony was inoculated in 5 ml of LB medium with appropriate antibiotic as a pre – culture for 8 hrs at 37˚C shaker. This pre – culture was added in a dilution 1:700 to a 50 or 100 ml LB medium with appropriate antibiotic and incubated overnight at 37˚C with shaking. The culture was centrifuged at 3273 g for 15 min. Plasmid DNA preparation was performed according to QIAGEN® Plasmid Purification Protocol supplied with the QIAGEN® Plasmid Maxi Kit.

2.2.1.2 Isolation of genomic DNA from tissue samples and cells.

(Laird et al., 1991)

1 cm of mouse tail, a fragment of a moue tissue or a cell pellet was incubated in 500µl lysis buffer containing Proteinase K (100µg/ml) at 37˚C overnight in Thermomixer compact. 450 µl of tissue lysate were transferred into a new tube and 450 µl of isopropanol were added, mixed by inverting for 5 min. To complete precipitation of DNA, then centrifuged at a speed of 16.000 g for 15 min, washed with 1ml of 70% ethanol and centrifuged again at a speed of 16.000 g for 10 min. DNA pellet was dissolved in 200 µl of miliQ water by incubation at 60˚C for 20 min.

2.2.1.3 Isolation and purification of genomic DNA for Southern blot and qPCR.

1 cm of the mouse tail, a fragment of a moue tissue or a cell pellet was incubated in 500µl lysis buffer containing Proteinase K (100µg/ml) at 37˚C overnight in Thermomixer compact. 450 µl of tissue lysate were transferred into a new tube and 450 µl of Phenol:Chlorophorm:Isoamyl Alcohol (25:24:1) were added, mixed by inverting for 1 min and centrifuged at a speed of 16.000 g for 5 min. The upper aqueous phase was transferred into a new eppendorf and equal amount of chlorophorm was added. Sample was mixed for 1 min and centrifuged at a speed of 16.000 g for 5 min. Upper, aqueous faze was transferred into a new eppendorf and equal amount of isopropanol was added together with $NaCl_2$ (final concentration 200mM). Sample was mixed by inverting for 5 min. to complete precipitation of DNA, then centrifuged at a speed of 16.000 g for 15 min, washed with 1ml of 70% ethanol and centrifuged again at a speed of 16.000 for 10 min. Obtained pellet was dissolved in 200 µl of miliQ water and incubated at 60˚C for 20 min.

2.2.1.4 Isolation of total RNA from tissue samples

(Sigma)

100 – 200 mg tissue samples were homogenized on ice in 200 µl Tri Reagent, then 800 µl of Tri Reagent were added and vortexed. The homogenate was stored at RT for 5 min to permit the complete dissociation of nucleoprotein complexes. Next 200 µl of chloroform were added, mixed vigorously, and stored at RT for 15 min. After centrifuging at a speed of 12000 g for 15 min. at 4˚C the upper aqueous phase was transferred into a new tube. The RNA was precipitated by adding 500 µl of isopropanol, incubating at RT for 10 min and centrifuging at a speed of 12000 g for 10 min at 4˚C. Finally the pellet was washed by 1 ml 75% ethanol, centrifuged again for 8 min, air-dried for 5 min at RT, dissolved in 20 µl of DEPC–H2O and incubated at 60 ˚C for 10 min.

2.2.2 Determination of the nucleic acids concentration

The concentration of nucleic acids was determined spectrophotometrically by measuring absorption of the samples at 260nm using the NanoDrop 3300. The quality of nucleic acids i.e. contamination with salt and protein was checked by measurements at 230, 280 and 320 nm.

2.2.3 Gel electrophoresis

2.2.3.1 Agarose gel electrophoresis of DNA

Usually, 2 g of agarose was added in 100 ml 1x TBE buffer, and boiled in the microwave to dissolve the agarose, then chilled to about 60 ˚C before adding 10 µl of Ethidium bromide

(10mg/ml) and then poured into a horizontal gel chamber.

2.2.3.2 SDS – PAGE for the separation of proteins

(Laemmli, 1970)

SDS gel electrophoresis can be used for separating protein for analysis and molecular weight determination. The proteins are denatured and rendered monomeric by boiling in the presence of reducing agents (β – mercaptoethanol or dithiothreitol) and negatively charged detergent (SDS). The proteins, which normally differ according to their charges, are all coated with negatively charged SDS molecules. Hence, all the proteins in the sample become negatively charged and achieve constant charge to mass ratio. In this way, the separation is according to the size of proteins. A SDS – PAGE consists of two gels; firstly 5% separating gel was poured. In order to achieve a smooth boundary between separating and stacking gel, the separating gel was covered with a layer of 95% ethanol. After polymerization of separating gel, the stacking gel was poured over it. Before loading, samples were mixed with LDS sample buffer and heated at 95˚C for 10 min and chilled on ice for 2 min. The gel was running at 70V and 30mA for 10 – 15 min and then at 150V for 1 – 1,5 hr.

2.2.4 Isolation of DNA fragments from agarose gel

DNA fragments appointed for isolation from the agarose gel and then for purification were run in 0,8% agarose gel. After separation in gel the DNA fragment was excised with a sterile scalpel and weighed. DNA isolation was performed according to protocol supplied with Wizard® SV Gel PCR Clean-Up system (Promega).

2.2.5 Restriction of DNA

2.2.5.1 Restriction of plasmid DNA

Restriction enzyme digestions were performed by incubating double – stranded DNA with an appropriate amount of restriction enzyme in its respective buffer as recommended by the supplier, at the optimal temperature for the specific enzyme. Standard digestions include 2 – 10 U enzyme per microgram of DNA. This reaction was usually incubated for 3 hrs to ensure complete digestion at the optimal temperature for enzymatic activity, which was typically 37˚C.

2.2.5.2 Restriction of genomic DNA for Southern blot

10 µg of genomic DNA isolated according to the protocol 2.2.1.3 was digested with PstI enzyme overnight at 37˚C. The reaction was carried out in the following reaction mix:

DNA	10 µg
10x Buffer	4 µl
BSA	0,4 µl
PstI enzyme	4 µl
In a total volume of 40µl	

PstI endocuclease recognises and cuts following sequence:

5’ CTGCA G 3’

3’ G ACGTC 5’

2.2.6 Electrocompetent *E.coli* cells production

A single colony of *Escherichia coli* was inoculated in 50ml of LB medium and incubated overnight at 37˚C with shaking. Culture was added in a dilution 1:20 to 500 ml LB medium and incubated at 37˚C with shaking. Rate of the bacterial growth was determined measuring OD_{600} (DU® 730 Spectrophotometer). At the OD_{600} = 0.4 the culture was transferred to an ice-old water bath for 15-30 min and mixed occasionally to ensure even cooling. Next the culture was centrifuged at 1000 g for 15 min at 4˚C. Obtained pellet was washed with 250 ml of 10% ice-cold glycerol and centrifuged at 1000 g for 20 min at 4˚C. This step was repeated two more times. The concentration of the culture was determined measuring the OD_{600} at the dilution 1:100. Cells were diluted to the final concentration 2-3 $x10^{10}$ cells/ml and aliquoted on the dry ice – ethanol bath (50µl/sample) and stored at -80˚C.

2.2.7 Electroporation of competent bacteria

An aliquot of electrocompetent *E.coli cells* was transferred to an ice cold electroporation cuvette (0.2-cm gap) and 10 – 25pg of a DNA purified with Wizard® SV gel and PCR Clean Up System Purification Kit were added. Cells with DNA were incubated on ice for 1 min. Cuvette with cells was placed in the electroporator and the electroporation was performed with the following settings:

Capacitance	25µF
Resistance	200Ω
Voltage	2,5 kV

After the electroporation, electroporator cells were immediately transferred to an eppendorf tube and 700µl of pre-warmed SOC medium were added. Cells were incubated for 1h at 37˚C with shaking in a thermomixer (Themomixer compact) and plated on an agar plate with the appropriate antibiotic.

2.2.8 Polymerase Chain Reaction (PCR) – PCR amplification of DNA fragments

(Chien et al., 1976; Saiki et al., 1985)

PCR reactions were performed on an automatic thermocycler (T3000 Thermocycler). The PCR reaction contained, in general, the following components:

10 ng	DNA
0,25 µl	forward primer (10 pM)
0,25 µl	reverse primer (10 pM)
0,75 µl	dNTPs (10 mM)
5 µl	5x PCR buffer
0,2 µl	Phusion™ High-Fidelity DNA Polymerase
up to 25 µl	H_2O

The reaction mixture was placed in 200 µl reaction tube and placed in thermocycler.

A standard PCR programme is shown here:

Initial denaturation	98 ˚C	30 sec

(35 cycles):	Denaturation	98 ˚C	8-10 sec[1]
	Annealing	depend. On Tm.	15-20 sec[2]
	Elongation	72 ˚C	15-55 sec[3]
	Final elongation	72 ˚C	5 min.

2.2.9 Genotyping of Mll2KO/Mll2F/CD21-Cre line

The genotypes of all offspring of Mll2KO/F/CD21-Cre line were analyzed by PCR reaction (2.2.8). DNA was extracted from mouse tails (2.2.1.2). For amplification of Mll2 allele (Fig. 9 A) were used primers Neo F and Neo. PCR reactions were run according to the following conditions:

10 ng	DNA
0,25 µl	Neo F (10 pM)
0,25 µl	Neo R (10 pM)
0,75 µl	dNTPs (10 mM)
5 µl	5x PCR HF buffer
0,2 µl	Phusion™ High-Fidelity DNA Polymerase
up to 25 µl	H_2O

using the following PCR programme:

Initial denaturation	98 ˚C	30 sec

[1] depending on a GCp content and length of the PCR product
[2] depending on the melting temperature (Tm) of primers
[3] depending on a length of the PCR product

(35 cycles):	Denaturation	98 ˚C	8 sec
	Annealing	66 ˚C	17 sec
	Elongation	72 ˚C	20 sec
	Final elongation	72 ˚C	5 min.

For amplification wild type, Mll2F and Mll2FC alleles were used primers 145 and 147 (Fig. 9 A). PCR reactions were run according to the following conditions:

10 ng	DNA
0,25 µl	forward primer (10 pM)
0,25 µl	reverse primer (10 pM)
0,75 µl	dNTPs (10 mM)
5 µl	5x PCR GC buffer
5%	DMSO
0,2 µl	Phusion™ High-Fidelity DNA Polymerase
up to 25 µl	H_2O

using the following PCR programme:

	Initial denaturation	98 ˚C	30 sec
(35 cycles):	Denaturation	98 ˚C	8 sec
	Annealing	55 ˚C	20 sec
	Elongation	72 ˚C	55 sec
	Final elongation	72 ˚C	5 min.

The presence of the CD21-cre allele was detected by PCR using primers 19 and 20. PCR reactions were run according to the following conditions:

10 ng	DNA
0,25 µl	forward primer (10 pM)
0,25 µl	reverse primer (10 pM)
0,75 µl	dNTPs (10 mM)
5 µl	5x PCR GC buffer
1 µl	$MgCl_2$ (50mM)
0,2 µl	Phusion™ High-Fidelity DNA Polymerase
up to 25 µl	H_2O

using the following PCR programme:

	Initial denaturation	98 ˚C	30 sec
(35 cycles):	Denaturation	98 ˚C	8 sec
	Annealing	55 ˚C	20 sec
	Elongation	72 ˚C	30 sec
	Final elongation	72 ˚C	5 min.

All PCR products were analysed by agarose gel electrophoresis in 2% gel. Neo allele gives 421 bp product (Fig. 7 and 7 A). while wild type, Mll2F and Mll2FC alleles give 1441 bp, 1618 bp and 760 bp products respectively (Fig. 7 A and C). CD21-cre allele gives 743 bp product (Fig. 7 D).

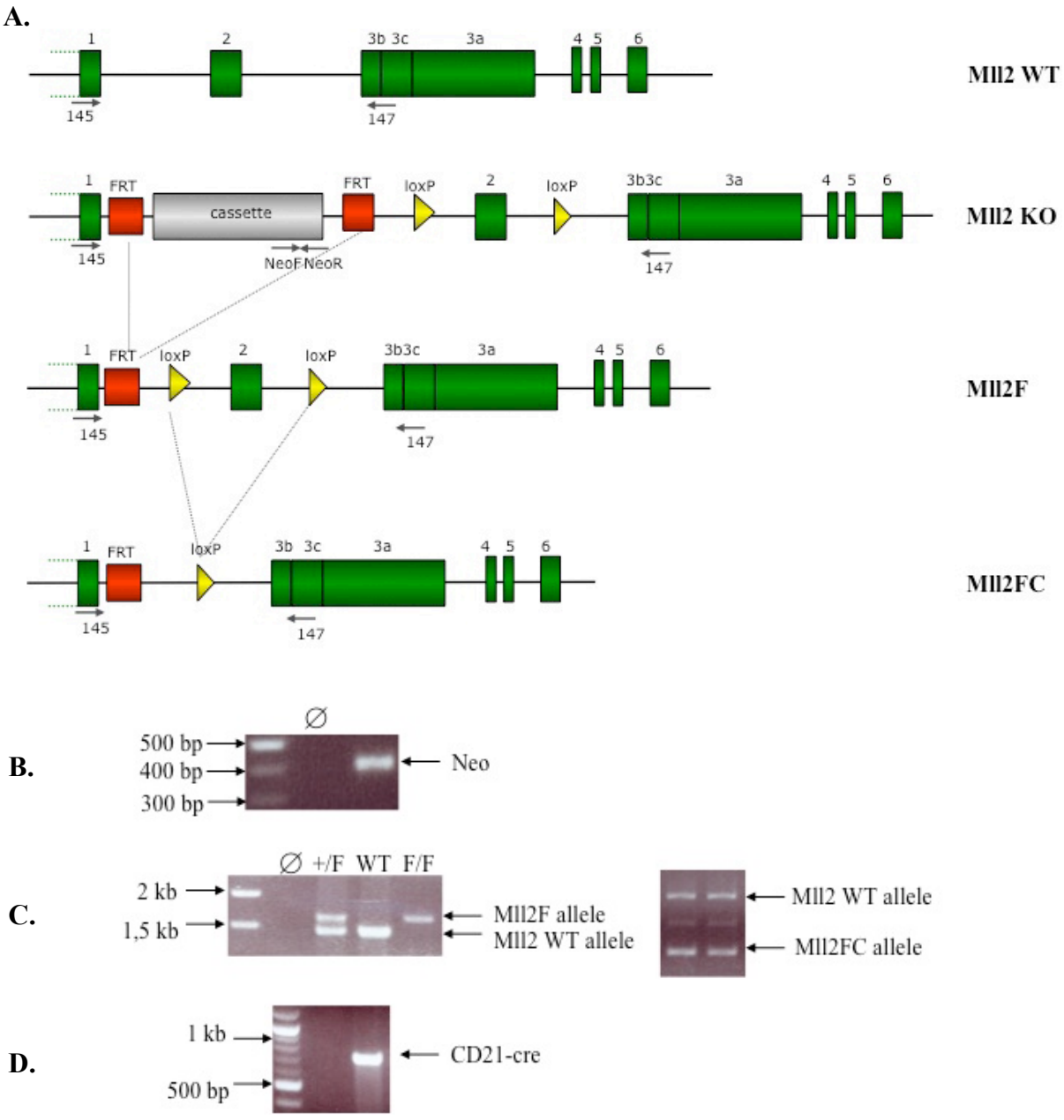

Figure 7. Genotyping of Mll2/F/CD21-Cre mouse line using PCR reaction; A. Schematic representation of genotyping strategy; **B**. PCR products of the reaction with primers Neo F – Neo R (421 bp) **C**.PCR products of the reaction with primers 145 – 147: wild type (1441bp), Mll2F (1618 bp) and Mll2FC (760 bp) alleles; **D**. PCR products of the reaction with primers 19 – 20: CD21-cre allele (743 bp); **Ø** – negative control, **Mll2 WT** – wild type Mll2, **Mll2 KO** – Mll2 straight knock out allele, **Mll2F** – Mll2 conditional knock out allele, **Mll2FC** – Mll2 frameshifted knock out allele

2.2.10 Reverse transcription PCR (RT – PCR)

RT – PCR generates cDNA fragments from RNA templates and is a technique to determine the expression of genes in specific tissues or in different development stages. 1 – 5 µg of total RNA was mixed with 1 µl of random primers (10 pmol/µl) and 1 µl of dNTPs (10mM) in a total volume 13 µl. To disrupt secondary structures of RNA, which might interfere with the synthesis, the mixture was heated to 65˚C for 5 min, and quickly chilled on ice for 2 min. After a brief centrifugation, the followings were added to the mix:

4µl	5x First standard buffer
1µl	0,1M DTT
1µl	RNaseOUT™
2 µl	SuperScript™ III Reverse Transcriptase

The content of the tube was mixed gently and incubated 50˚C for 1h for the first strand cDNA synthesis. Next, the reaction was inactivated by heating at 70˚C for 15 min.
One µl of the first strand reaction was used for the PCR (2.2.8) or Q-PCR (2.2.10) reactions.

2.2.11 Real Time PCR (qPCR)

Real Time PCR called also Quantitative PCR (qPCR) enables both detection and quantification (as absolute number of copies or relative amount when normalized to DNA input or additional normalizing genes) of targeted DNA sequence(s) and therefore has found brought application in both diagnostic and basic research. The procedure follows the general

principle of PCR. Its key difference however is that the amplified DNA is detected as the reaction progresses in real time, in contrast to the standard PCR, where the product of the reaction is detected at its end. Detection of products in real-time PCR is carried with use non-specific fluorescent dyes (such as SYBR green) that intercalate with any double-stranded DNA, or sequence-specific DNA probes consisting of oligonucleotides that are labeled with a fluorescent reporter which permits detection only after hybridization of the probe with its complementary DNA target. An increase in DNA product during PCR leads to an increase in fluorescence intensity and is measured at each cycle, thus allows quantification of the DNA concentrations.

qPCR reactions with use of primers were run in the following mix:

12,5 µl	2x SYBR® Green PCR Master Mix
0,5 µl	forward primer (10 µmol)
0,5 µl	reverse primer (10 µmol)
X[4] µg	cDNA
up to 25 µl	miliQ H_2O

A standard SYBR® Green qPCR programme is shown here:

AmpErase® UNG activation	50°C	2min
AmpliTaq Gold® DNA Polymerase activation	95°C	10min
and UNG inactivation		
(35 cycles) Denaturation	95°C	15sec

[4] 5µg of cDNA

Annealing and Elongation	60°C	1min

TaqMan qPCR reactions were run in the following mix:

7,5 µl	TaqMan PCR Mastermix
0.75	TaqMan Gene expression assay 20x
	template[5]
up to 15 µl	miliQ H_2O

A standard TaqMan qPCR programme is shown here:

AmpliTaq Gold® DNA Polymerase activation	95°C	10min
and UNG inactivation		
(40 cycles) Denaturation	95°C	15sec
Annealing and Elongation	60°C	1min

qPCR reactions were run using the ABI PRISM® 7900 Fast Real Time PCR System and ABI PRISM® 7900HT Sequence Detection System (Applied Biosystems) and analyzed with the SDS Software 2.3 (Applied Biosystems). Each sample was analyzed in triplicates. When cDNA was used as the template qPCR data were normalized to TATA-Binding Protein (Tbp) as endogenous control. In case of analysis of genomic DNA template samples were normalized to Telomerase Reverse Transcriptase (Tert). Normalization was used to correct sample-to-sample variations in RNA concentration and integrity. Relative mRNA amounts were calculated by the comparative cycle threshold (Ct) method using the formula

[5] 5µg of cDNA or 10 - 20µg of genomic DNA

$2^{-\Delta Ct}$. qPCR reactions were performed by Real Time PCR Unit of Cogentech on the IFOM-IEO-Campus, Milan (Italy).

2.2.12 Blotting techniques

2.2.12.1 Southern Blotting of DNA onto nitrocellulose membrane

(Southern, 1975)

A Southern blot allows detection of a specific DNA sequence in DNA samples. Southern blotting combines transfer of electrophoresis-separated DNA fragments to a filter membrane and subsequent fragment detection by probe hybridization. In Southern blotting, the transfer of DNA from agarose gels to nitrocellulose membrane is achieved by capillary flow and gravity force. 20x SSC buffer, in witch nucleic acids are highly soluble, is drawn up through the gel into nitrocellulose membrane, taking with in DNA that becomes immobilized in the membrane matrix.

Following gel electrophoresis digested genomic DNA was transferred as bellow (in order from the top):

20xSSC buffer in the gutter of blotter	
2x Whatman paper (GB 002) (bridge)	20x SSC
4x Whatman paper (GB 002)	20x SSC
Agarose gel with DNA	2xSSC
Nitrocellulose membrane	2x SSC
4x Whatman paper (GB 002)	20x SSC
40 Whatman paper (GB 002)	dry

DNA was purified (2.2.1.3), digested with PstI enzyme (2.2.5.2) and subsequently separated by electrophoresis in a 1% agarose gel (2.2.3.1) (without Ethitium bromide). Prior to blotting DNA fragments were denaturated by washing 3 times for 15 min at room temperature (RT) in Denaturation buffer (2.1.2.1.). All Whatman filter paper (GB 002) were soaked with 20x SCC buffer. Gel was washed shortly in 2x SSC buffer and nitrocellulose membrane was soaked with 2x SSC buffer for 10min. Transfer was carried for overnight at RT. Finally after disassembling of the blot, DNA was fixed into membrane by baking for minimum 2 hrs at 80˚C.

2.2.12.2 Western Blotting of proteins onto nitrocellulose membrane

(Gershoni and Palade, 1982)

Following electrophoresis in a SDS – PAGE gel (2.2.3.2) proteins were blotted onto nitrocellulose membrane as described below (in order from the top):

2x Extra thick blot paper Protean®

SDS – PAGE gel with proteins

Protran® membrane

2x Extra thick blot paper Protean®

All paper sheets (Protean®) and membrane were cut out for the size of the gel. All Whatman paper sheets were soaked in transfer buffer; membrane was soaked in transfer buffer for 10 min. The SDS – PAGE gel with proteins was washed shortly in transfer buffer. Transfer was carried out according to the 2.2.3.2 protocol.

To asses transfer efficiency of proteins onto nitrocellulose membrane, the gel was incubated 1h in Coomasie blue staining solution at RT with shaking and next in Coomasie blue destaining solution at RT with shaking. Stained gel was closed in plastic bag and stored at 4ºC.

2.2.13 "Random Prime" method for generation of 32P labelled DNA

(Denhardt, 1966; Feinberg and Vogelstein, 1983)

2.2.13.1 Random Prime" method for generation of 32P labelled DNA using Rediprime™ II Random Prime Labelling System

Rediprime™ II Random Prime Labelling System (Amersham Pharmacia) was used for labelling of DNA probes. The method depends on the random priming principle developed by Feinberg and Vogelstein (1989). The reaction mix contained dATP, dGTP, dTTP, Klenow fragment (4 – 8 U) and random oligodeoxyribonucleotides. Firstly, 25 – 50 ng of DNA were denatured in a total volume of 46 µl at boiling water for 10 min and quick chilled on ice for 5 min. After pippeting denatured probe to Rediprime™ II Random Prime Labelling System cup, 5 µl pf [α-32P]dCTP (50µCi) was added to the reaction mixture. The labelling reaction was carried out at 37˚C for 1 hr. The labelled probe was purified from unincorporated [α-32P] dCTP by using ProbeQuant™ G-50 Micro Columns (GE Healthcare)..

2.2.13.2 Random Prime" method for generation of 32P labelled DNA using Ladderman™ labelling Kit

Principle of the method is similar to the previously described (2.2.12.1). The reaction mix was the following:

Probe	100 ng
Random Primers	2 µl
H_2O	up to 14 µl

Probe was denatured for 5 min and quickly chilled on ice for 5 min. And following reagents were added:

10x buffer	2,5 µl
dNTPs	2,5 µl
[α-32P]dCTP	5 µl (50 µCi)
DNA polymerase	1 µl

and mixed by pipetting. The labelling reaction was carried out at 55˚C for 1 hr after which 100 µl of H_2O were added and the labelled probe was purified from unincorporated [α-32P] dCTP by using ProbeQuant™ G-50 Micro Columns (GE Healthcare).

2.2.14 Hybridization of nucleic acids

(Denhardt, 1966)

The membrane to be hybridized was equilibrated in 2x SSC for 10 min and transferred into hybridization bottle. 10 ml of 1x PerfectHyb™ Plus Hybridization Buffer (Sigma) was wormed up to 65˚C. Membranes were prehybridized 1 hr at 65˚C. The labelled probe (2.2.12) was denatured at 95˚C for 5 min and quick chilled on ice for 5 min and added into the hybridization bottle. Hybridization was carried out overnight at 65˚C in the oven. On the following day, the membranes were washed for 15 min with Washing buffers (I – III) (2.1.2.1.6) at 65˚C, 15 – 20 min each. After drying the membranes were sealed in plastic bag

and exposed to Storage phosphor screen (Amersham Bioscence) for at least 24h. The radioactive signal was visualized using Typhoon TRIO (GE Healthcare) and Typhoon Scamner Control v.5.0 (GE Healthcare) and Photoshop CS3 10.0.1 (Adobe System).

2.2.15 Protein methods

2.2.15.1 Isolation of total protein from eukaryotic cells

Cells were collected in the eppendorf or Falcon tube, centrifuged for at 335 *g* for15min at RT. Cell lysis was performed using lysis buffer (2.1.2.1.5) for 25 min at RT. Lysed cells were sonicated 3 times for 45 sec (with 1 min of pause between cycles on ice) with water bath sonicator Bioruptor™ UCD-200 (Diagenode) and subsequently centrifuged at 16.000 *g* for 20 min at 4˚C. Supernatant was transferred into a new tube and stored at -80˚C.

2.2.15.2 Determination of protein concentration

To determine the protein concentration, Bio – Rad protein assay was employed which is a dye-binding assay based on differential colours change of a dye in response to various concentration of protein. The assay is based on the observation that the absorbance maximum for an acidic solution of Coomasie Blue G – 250 shifts from 494 to 595 nm when the binding to proteins occurs. The bovine serum albumin (BSA) stock solution of 1 mg/ml was diluted in order to obtain standard dilutions in range of 1 µg/ml to 10 µg/ml. The Bradford (Bio-Rad) reagent was diluted 1 : 5 with H2O and filtered through 0,45 µm filters. 2 of a sample were mixed with 1 ml of Bradford solution and transferred into a cuvette. As a blank sample 2 µl of

lysis buffer were mixed with the Bradford solution. The absorption of the colour reaction was measured at 595 nm in DU® 730 Spectrophotometer (Beckman Coulter®).

2.2.15.3 Incubation of protein – bound membranes with antibodies

After the electrophoretical separation on SDS-PAGE gel (2.1.2.1.7.1), proteins were transferred onto nitrocellulose membrane using Transblot® SD Semi-dry transfer cell (Bio-rad) in Transfer buffer. Next, the membranes were blocked in Blocking buffer (2.1.2.1.7.2) for 1 hr at RT with shaking in order to block unspecific bind sites and incubated with primary antibody diluted in Blocking buffer, overnight at 4˚C. On the following day the membranes were washed three times, 5 min each, with TBST buffer at room temperature. A secondary antibody was applied, with which the membrane was incubated for 1 hr at room temperature. The membrane was washed three times as described abouve and proteins were detected using ECL Plus Western Blotting Detection System (Amersham GE Healthcare) and subsequently visualised on Hyperfilm™ ECL (Amersham GE Healthcare).

2.2.16 Enzyme-Linked Immunosorbent Assay (ELISA)

(Engvall and Perlmann, 1971)

Enzyme-Linked Immunosorbent Assay (ELISA) methods are immunoassay techniques that, by combining the specificity of immunological reaction with the sensitivity of enzyme assays allow detection and quantification of a substance (immunoglobulin or antigen). One of the most common application of this method is to measure the amount of an immunoglobulin anti-antigen of interest in blood serum.

Coating was performed overnight at 4˚C in Coating buffer (2.1.2.1.3). The concentration of antibodies and antigen used for coating is listed in the table below.

antibodies/antigene	concentration
Goat-anti Mouse IgG3	1 : 100
Goat-anti Mouse IgM	1 : 100
NP_{23} - CGG	1 µg/ml
BSA	1 µg/ml

ELISA based quantification of anti NP-Ficoll IgM and IgG3 in blood serum of immunized mice (2.2.18) was performed according to the Bethyl ELISA Protocol supplied with Mouse IgM / IgG3 ELISA Quantitation Set. Absorbance measurement was performed using Victor^{3} ™ 1420 Multilabeled Counter and Wallac 1420 Workstation Software (Perkin Elmer™).

2.2.17 Immunostaining techniques

2.2.17.1 Immunostaining of cells for flow cytometry and fluorescence-activated cell sorting (FACS).

In order to analyze lymphocytes by flow cytometry, cells from different lymphoid organs were isolated in the B cell medium (2.1.1.8). Samples from spleen and bone marrow were subjected to erythrocyte lysis by incubating them in the Gey's solution (2.1.1.4.1) for 5 min on ice. Lysis was stopped by adding 40 ml of B cell medium to the sample. Next cells were centrifuged at 335g for 15 min, at 4˚C and diluted in FACS buffer (2.1.1.4.1). Live cells were counted with Trypan blue and 1 mln cells were used for each staining. Cells were stained in 100µl of FACS buffer containing antibodies of choice for 20 min at 4˚C in darkness and subsequently washed

twice with 200µl of FACS buffer and fixed with Fixing solution (2.1.1.4.1). For FACS analysis cells were prepared in the similar way. The volume of staining mixture used for FACS was 20 µl/ 1 mln of cells. Antibodies for both flow cytometry and FACS is listed in table below. Samples were acquired and analyzed using FACSCAlibur (BD Biosciences) and CellQuestPro software.

antibodies	concentration
Monoclonal Mouse-anti BrdU (FITC)	1 : 50
Monoclonal Mouse-anti BrdU (APC)	1 : 50
CD1d (FITC)	1 : 300
CD4 (PE)	1 : 400
CD5 (PE)	1 : 200
CD8 (FITC)	1 : 100
Monoclonal Rat-anti mouse CD19 (Cy7 PE)	1 : 250
Monoclonal Rat-anti mouse CD21/CD35 (FITC)	1 : 100
Monoclonal Rat-anti mouse CD23 (PE)	1 : 200
Monoclonal Rat-anti mouse CD38 (APC)	1 : 200
Monoclonal Rat-anti mouse CD38 (FITC)	1 : 200
Monoclonal Rat-anti mouse CD43 (PE)	1 : 200
Monoclonal Rat-anti mouse/human CD45R(B220) (FITC)	1 :200
Monoclonal Rat-anti mouse/human CD45R(B220) (Cy7PE)	1 : 200
Monoclonal Mouse-anti mouse CD45.1 (Ly5.1) (FITC)	1 : 200
Monoclonal Mouse-anti mouse CD45.2 (Ly5.2) (APC)	1 : 200
CD93 (AA4.1) (PE)	1 : 250
CD95 (Fas)	1 : 150
IgM Alexa 488	1 : 500
Monoclonal Rat-anti mouse IgD (PE)	1 : 600
Streptavidin (APC)	1 : 500
Streptavidin (FITC)	1 : 400

2.2.17.2 Immunostaining of cells for magnetic-activated cell sorting (MACS®)

(Miltenyi Biotec)

Magnetic-activated cell sorting (MACS®) is a method for separating various cell populations on the basis of their surface antigens. Depending on the purposes of the experiments cells of interest can be separated positively or negatively.

In order to analyze lymphocytes by flow cytometry, cells from different lymphoid organs were isolated in the B cell medium (2.1.1.8). Samples from spleen and bone marrow were subjected to erythrocyte lysis by incubating them in the Gey's solution (2.1.1.4.1) for 5 min on ice. Lysis was stopped by adding 40 ml of B cell medium to the sample. Next cells were centrifuged at 335g for 15 min, at 4˚C and diluted in FACS buffer (2.1.1.4.1). Live cells were counted with using Trypan blue and 10^6 cells were used for each staining. The MACS® - based cell separation was performed according the Miltenyi Biotec protocol supplied with CD19 MicroBeads Kit and Pan T Cell Isolation Kit. All staining and column washing were done in MACS® buffer (2.1.2.1.4.2).

2.2.17.3 Immunofluorescence

Spleen section preserved in O.C.T Compound (Tissue-Tek) were cut in 6µm thick slices and placed on Microscope Slides Superfrost ultra Plus® (Thermo Scientific). Samples were fixed with cold Fixing solution (2.1.2.1.4.3) for 20 min at room temperature, washed 3 times in PBS, 10 min each and subsequently blocked with blocking solution (2.1.2.1.4.3) for 1h at room temperature and washed again 3 times in PBS, 10 min each. A primary antibody was applied in the blocking solution for 1 h at room temperature. Next samples were washed as previously described and a secondary antibody was applied for 1 h at room temperatures in

darkness. After incubation with the secondary antibody samples were washed 3 times in PBS, 10 min and DAPI was applied for 5 min at room temperature, in darkness and again washed as described above. Covered glass was mounted with a use of moviol. Concentration of antibodies used in the immunofluorescence staining is indicated in the table below. Samples were acquired using Confocal Microscope TCS SP2 AOBS (Leica) and analyzed with ImageJ 1.42q software.

antibodies	concentration
IgM Alexa 488	1 : 300
Monoclonal Rat-anti mouse Macrophages MOMA-1(biotin)	1 : 100
Monoclonal Rat-anti mouse/human CD45R(B220) (FITC)	1 : 200
Monoclonal Rat-anti mouse Macrophages MOMA-1(biotin)	1 : 10
Streptavidin (Cy5)	1 : 200
DAPI	1: 1500

2.2.18 *In vitro* proliferation assay

Thanks to the covalent character of binding between Carboxyfluorescein succinimidyl ester (CFSE), a fluorescent dye, and intracellular molecules it is possible to track a stained cell up to 8 divisions hence it is possible to study cell viability and proliferation.

Lymphocytes from spleen were isolated in the B cell medium (2.1.1.8). Erythrocyte were lysed by incubating sample in Gey's solution (2.1.1.4.1) for 5 min on ice. Lysis was stopped by adding 40 ml of B cell medium to the sample. Next cells were centrifuged at 335g for 15 min, at 15˚C and live cells were counted with Trypan blue. B cells were separated using CD19 MicroBeads Kit according the Miltenyi Biotec protocol supplied the kit (2.2.16.2). Cells were stained with CFSE for 10 min at room temperature. Concentration of CFSE used for staining was 1μM. The staining reaction was stopped by adding B cell medium, next cells were

centrifuged at 335g for 15 min and counted as previously. Cells were plated at the concentration 1 mln/ml in the duplicates in the medium containing LPS (20 μg/ml)) and Il-4 (10pg/μl). Cells were counted daily for 4 consecutive days. At day 2, 3 and 4 cells were stained as indicated in the table below. Samples were analyzed by flow cytometry (2.2.17.1) using FACSCAlibur (BD Biosciences) and CellQuestPro software.

antibodies	concentration
IgG1 APC	1 : 500
CD19 Cy7 PE	1 : 200
CD138 PE	1: 200

2.2.19 *In vivo* immunization of mice with NP-Ficoll

Mice were immunized by intraperitoneal application with 50μg of NP-Ficoll diluted in sterile PBS. Blood serum samples were taken at the day 0 (immediately prior immunization), 3rd, 7th, 14th, 21st and 28th. Changes of the level of NP-Ficoll specific immunoglobulins and their class switch were approached by ELISA (2.2.16).

2.2.20 *In vivo* BrdU labelling

BrdU was administrated in drinking water at the concentration 0,8mg/ml. 5 % of Glucose was added and the BrdU-Glucose solution was filtered using 0,22μm Stericups. BrdU was applied for 28 days to age and sex matched controlled and mutant mice. Cells were analyzed on the days 7, 14 and 28 by flow cytometry according the staining indicated in the table below. BrdU staining was performed according the BrdU Flow Kit Staining Protocol supplied with BrdU

Flow Kit (BD Pharmingen™) Samples were analyzed by FACS (2.2.17.1) using FACSCAlibur (BD Biosciences) and CellQuestPro software.

lymphoid organ	antibodies	concentration
bone marrow	BrdU FITC	1 : 50
	CD43 PE	1 : 200
	B220 Cy7 PE	1 : 200
	IgM APC	1 : 400
spleen	CD21 FITC	1 : 100
	CD23 PE	1 : 200
	CD19 Cy7 PE	1 : 200
	BrdU APC	1 : 50

2.2.21 Microarray profiling of marginal zone B cell gene expression in Mll2KO/F/CD21-Cre line

A microarray is a multiplex technology that enables a expression profiling of thousands genes or transcripts in a single sample as well as in different tissues and cell types. There are a variety of microarray platforms that have been developed to accomplish this. Their common feature is a glass slide or membrane spotted (arrayed) with DNA or RNA probes or as used in this work silicone chip GeneChip® Mouse Gene 1.0 ST Array (Affymetrix). In order to quantitate transcriptome of a sample first, cDNA synthesized from total RNA extracted from the sample is labeled and next hybridized to a microarray platform. Laser excites the dye, which fluoresces are proportional to the degree of hybridization that has occurred. Relative gene expression is measured as the difference in fluorescence intensity between control and mutant. Upregulation of the experimental transcriptome relative to the control is visualized as one (green) pseudo-colour, while downregulation is shown as another one (red), and

constitutive expression (1:1 mutant versus control) as a neutral (gray). Intensity of fluorescence is proportional to the difference in the expression.

Total RNA from control and mutant samples was purified in parallel using RNeasy® Plus Micro Kit (QIAGEN). cDNA synthesis and biotinylation as well as hybridization and analysis was performed by Affymetrix Microarray Unit of Cogentech on the IFOM-IEO-Campus, Milan (Italy) according to the indications of Affymetrix[6]. Statistical analysis was done using Partek GS 6.5 (Partek, 2008) software.

2.2.22 Computer analysis

For the analysis of the nucleotide sequences, standard programs like BLAST (Altschul et al. 1990), BLAST2 (Tatusova et al. 1999), and related softwares from the National Center for Biotechnology Information (NCBI) were used. Information about mouse gene sequences and other analysis of genes, transcript and proteins were downloaded from Jackson Laboratory (Begley and Ringwald 2002; Blake et al. 2003) and from Sanger Institute (Hubbard et al. 2005). For restriction analysis of DNA NEBcutter V2.0 program (Vincze et al. 2003) and REBASE (Roberts et al. 2005) were used. For proteins studies ExPASy tools (Gasteiger et al. 2003) were used. Mll2 gene trap constructs were analysed using Gene Construction Kit® 2.5 (Textco BioSoftware). Flow cytometry and FACS data were acquired and analyzed using CellQuest Pro v5.2.1 (BD Biosciences). Microscope data analysis was done using ImageJ 1.42q (Burger and Burge, 2007). Southern blot were visualised and analysed using Typhoon Scamner Control v.5.0 (GE Healthcare) and Photoshop CS3 10.0.1 (Adobe System). ELISA data were acquired and analysed with a use of Wallac 1420 Workstation software (Perkin Elmer). qPCR analysis was performed using SDS Software 2.3 (Applied Biosystems).

[6] (http://www.affymetrix.com/support/technical/manual/expression_manual.affx).

3. Results

3.1 Experimental system

The rationale of choice of B cell lymphopoiesis as an experimental system was confirmed in a scrupulous analysis of the expression of Mll2 throughout B cell development. Expression of Mll2 was analysed in various mouse tissues and at the different stages of B cell maturation as well as in the different subpopulation of mature B cells in wild type animals (Fig. 1 and 2).

3.1.1 Mll2 conditional knock out and CD21-Cre mouse lines

In order to study role of Mll2 in mature differentiated cells it is necessary to overcome the embryonic lethality of Mll2 deletion (Glaser et al., 2006). Therefore to investigate the function of Mll2 in the mature B cell compartments, I chose a conditional mutagenesis approach. In order to knock out Mll2 specifically in mature B cells I selected the CD21-Cre3A mouse line that expresses Cre recombinase under the CD21 promoter. The line was established by inserting Cre gene into CD21/35 locus on a bacterial artificial chromosome (Kraus et al., 2004). The expression of CD21 and Cre recombinase proteins and in the consequence Cre-mediated deletion occur at the moment of the transition from immature B into long-lived mature B cell (Kraus et al., 2004; Takahashi et al., 1997) (Fig. 5 and 6).
Combining the conditional knock out strategy (Glaser et al., 2009; Testa et al., 2004) and the B lymphocyte development stage specific Cre expressing line, I generated a line in which for the very first time an epigenetic regulator was ablated specifically in mature B cell compartments.

3.1.2 Generation Mll2KO/Mll2F/CD21-Cre line - breeding strategy

In order to set up the experimental mouse cohorts, mice heterozygous for the Mll2 straight knock-out allele (Mll2 KO; Fig 4) were bred with mice heterozygous for the CD21-Cre allele (Fig. 5). Offspring positive for both Mll2 KO allele and CD21-cre allele (Mll2KO/CD21-cre) (Fig. 4, 7 and 8) was further bred to mice homozygous for the Mll2F conditional allele. For experimental procedures I chose mice that carried homozygous Mll2 conditional knock out allele and expressing CD21-Cre (Mll2KO/Mll2F/CD21-Cre) (Fig. 4, 5, 7 and 8). As demonstrated further in a careful analysis, mice homozygous for the Mll2 conditional knock-out allele in both forms: Mll2KO/Mll2F and Mll2F/Mll2F show similar phenotype, therefore for the experiment procedures were chosen both allelic conditions. As a control I used heterozygous Mll2 conditional knockout mice positive for CD21-Cre (+/Mll2F/CD21-Cre) (Fig. 4, 5, 7 and 8). Control and mutant animals used in all experiments were always sex-matched littermates. For simplification Mll2KO/Mll2F/CD21-Cre line will be further called Mll2KO/F/CD21-Cre line, while Mll2KO/Mll2F/CD21-Cre, Mll2F/Mll2F/CD21-Cre and +/Mll2F/CD21-Cre mice will be further named Mll2KO/F/CD21-Cre and Mll2F/F/CD21-Cre (mutant) and +/F/CD21-Cre (control) respectively (Fig. 8).

It is important to mention that mice heterozygous for Mll2 KO allele were backcrossed with the C57BL/6J line in order to obtain a line of a pure genetic background. Mice hetero- and homozygous for Mll2F allele were not backcrossed and therefore were of a mixed C57BL/6J and Sv-129 background[1]. Line CD21-Cre3A was of a pure C57BL/6J background (Takahashi et al., 1997). In the consequence, obtained Mll2KO/Mll2F/CD21-Cre line was of partially mixed C57BL/6J and Sv-129 background. Therefore, in order to obtained reliable results I analyzed large number of animals. Due to the fact that heterogeneity of the genetic background is associated with the presence of Mll2F allele

[1] Personal information – Dr. Giuseppe Testa

Mll2F/F/CD21-Cre cohort has higher percentage of Sv-129 background, and in the consequence more mixed background, than Mll2KO/F/CD21-Cre. This observation should be taken into account while interpreting the results.

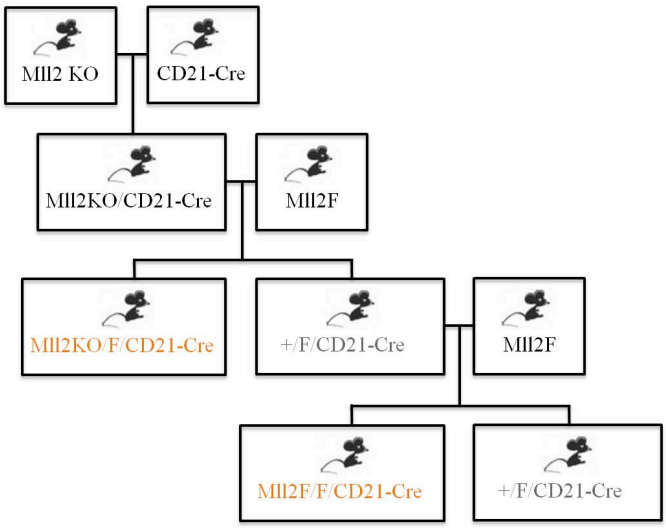

Figure 8. Schematic representation of breeding strategy - generation of Mll2KO/F/CD21-Cre line. Mll2 KO – knock out allele (heterozygous), **Mll2F** – Mll2 conditional allele (homozygous), **CD21-Cre** - CD21-Cre3A, **Mll2KO/F/CD21-Cre** and **Mll2F/F/CD21-Cre** - mutant (**orange**), **+/F/CD21-Cre –** control (**grey);** Detailed description in the text (3.1.2)

3.2 Analysis of CD21-Cre - mediated deletion of Mll2

It order to validate that observed phenotype is due to the ablation of Mll2 in mature B lymphocytes and the same to ensure reliability of following results it is essential to control the occurrence and specificity of Mll2 CD21-Cre mediated deletion. I assessed the Mll2 deletion in Mll2KO/F/CD21-Cre line by Southern blot (3.2.2; Fig. 9 and 11) and qPCR analysis of genomic DNA from different lymphoid organs and confirmed its restriction to the mature B cells.

3.2.1 Generation of Mll2F/PGK-Cre line

With a purpose of generating a reliable reference of the occurrence of CD21-Cre mediated deletion of Mll2 flexed allele, I bred mice homozygous for the Mll2 floxed allele (Mll2F) to the PGK-Cre mouse strain expressing Cre recombinase ubiquitously under the PGK promoter (Lallemand et al., 1998). Hence, in the offspring (Mll2F/PGK-Cre), Mll2F allele is expected to be deleted in all cell types. Through one more round of breeding with C57BL/6J line, I segregated the Cre-recombined Mll2 allele and obtained a reference control mouse heterozygous in all cells for the recombined Mll2FC allele (Fig. 4). Genomic DNA from this mouse served then as standard to assess the degree of Cre-mediated deletion in the further experiments.

To confirm the PGK-Cre mediated deletion 10µg (2.2.2) of genomic DNA was digested using PstI enzyme (2.2.5.2). DNA fragments were electrophoretically separated on 1% gel without Ethidium bromide (2.2.3.1) and subsequently blotted onto nitrocellulose membrane (2.2.12.1). Blotted DNA was hybridized with labeled (2.2.13) Probe C (2.1.11). The bands of 3542 bp and 3440 correspond to the MllF and Mll2 wild type alleles respectively. The band of 2684 bp corresponds to the Mll2FC allele (Fig. 10). Schematic representation of Southernblot strategy is shown in Figure 9.

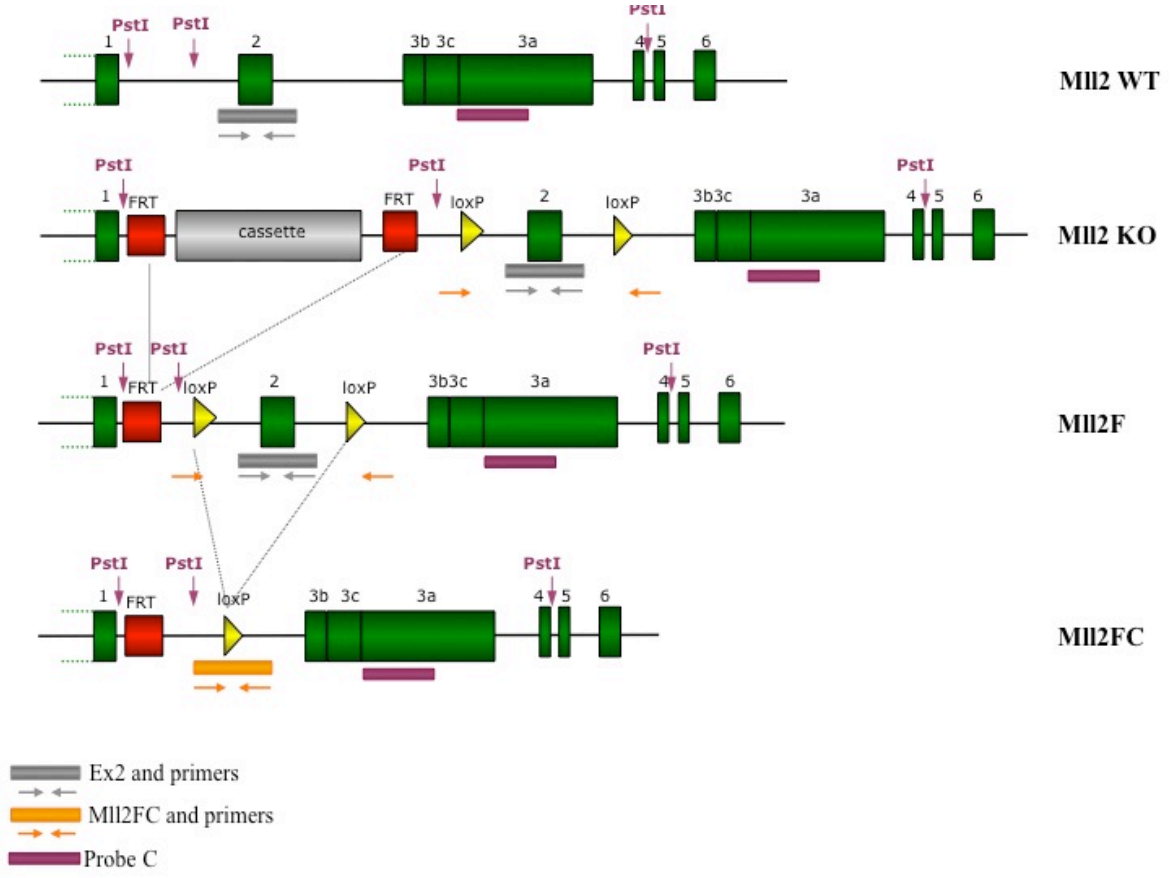

Figure 9. Schematic representation of TaqMan qPCR and Southernblot strategies. Schematic representation of the Taqman qPCR probes localization: **grey** – probe Ex2 and its primers, **orange** – probe Ex2 and its primers; Schematic representation of localization of probe C **(purple)**; **Mll2 WT** – wild type Mll2, **Mll2 KO** – Mll2 straight knock out allele, **Mll2F** – Mll2 conditional knock out allele, **Mll2FC** – Mll2 frameshifted knock out allele

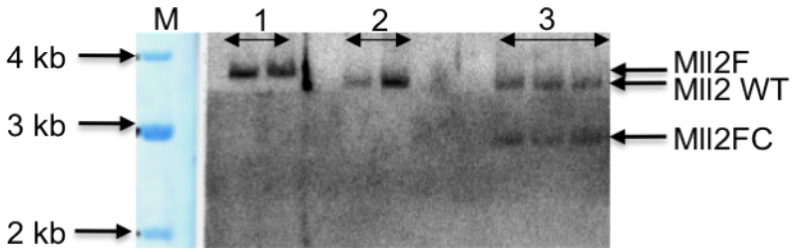

Figure 10. Southern blot analysis of Cre-mediated deletion of the Mll2F allele in Mll2F/PGK-Cre line. **M** – 1 kb DNA marker stained with Methylene blue, **1** – Mll2F homozygous, **2** - PGK-Cre , **3** – Mll2F/PGK-Cre genomic DNA, **Mll2 WT** - Mll2 wild type allele, **Mll2F** – Mll2 conditional knock out allele, **Mll2FC** – Mll2 Cre-recombined frame shifted allele (Fig. 4 and 9).

3.2.2 Southern blot analysis of the CD21-Cre - mediated deletion in different lymphoid organs

I accessed the occurrence and specificity of the Mll2 CD21-Cre mediated deletion by Southern blot. 10µg (2.2.2) of genomic DNA isolated from the lymphoid organs - bone marrow (BM), spleen (SP), mesenteric lymph nodes (MLN), Peyer's patches (PP), thymus (T) and peritoneal cavity (PC) was digested with PstI, resolved on 1% gel without Ethydium bromide and subsequently blotted onto nitrocellulose membrane, which was then hybridized with Probe C (2.1.11). As predicted we can observe the 2684 bp fragment corresponding to the Mll2FC allele only in the spleen, mesenteric lymph nodes, Peyer's patches and peritoneal cavity (Fig. 11 – lane SP, MLN, PP, PC). Consistent with the mature B cell restricted Cre expression pattern in the CD21-Cre line, the Mll2FC allele was not detected either in the bone marrow or in the thymus (Fig 11 – lane BM and T). The bands of 4325 bp and 3542 bp correspond to the Mll2 KO and Mll2F alleles respectively.

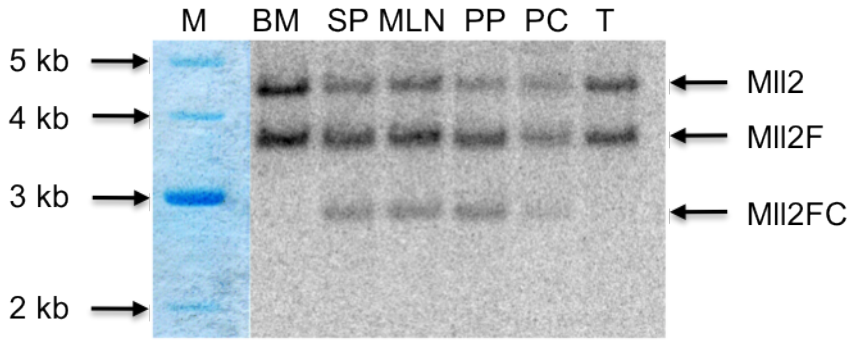

Figure 11. Southern blot analysis of Mll2 Cre-mediated deletion in the Mll2KO/F/CD21-Cre line. M – 1 kb DNA marker stained with Methylene blue, **BM** – bone marrow, **SP** – spleen, **MLN** – mesenteric lymph nodes, **PP** – Peyer's patches, **PC** – peritoneal cavity, **T** – thymus, **Mll2** - Mll2 knock-out first allele, **Mll2F** – Mll2 conditional knock out allele, **Mll2FC** – Mll2 frame shifted allele (Fig. 4). Schematic representation of Southernblot strategy is shown in Figure 9.

3.2.3 qPCR analysis of the CD21-Cre - mediated deletion in Mll2KO/F/CD21-Cre line

With a purpose of developing the fast and reliable strategy of detection CD21-Cre - mediated deletion, I designed TaqMan qPCR probes that allow to score at the genomic level the occurrence and level of Mll2 deletion. Thanks to its high sensitivity, the qPCR method requires low amount of the template, therefore allows detection of the Cre-mediated deletion also in sorted lymphoid subpopulations. Probes were designed in order to detect the presence of exon 2 (probe Ex2) and a unique sequence that is generated by Cre mediated deletion (probe Mll2FC). Primers for the first probe are localized before and after the exon 2. Forward primer of probe Mll2FC comprises the sequence before the first loxP site and its first half, while the sequence of the reverse primer consists of the second half of the second loxP site and the sequence after it (Fig. 9 and 12 A).

qPCR was performed with TaqMan probes on genomic DNA isolated from bone marrow (BM), spleen (SP), Peyer's patches (PP), and thymus (T) cells and a fragment of a tail. As shown in Figure 12 B, Cre-mediated deletion occurred only in the spleen and Peyers' patches. The deletion was not detected either in bone marrow or thymus or tail, confirming the restriction of the deletion only to the CD21 expressing cell types – mature B cells (Fig. 11 and 12 B). It is important to highlight that the qPCR analysis was done on the genomic DNA from total cells of each organ, hence the still present expression of exon 2 (probe Ex2 – grey) in SP and PP is expected. The occurrence of Cre- mediated deletion on genomic DNA from sorted lymphocytes was analyzed further (3.2.4; Fig. 13)

So high level of the sequence detected by Mll2FC probe (orange) in comparison to the sequence detected by probe Ex2 (gray) is due to the different efficiency of both reactions. Therefore there simple correlation between levels of expression of both probes is not warranted.

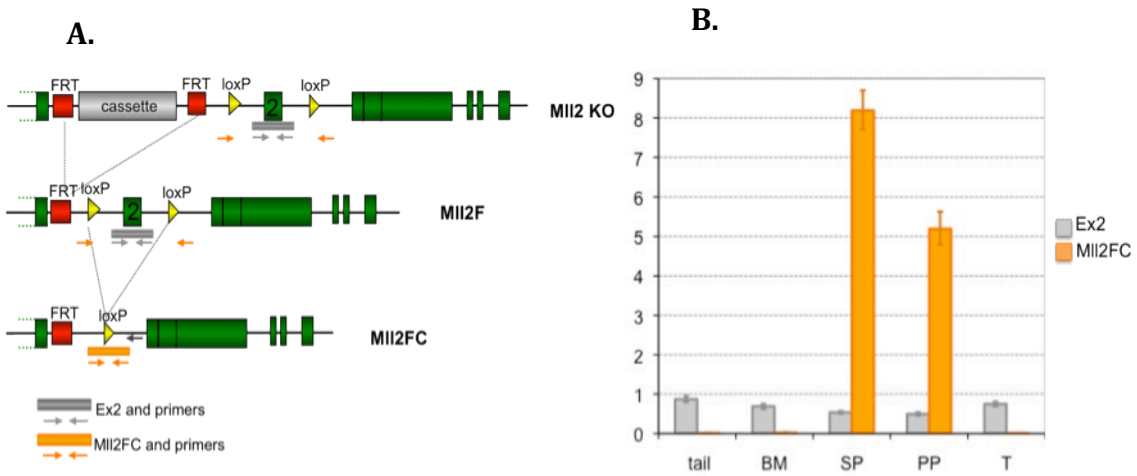

Figure 12. qPCR analysis of the Cre-mediated deletion in MllKO2/F/CD21-Cre line. A. Schematic representation of the TaqMan qPCR probes localization: **grey** – probe Ex2 and its primers, **orange** – probe Mll2FC and its primers; **Mll2 KO** – Mll2 straight knock out allele, **Mll2F** – Mll2 conditional knock out allele, **Mll2FC** – Mll2 frameshifted knock out allele; **B.** qPCR analysis of the Cre-mediated deletion in Mll2/F/CD21-Cre line **BM** – bone marrow, **SP** – spleen, **PP** – Peyer's patches, **T** – thymus, **Ex2** – probe detecting exon 2, **Mll2FC** – probe detecting Mll2FC allele.

3.2.4 qPCR analysis of the Cre-mediated deletion in FACS sorted lymphocytes

In order to perform more accurate analysis of the specificity of the Cre - mediated Mll2 deletion, I analyzed its extent in different sorted lymphocyte subpopulations. To this end lymphocytes from bone marrow, spleen and peritoneal cavity were isolated and stained for the following markers: bone marrow (IgM, B220), spleen (CD21, CD23, CD19, CD4, CD8), peritoneal cavity (B220, CD5, CD19) in following staining mix in FACS buffer as indicated in the table below:

lymphoid organ	staining	antibodies
bone marrow	1	IgM-Cy2
		B220 Cy7 PE
spleen	2	CD21 FITC
		CD23 PE
		CD19 Cy7 PE
	3	CD8 FITC
		CD4 PE
		CD19 Cy7 PE
peritoneal cavity	4	B220 FITC
		CD5 PE
		CD19 Cy7 PE

Used combination of antibodies allowed to distinguish and FACS sort the following lymphocyte populations: bone marrow : Pre/Pro B cell ($B220^{high}$ – $IgM^{neg\text{-}low}$), IgM – positive (IgM+) ($B220^{high}$ - IgM^{high}), spleen: marginal zone B cell (MZ) ($CD19^{high}$ - $CD21^{high}$ - $CD23^{low}$), follicular B cell (Fo) ($CD19^{high}$ - $CD21^{interm}$ - $CD23^{high}$), T CD4+ cell ($CD19^{neg}$ - $CD4^{high}$ - $CD8^{low}$), T CD8+ cell ($CD19^{neg}$ - $CD4^{low}$ - $CD8^{high}$) and peritoneal cavity: B1 ($CD19^{high}$ - $B220^{high}$ - $CD5^{low\ to\ interm}$). TaqMan qPCR was performed on genomic DNA isolated from sorted cells. Detected DNA sequence corresponding to the exon 2 was normalized to the Pre/Pro B sample from the control mouse (+/F/CD21-Cre), which is expected to carry 2 copies of exon 2 – one on the wild type allele and one on the conditional allele before the Cre mediated deletion (Mll2F). Similarly, the level of the Mll2FC amplicon was normalized to the follicular B sample from the mutant (Mll2KO/F/CD21- Cre), where both copies of Mll2 floxed allele undergo the deletion.

As we can observe in Figure 13, the deletion takes place in IgM - positive bone marrow B cells, MZ B, Fo B and B1 cells, while in Pre/Pro B population as well as in splenic T lymphocytes the level of deletion is not detectable or minimal. Possible explanation for the detection of the Cre-mediated deletion in the splenic T cells from control animals may be the incomplete purity of the FACS sorting combined with the high sensitivity of the qPCR assay. Analysis confirmed restriction of the CD21-Cre mediated Mll2 deletion to mature B lymphocytes.

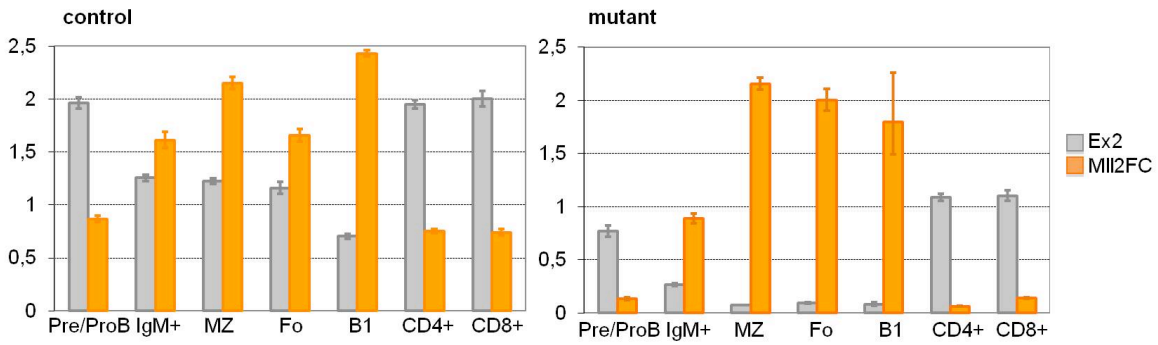

Figure 13. qPCR analysis of the Cre-mediated Mll2 deletion in different subpopulation of B and T lymphocytes in Mll2KO/F/CD21-Cre line. control - +/F/CD21-Cre mouse, **mutant** – Mll2KO/F/CD21-Cre mouse **Ex2** – probe detecting exone 2, **Mll2FC** – probe detecting Mll2FC allele, **Pre/Pro B** – Pre/Pro B cell, **IgM+** - IgM positive B cell from bone marrow, **MZ** – marginal zone B cell, **Fo** – follicular B cell, **B1** – B1 B cell from peritoneal cavity, **CD4+** – splenic T CD4+ cells, **CD8+** – splenic T CD8+ cells; **control** - +/F/CD21-Cre, **mutant** – Mll2KO/F/CD21-Cre

3.3 Analysis of Mll2 function in mature B cells

In order to characterize the effect of the loss of Mll2 in mature B lymphocyte, I performed flow cytometry analysis of B cells at the different stages of development, from different lymphoid organs. Careful flow cytometry analysis revealed the reduction of the marginal zone B cell compartment, which I further confirmed by examining spleen sections by immunofluorescence. Immunization with NP-Ficoll yielded information about fitness of residual marginal zone B cell population, while proliferation assay and BrdU *in vivo* labelling about its dynamics. Further described experiments allowed to better understand the role of Mll2 in the context of commitment to a given differentiation program.

3.3.1 Absolute numbers of splenic B cell subpopulations

In order to control if Mll2 deletion leads to global changes in total number of B cells absolute numbers of B cell subpopulations were counted. To eliminate variability of the dissection procedure that may affect the result, I limited the analysis to absolute numbers of the splenic B cell compartments. In addition, spleen weight of control and mutant animals was monitored. Data were collected from 22 pairs of experimental and control mice (3.2.2 – 3.5.3). The average spleen weight of control and mutant animals was found to differ by only 3,99% (0,096g – control versus 0,092g – mutant) (Fig. 14 A). Similarly, numbers of $CD19^{high}$ B cells, as well as the follicular B cell (Fo) and immature/transitional (Imm/Tr) compartments were found to be comparable. The number of $CD19^{high}$ B cells in control animals differed on average 4,02% ($5,1\times10^7$ cells – control vs. $5,3\times10^7$ cells - mutant), Fo B cells by 3,28% ($3,9\times10^7$ cells – control vs. $4,0\times10^7$ cells - mutant) and Imm/Tr population by 24,55% ($3,2\times10^6$ cells - control vs. $3,9\times10^6$ cells - mutant) (Fig. 14 B). In contrast the number of marginal zone B cells (MZ) in mutant mice was lower by 28,13% in comparison to the control (Fig. 14 B) with a p value of 0,02.

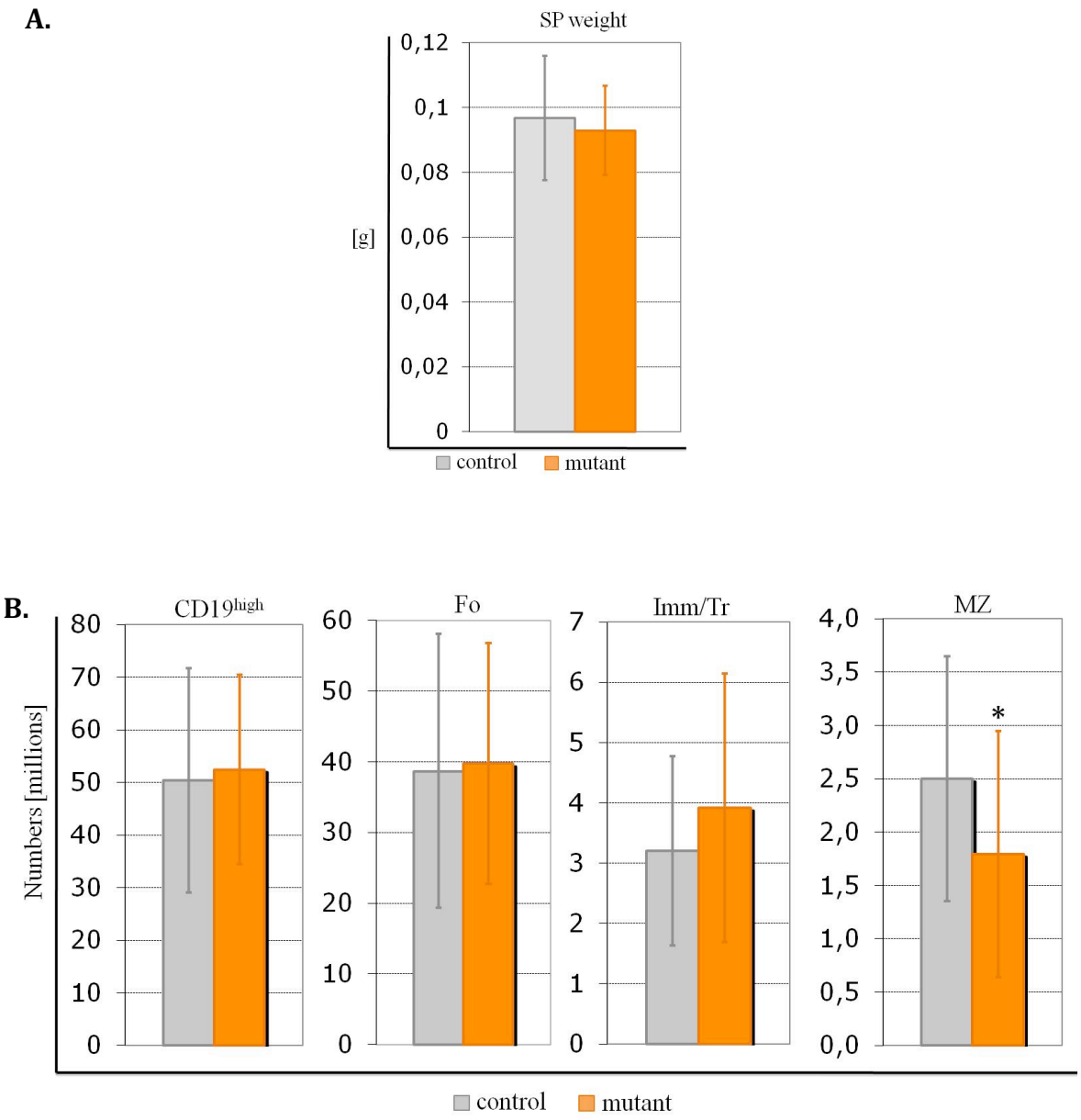

Figure 14. Absolute numbers of splenic B lymphocytes in Mll2KO/F/CD21-Cre mice; A. Spleen weight in Mll2KO/F/CD21-Cre line, [g]**; B.** Absolute numbers of splenic CD19^{high} B cells, follicular B cells (**Fo**), immature/transitional B cells (**Imm/Tr**), marginal zone B cells (**MZ**), numbers in millions; **grey** – control, **orange** – mutant; * p = 0,02; **control** - +/F/CD21-Cre, **mutant** – Mll2KO/F/CD21-Cre and MllF/F/CD21-Cre

3.3.2 Flow cytometry analysis of lymphocytes from Mll2KO/F/CD21-Cre mice

In order to analyze the effect of Mll2 deletion in mature B lymphocytes, cells from various lymphoid organs and at different stages of B lymphopoiesis were analyzed by flow cytometry.

Cells from bone marrow, spleen, peritoneal cavity, Peyer's patches, mesenteric lymph nodes and thymus were isolated in B cell medium (2.1.1.8) and stained with the following markers: bone marrow (BM) (IgM, CD43, B220), spleen (SP) (CD21, CD1d, CD38, CD23, CD19, CD4, CD8), peritoneal cavity (PC) (B220, CD5, CD19), Peyer's patches (PP), mesenteric lymph nodes (MLN) (CD38, Fas, CD19, CD4, CD8), thymus (T) (B220, CD4, CD8) as indicated in the table below.

These combinations of antibodies allowed to distinguish the following lymphocyte subpopulations: bone marrow : Pro B cell ($B220^{high}$ - IgM^{low} - $CD43^{high}$), Pre B cell ($B220^{high}$ - IgM^{low} - $CD43^{neg}$), IgM positive (IgM+) of both fractions immature and recirculating B cells ($B220^{high}$ - IgM^{high}), spleen: marginal zone B cell (MZ) ($CD19^{high}$ - $CD21^{high}$ - $CD23^{low}$), follicular B cell (Fo) ($CD19^{high}$ - $CD21^{interm}$ - $CD23^{high}$) transitional/ immature B cell (Tr/Imm) ($CD19^{high}$ - $CD21^{low}$ - $CD23^{low}$), peritoneal cavity: B1 cell (B1) ($CD19^{high}$ - $B220^{high}$ - $CD5^{low\text{-}interm}$), Peyer's patches, mesenteric lymph nodes and splenic: Non-germinal center (Non-GC) ($CD19^{high}$ – $CD38^{high}$ – Fas^{neg}), transitional ($CD19^{high}$ – $CD38^{high}$ – Fas^{interm}), germinal center (GC) ($CD19^{high}$ – $CD38^{low\text{-}neg}$ – Fas^{high}), T CD4+ cell ($CD19^{neg}$ - $CD4^{high}$ - $CD8^{neg}$), T CD8+ cell ($CD19^{neg}$ - $CD4^{neg}$ - $CD8^{high}$), thymus: double negative (DN) ($CD19^{neg}$ - $CD4^{neg}$ - $CD8^{neg}$), double positive (DP) ($CD19^{neg}$ - $CD4^{high}$ - $CD8^{high}$), T CD+ cell ($CD19^{neg}$ - $CD4^{high}$ - $CD8^{neg}$), T CD8+ cell ($CD19^{neg}$ - $CD4^{neg}$ - $CD8^{high}$). Cells were analyzed by flow cytometry (2.2.17.1) using FACSCalibur and CellQuest Pro software.

Cells of age and sex matched control and mutant littermates were isolated, stained and analyzed in parallel. Due to the expectedly high variability observed between different litters, collected data are presented, for each B cell subpopulation, as the average percentage of B cells in mutant with respect to the average percentage in control animals (Fig. 16). For each B cell population the percentage of B cells in control mice scored by flow cytometry was set to 100%. The relative percentage of B cells in mutant mice with respect to controls was then calculated in the following way:

$$X = [\%]^{M} \times 100\% \div [\%]^{C}$$

X [%] relative percentage of B cells in mutant mouse with respect to the control

$[\%]^{M}$ percentage of B cell of a particular population scored by flow cytometry in a mutant mouse

$[\%]^{C}$ percentage of B cell of a particular population scored by flow cytometry in a control mouse

Flow cytometry analysis of cells at the various stages of lymphopoiesis did not reveal significant changes for most of the populations I analyzed. Thus, the percentages of the Pre and Pro B cell compartments as well as the Imm/Tr compartments from bone marrow and spleen were comparable in control and mutant mice. On average, mutant Pre and Pro B cell population accounted for, respectively, 105,87% and 94,72% of the values observed in control animals, and Imm/Tr compartment for, respectively, 93,93% - BM and 109,25% - SP (Fig. 15 A and 16 A). This observation is not surprising since the Cre-mediated deletion of Mll2, as confirmed previously (3.2.2 – 3.2.4), takes place later - during the immature B cell into mature B cells transition. Similarly, the percentage of peritoneal cavity's B1a and B1b populations did not differ between control and mutant mice. The percentage of B1a cells in the mutant was found to be 98,01% of the control and B1b to be

85,13%. (Fig.15 B and 16 B). Average sizes of Non GC B cell populations from all analyzed organs (SP, MLN, PP) were also comparable (Fig.15 C and 16 C). Thus, GC population from Peyer's patches was of the same size in control and mutant animals (Fig. 16 C). Differences observed in the case of germinal center B cell populations (GC) from spleen (SP) and mesenteric lymph nodes (MLN) (SP GC - 33,82% reduction and MLN GC - 29,59% reduction with respect to the control mice) were not statistically significant ($p > 0,1$). Analogously, mutant B2 population accounted for 131,94% with respect to the control and BM mature recirculating B cells for 72,44% of control, have a weak statistical support (Fig. 15 C and A and 16 C and A - respectivly). Instead I found a very pronounced difference between mutants and controls in the splenic marginal zone B cell compartment (MZ). Its average size in mutant mice was only 56,82% of the size in a population found in control animals (Fig. 17 A). The mean size of MZ B cell population in mutant animals accounted for 4,21% of splenic B cells, while in control mice for 7,4%. This result was in agreement with the reduction in total number of MZ B cells (3.3.1; Fig. 14 B). As expected, given the high variability in the size of B cell subpopulation among individual mice, the expressivity of this phenotype varied between different litters. Thus, the highest degree of reduction I observed in the mutant MZ B cell compartment with respect to the control, accounted for 88,3% while the lowest for 4,95%. Equally expected was the observation that penetrance of the phenotype was nearly but not completely full. In 5 out 53 control-mutant pairs I analyzed, the MZ B cell population was bigger than in their respective control, with an increase up to 253,61% of the size of the control population. Such increase of the size of mutant population was however singular. In 4 other cases, the size of mutant MZ B sell population accounted for 131,61%, 132,98%, 156,04% and 173,73% of the size of their respective control. Lack of full penetrance and differences in the expressivity may result from mentioned before still partially mixed genetic background of animals used for the experiments.

As mentioned previously (3.2.1) in the experimental procedures, these results come from experiments performed on mutant mice of both allelic configurations, namely mice homozygous for the Mll2 conditional knock-out allele carrying one Mll2 KO allele and one Mll2F conditional allele (Mll2KO/F/CD21-Cre) or mice carrying both Mll2F alleles (Mll2F/F/CD21-Cre) (Fig. 2 and Fig. 7). In total 53 control-mutant pairs were analysed, of which 21 were of the Mll2KO/F/CD21-Cre genotype and 32 of the Mll2F/F/CD21-Cre. Hence, it was important to exclude haploinsufficiency of Mll2 in case of Mll2KO/F/CD21-Cre cohort. A separate analysis of the results obtained from the two distinct allelic configurations, showed only minor differences. While the average percentage of the MZ B cells of all mutant animals was accounted for 55,56% of the values observed in control, the percentage of MZ B cell population in Mll2KO/F/CD21-Cre animals equalled 46,69% and in Mll2F/F/CD21-Cre 57,45% (Fig. 16 A and unpublished data). Furthermore, this minor difference results most likely from the fact that 4 out of the 5 control-mutant pairs presenting an opposite phenotype (increase of the MZ B cell compartment in mutants) belonged to the Mll2F/F/CD21-Cre cohort.

Finally, as predicted, T lymphocytes from thymus, spleen and mesenteric lymph nodes were not affected (Fig. 15 D), confirming that CD21-Cre mediated Mll2 deletion is limited to mature B cells. Surprisingly however, I found that thymic T CD4+ cells were also significantly reduced in the mutant. Size of the T CD4+ cell subpopulation in mutant mice was on average reduced by 21,4% ($p = 0.01$) (Fig. 15 D). As this observation was not further followed it is difficult to make a final conclusion, however based on several previously published articles, it is possible to speculate that reduced number of MZ B cells indirectly leads to decreased number of T cells. It is known that MZ B cells shuttle between the centre and margin of the follicle (Cinamon et al., 2008) transporting IgM containing immune complex (IgM-IC) and placing it onto follicular dendritic cells (Ferguson et al., 2004) what further stimulates germinal center (GC) formation. Though this process MZ B cells initiate the early stage of the T dependent immune response – and

indeed it was demonstrated that mice with reduced MZ B cell compartment form germinal center less efficiently (Ferguson et al., 2004). It is likely that reduced MZ B cell compartment giving weaker stimulus for the activation of T dependent immune response leads to the stabilization of T cell compartment at its low (not stimulated) level. Furthermore it is possible that this lower requirement for the T CD4+ compartment in the spleen is signalled to the thymus and in effect leads to the decreased proliferation of T CD4+ cells in mutant animals. This potential signalling loop would indicate that decreased size of T CD4+ cells is a secondary effect of loss of Mll2. However as this results were not further followed, a specific role of Mll2 in the development of T CD4+ cells cannot be excluded.

The relative percentages of population discussed above are presented in the figure 15 and 16, while the examples of flow cytometry analysis are collected in the figures 16B (spleen) and 17. As Loss of Mll2 in mature B cells was found to impact selectively the marginal zone B cell compartment, and in light of the very interesting biology of this cell type, I focused my further work on the dissection of this phenotype.

lymphoid organ	staining	antibodies
bone marrow	1	IgM ALEXA488
		CD43 PE
		B220 Cy7 PE
spleen	2	CD21 FITC
		CD23 PE
		CD19 Cy7 PE
	3	CD1d – biotin Sa - FITC
		CD23 PE
		CD19 Cy7 PE
	4	CD38 – biotin Sa - FITC
		CD23 PE
		CD19 Cy7 PE
	5	CD8 FITC
		CD4 PE
		CD19 Cy7 PE
peritoneal cavity	6	B200 FITC
		CD5 PE
		CD19 Cy7 PE
Peyer's patches	5	CD38 – biotin Sa - FITC
		Fas PE
		CD19 Cy7 PE
	6	CD8 FITC
		CD4 PE
		CD19 Cy7 PE
mesenteric lymph nodes	5	CD38 – biotin Sa - FITC
		Fas PE
		CD19 Cy7 PE
	6	CD8 FITC
		CD4 PE
		CD19 Cy7 PE
thymus	6	CD8 FITC
		CD4 PE
		CD19 Cy7 PE

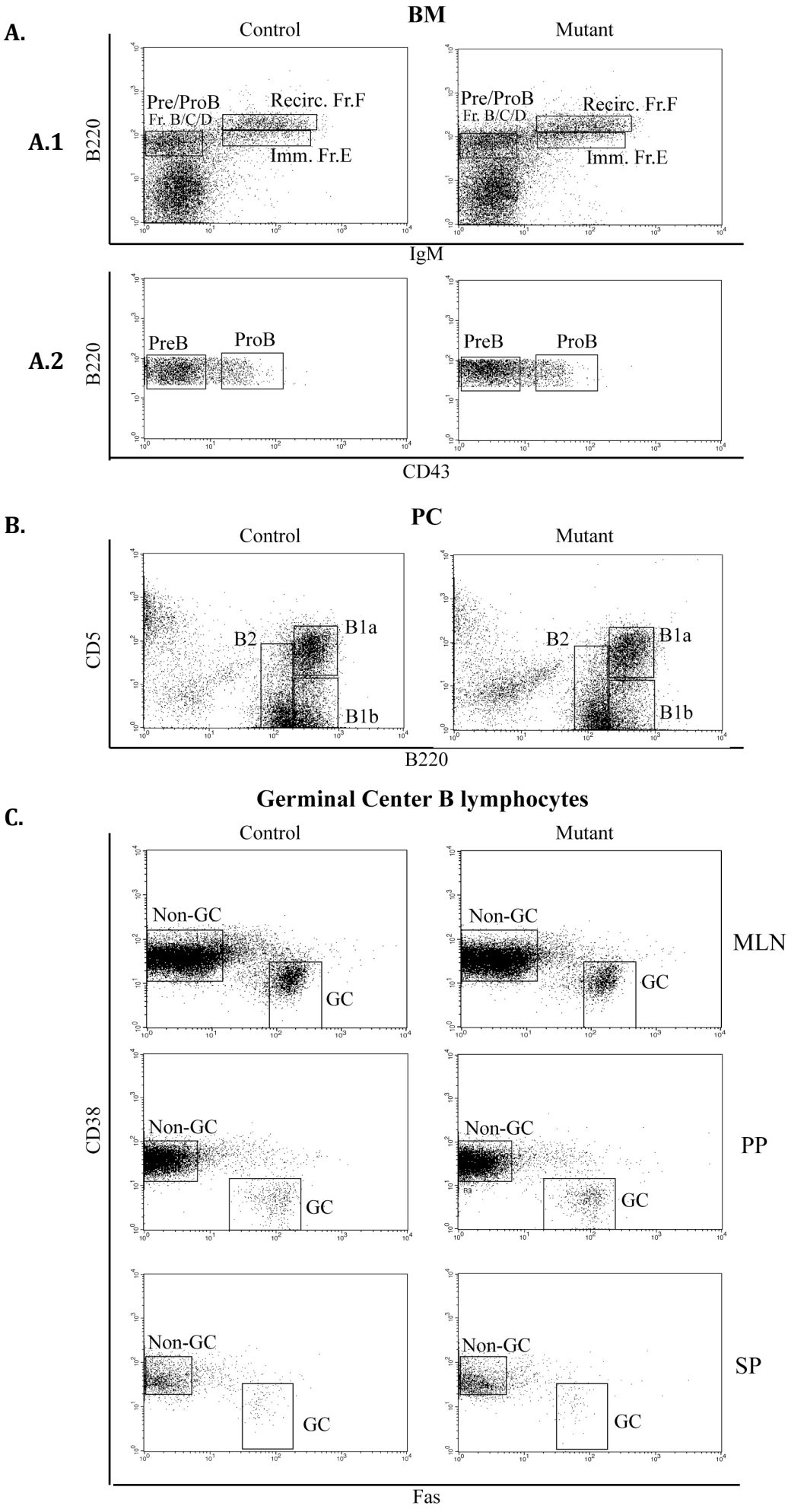
A.
BM
Control
Mutant
A.1
B220
Pre/ProB
Fr. B/C/D
Recirc. Fr.F
Imm. Fr.E
IgM
A.2
B220
PreB
ProB
CD43
B.
PC
Control
Mutant
CD5
B2
B1a
B1b
B220
C.
Germinal Center B lymphocytes
Control
Mutant
CD38
Non-GC
GC
MLN
PP
SP
Fas

D. **T lymphocytes**

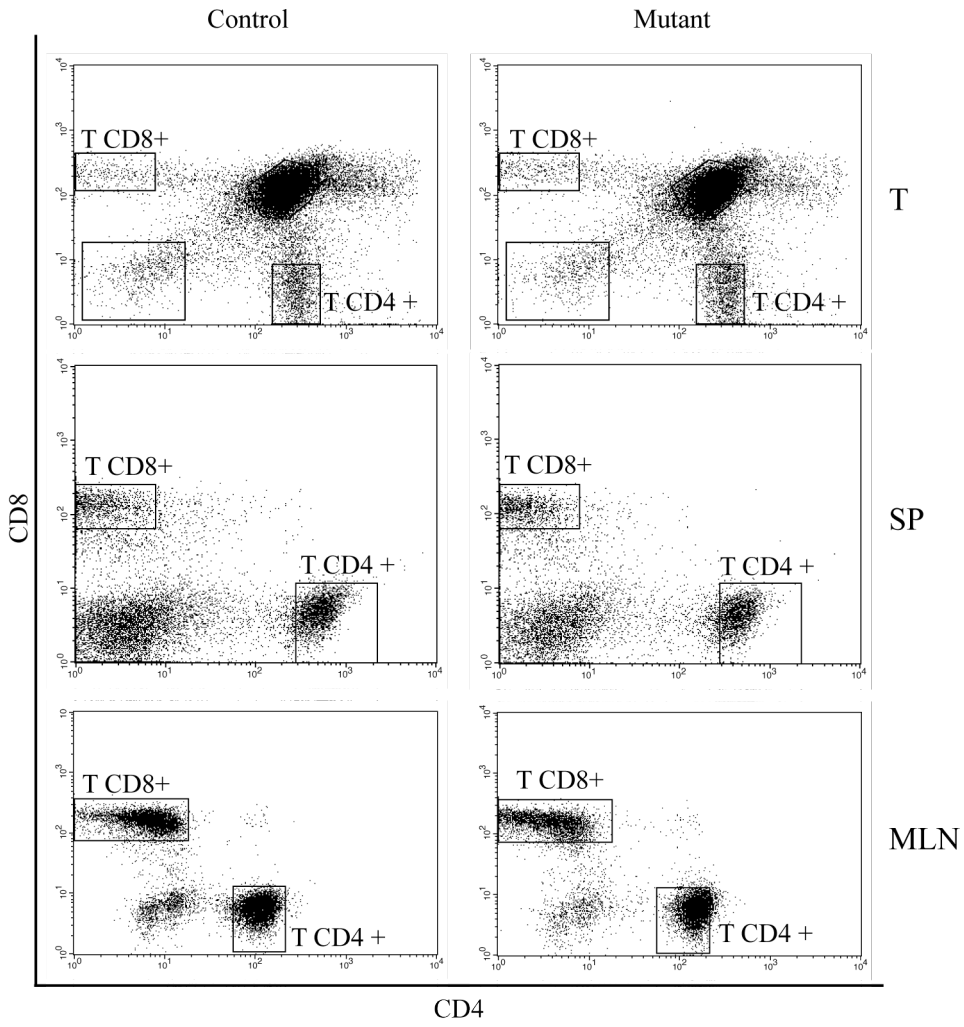

Figure 15. Representative examples of flow cytometry analysis of lymphocytes from Mll2KO/F/CD21-Cre line; A. bone marrow B lymphocytes stained with **A.1** IgM (ALEXA488) and B220(Cy7 PE) and **A.2** CD43 (PE) and B220(Cy7 PE, **B.** peritoneal cavity CD19^{high} B lymphocytes stained with CD5 (PE) and B220(FITC), **C.** germinal center B lymphocytes from mesenteric lymph nodes, Peyer's patches and spleen stain with CD38-Sa(FITC) and Fas (PE), **D.** T lymphocytes stained from thymus, spleen and mesenteric lymph nodes stained with CD8 FITC and CD4 PE; **Pre/Pro B** – Pre/Pro B cell, **Imm. (E)** – immature B cells (fraction E), **Recir. (F)** – mature, recirculating B cells (fraction F) **B1a** – B1a cells, **B1b** – B1b cells, **B2** – B2cells; **Non GC** - Non germinal center B cells, **GC** - Germinal center B cells, **DN** – double negative T cells, **DP** – double positive T cells, **T CD4+** – T CD4+ cells, **T CD8+** – T CD8+ cells, **BM** – bone marrow, **PC –** peritoneal cavity, **MLN** – mesenteric lymph nodes, **PP** – Peyer's patches, **SP** – spleen, **T** – thymus

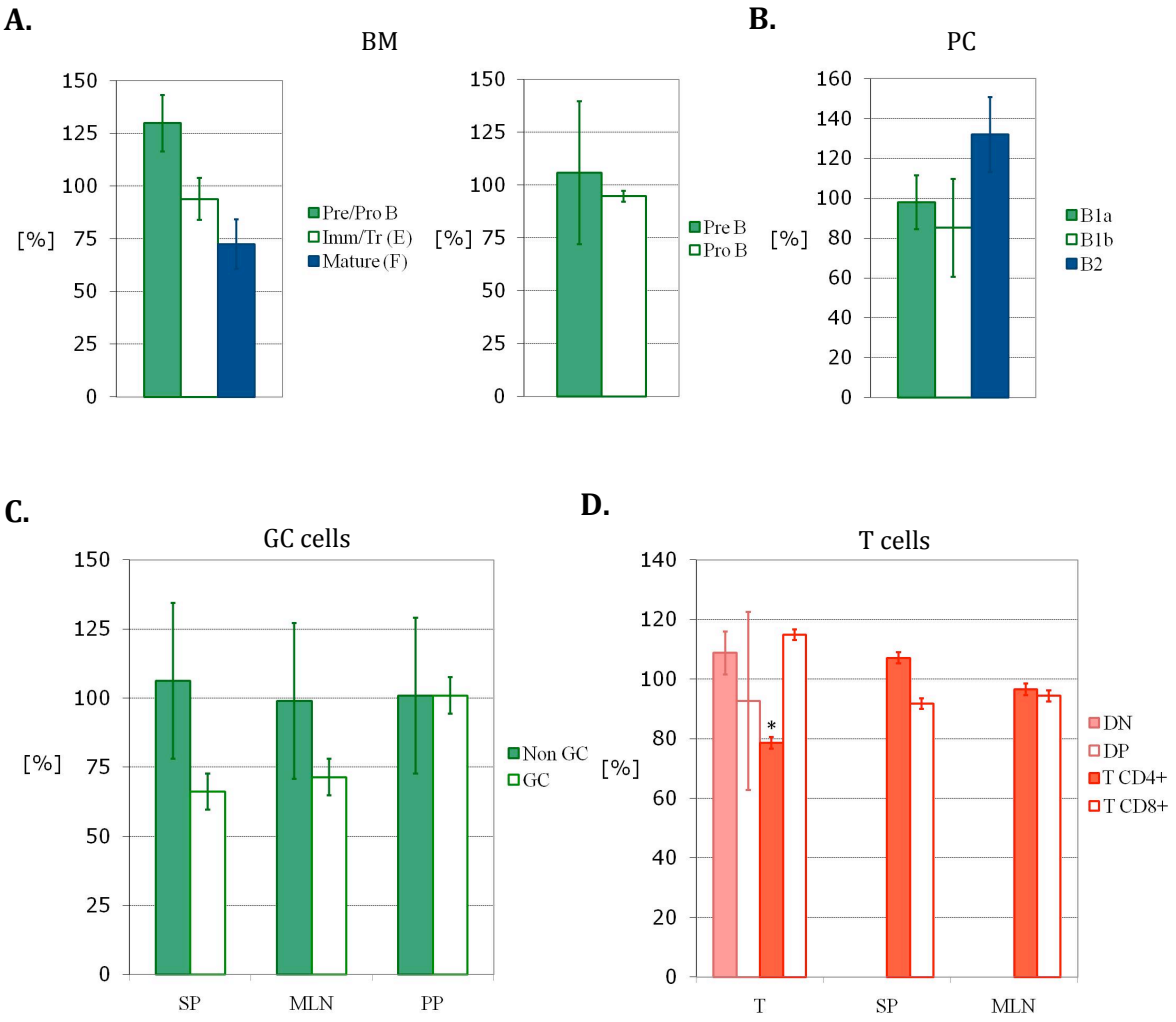

Figure 16. Relative average percentage of lymphocyte subsets in Mll2KO/F/CD21-Cre mice. The values of control mice are set to 100%. A. Lymphocytes subsets from bone marrow: **Pre/Pro B** – Pre/Pro B cell (green), **Imm/Tr (E)** – immature/transitional B cells (fraction E) (white), **Mature (F)** – mature, recirculating B cells (fraction F) (blue); **B.** Lymphocytes subsets from peritoneal cavity: **B1a** – B1a cells (green), **B1b** – B1b cells (white), **B2** – B2cells (blue); **C. Non GC** - Non germinal center B cells (green), **GC** - Germinal center B cells (white) from **SP** – spleen, **MLN** – mesenteric lymph nodes, **PP** – Peyer's patches; **D.** T lymphocytes subsets from **T** – thymus, **SP** – spleen, **MLN** – mesenteric lymph nodes; **DN** – double negative T cells (salmon), **DP** – double positive T cells (white with salmon line), **T CD4+** – T CD4+ cells (red), **T CD8+** – T CD8+ cells (white with red line). ***** p = 0.01. Detailed description in the text (3.4.2). Average percentage values of flow cytometry analysis from at least 10 pairs of control and experimental mice are shown.

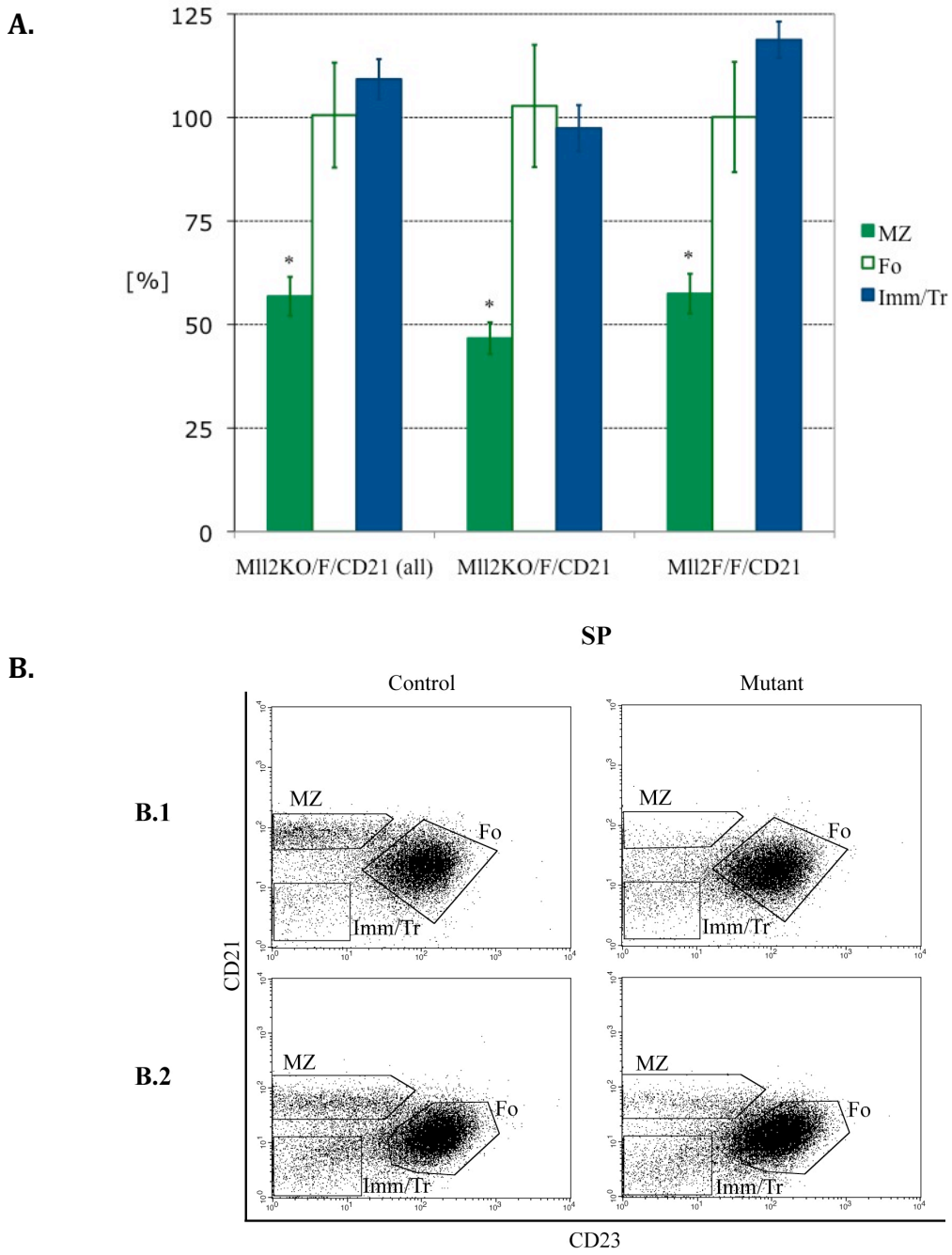

Figure 17. Analysis of splenic B lymphocytes subsets in Mll2KO/F/CD21-Cre mice. A. Average percentage of lymphocyte subsets of splenic B lymphocytes in all analysed Mll2/F/CD21-Cre animals (N = 53), Mll2KO/F/CD21-Cre animals (N = 21) and Mll2F/F/CD21-Cre animals (N = 32) - the values of control mice are set to 100%: **MZ** – marginal zone B cells (green), **Fo** – follicular B cells (white), **Imm/Tr** – immature/transitional B cells (blue) ***** $p < 0{,}003$. Detailed description in the text (3.4.2). **B.** Flow cytometry analysis of splenic $CD19^{high}$ B lymphocytes stained with CD21(FITC) and CD23(PE): **B.1.** Flow cytometry analysis of splenic $CD19^{high}$ B lymphocytes from a couple of mice with high reduction of MZ B cell subset, **B.2.** - Flow cytometry analysis of splenic $CD19^{high}$ B lymphocytes from a couple of mice with average reduction of MZ B cell subset.

3.3.3 Flow cytometry analysis of marginal zone B cell compartment

In order to gain independent confirmation of the reduction of the (MZ) population upon loss of Mll2 (3.3.2; Fig. 17) splenic cells from 10 animals were stained also for an alternative combination of markers (CD1d-CD23-CD19 and CD38-Cd23-CD19) (2.1.2.1) according to the table 3.3.2 (stainings 3 and 4). Importantly, this experiment was also meant to exclude that the reduction in MZ cells could simply result from Mll2-dependent regulation of the CD21 gene itself, and hence from its downregulation upon loss of Mll2. Cells were analyzed by flow cytometry (2.2.17.1) using FACSCalibur and CellQuest Pro software.

Also with this staining I confirmed the reduction of the marginal zone B cell compartment (MZ) in the mutant that I have presented above (3.3.2 Fig. 17). Mutant $CD19^{high}$ – $CD1d^{high}$ - $CD23^{low}$ and $CD19^{high}$ – $CD38^{high}$ - $CD23^{low}$ MZ B cells population was decreased by 55,15% (7,85% - control vs. 3,52% - mutant) and 49,59% % (10,91% - control vs. 5,50% - mutant) respectively. Follicular B cell compartment (Fo) ($CD19^{high}$ - $CD21^{interm}$ - $CD23^{high}$) and transitional/ immature B cells (Tr/Imm) ($CD19^{high}$ - $CD21^{low-interm}$ - $CD23^{low-interm}$) were not affected (Fig. 18). To ensure the unbiased flow cytometry analysis of all 3 straining (CD19 - CD21 - CD23, CD19 - CD1d - CD23 and CD19 – CD38 - CD23), I have chosen for comparison the same animals.

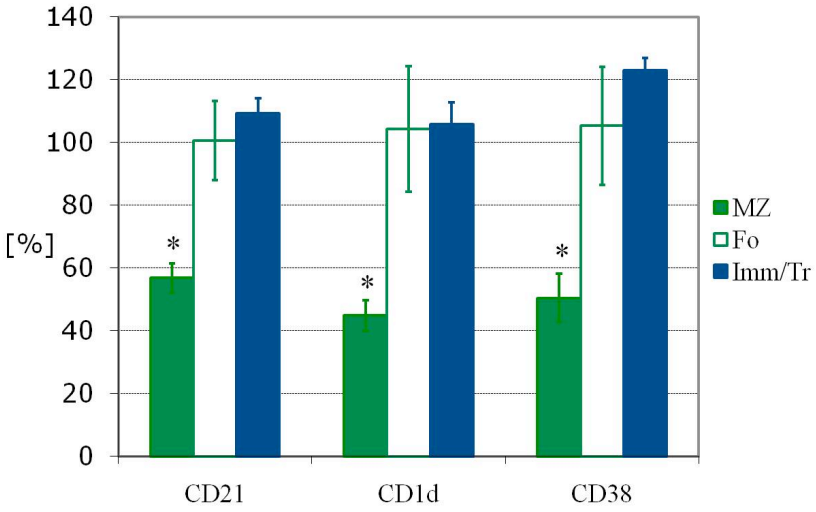

Figure 18. Analysis of splenic CD19^{high} B lymphocytes subsets in Mll2KO/F/CD21-Cre mice. 10 animals were stainted for: **CD21** (CD21-CD23-CD19**), CD1d (**CD1d-CD23-CD19**), CD38 (**CD38-CD23-CD19**).** The values of control mice are set to 100%. **MZ** – marginal zone B cells (green), **Fo** – follicular B cells (white), **Imm/Tr** – immature/transitional B cells (blue) * $p < 0,02$. Detailed description in the text (3.4.2).

3.3.4 Immunofluorescence analysis of spleen sections of Mll2KO/F/CD21-Cre mice

Murine marginal zone B cells (MZ) are defined i) by the expression of the following markers: CD19^{high} - CD21^{high} – CD1d^{high} – CD38^{high} - CD23^{low} and ii) by their localization around the margins of splenic follicles (Oliver et al., 1997a; Oliver et al., 1997b; Roark et al., 1998) (Fig. 19 A). Therefore in order to confirm the reduction of the MZ B cell compartment in the splenic tissue I performed an immunofluorescence analysis of spleen sections from control and mutant Mll2/F/CD21-Cre mouse pairs.

Spleen sections from two control-mutant mouse pairs of the Mll2KO/F/CD21-Cre allelic cohort were stained (2.2.17.3) for IgM (green) to localize all B cells and MOMA-1 (red) to mark metallophilic macrophages (MM), whose ring separates marginal zone B cells from

follicular B cells. Cell DNA was marked with DAPI. Spleens from control and mutant animals were dissected, sectioned and stained in parallel. 40 different follicles of each control and mutant sample were analyzed by confocal microscopy. Antibodies and DAPI concentration used in straining are listed in table in (2.1.2.3 and 2.2.17.3). Data were acquired using Confocal Microscope TCS SP2 AOBS (Leica) and analyzed with ImageJ 1.42q software. For both control and mutant samples, the thickness of the marginal zone cell layer was measured using ImageJ 1.42q software at its thickest part.

The analysis showed significant differences in the thickness of the MZ layer between control and mutant samples. While the marginal zone B cell layer in control samples was invariably easy to distinguish, with cells uniformly distributed around entire follicle sections, MZ B cells in the mutant mice were much fewer and clustered in small groups (Fig. 19 C). On average the MZ B cell layer in the control mice was thicker by 144,52% than in mutants animals, measuring 32,651µm against the 13,353µm of the mutant (Fig.19 B). This evident reduction of MZ B cell population demonstrated by immunofluorescent staining of spleen sections from Mll2KO/F/CD21-Cre animals (Fig. 19) confirmed previously observed strong reduction of this specific compartment (3.3.1 – 3.3.3; Fig. 14 - 18) indicating again role of Mll2 in the MZ B cell development.

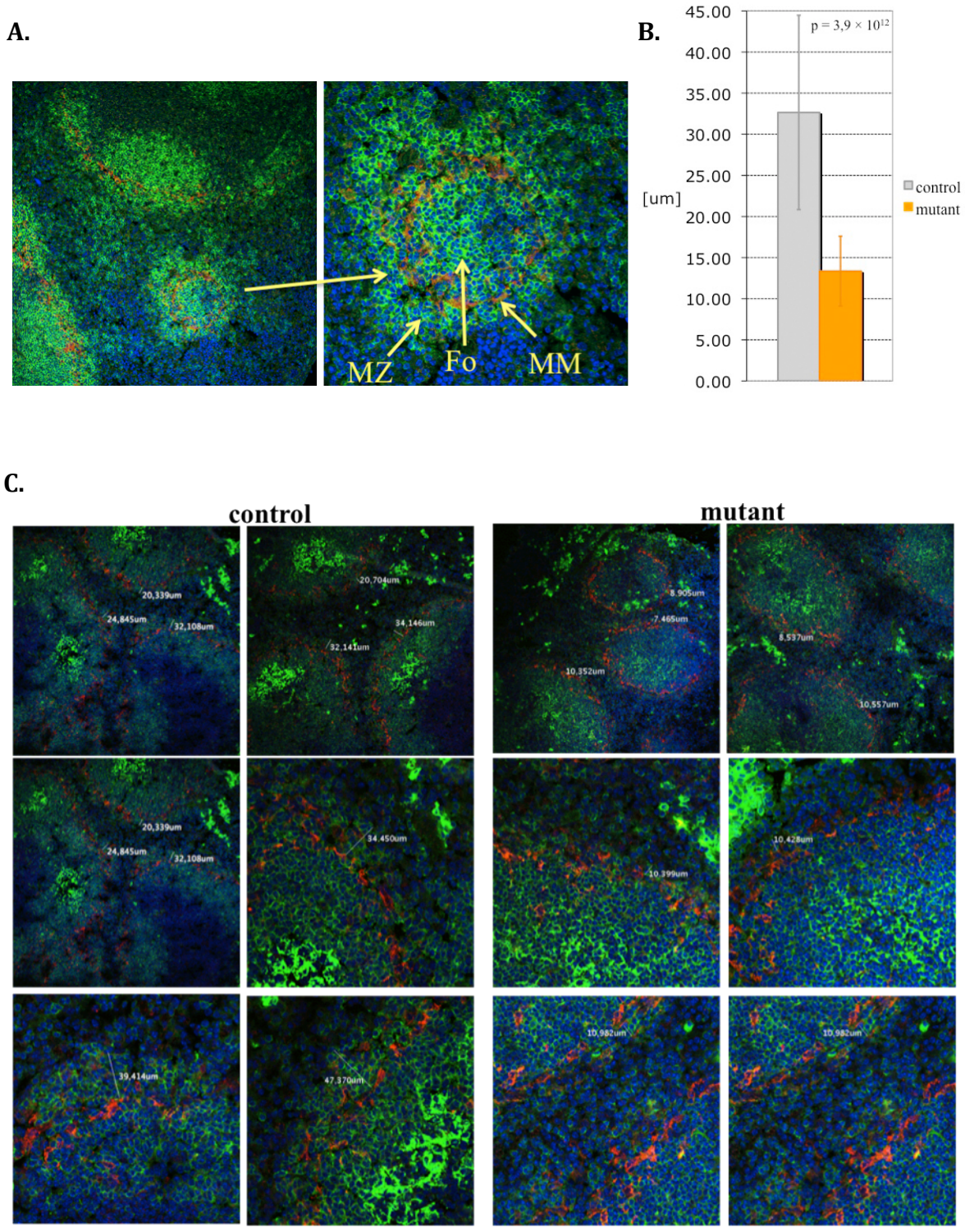

Figure 19. Immunofluorescence analysis of spleen sections of Mll2KO/F/CD21-Cre mice; A. Confocal microscope analysis of wild type spleen section stained for B220 (**green)**, Moma-1 **(red**), DAPI **(blue).** With arrows are indicated **MZ** – marginal zone B cells, **Fo -** follicular B cells, **MM** – metallophilic macrophages; **B.** Thickness of marginal zone B cell layer [µm]; **grey** – control, **orange** –mutant. **C.** Confocal microscope analysis of control and mutant spleen section stained for IgM (**green)**, Moma-1 **(red**), DAPI **(blue**); **control** - +/F/CD21-Cre, **mutant** – Mll2KO/F/CD21-Cre

3.3.5 qPCR analysis of Mll2 CD21-Cre - mediated deletion in marginal zone B cell compartment

Previous analysis revealed significant reduction of marginal zone B cell compartment upon Mll2 ablation (3.3.1 – 3.3.4; Fig.14 - 19). Variable expressivity of the phenotype between animals from different litters was expected, however it became crucial to confirm Mll2 CD21-Cre - mediated deletion in the MZ B cells in order to exclude that cases with less pronounced phenotype are the consequence of heterogenic population composed of cells that did deleted Mll2 gene and those that did not. To this end I performed TaqMan qPCR analysis on the genomic DNA from FACS sorted marginal zone B cells from various experiments (chosen randomly).

Genomic DNA was isolated (2.2.1.3) from sorted (2.2.17.1) marginal zone B cell ($CD19^{high}$ - $CD21^{high}$ - $CD23^{low}$). qPCR analysis (2.2.11) was performed with TaqMan probes Ex2 and Mll2FC (3.2.3; Fig. 9 and 12 A). DNA sequences detected by both probes were normalized to the DNA sample from Mll2F/PGK-Cre mouse (3.2.1, Fig. 10) that carries one wild type Mll2 allele and one Cre deleted – Mll2FC. For the analysis I chosen samples from 2 control and 6 mutant animals.

qPCR analysis confirmed very high level of deletion of Mll2 gene in all mutant samples (Fig. 20) excluding the same that variability in the expressivity is accounted to the low level of the CD21-Cre-mediated deletion but is rather due to the still partially mixed background of the animals.

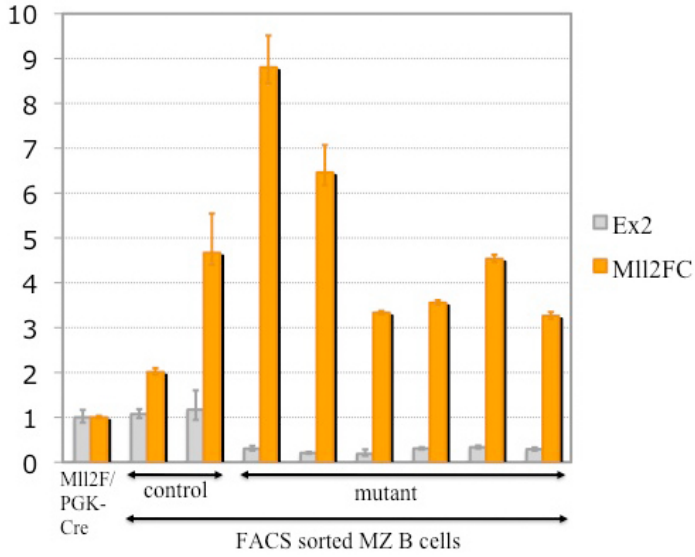

Figure 20. qPCR analysis of the Cre-mediated deletion in MZ B cells in Mll2KO/F/CD21-Cre line. control - +/F/CD21-Cre mouse, **mutant** – Mll2KO/F/CD21-Cre mouse **Ex2** – probe detecting exone 2 **(grey)**, **Mll2FC** – probe detecting Mll2FC allele **(orange)**, **MZ** – marginal zone B cell, **control** - +/F/CD21-Cre, **mutant** – Mll2KO/F/CD21-Cre and Mll2F/F/CD21- Cre

3.4 Functional analysis of Mll2 in mature B cells

3.4.1 NP-Ficoll immunization of Mll2KO/F/D21-Cre mice

Following the consistent reduction of the size of marginal zone B cell compartment associated with the loss of Mll2, it became essential to examine their principal function as B cells - the ability to mount the immunological response against antigens. To this end pairs of control-mutant mice of the Mll2F/F/CD21-Cre allelic cohort were immunized with NP-Ficoll. MZ B cells constitute the first line in the T-independent immunological response, and are involved in the reaction against polysaccharides present on the surface of encapsulated bacteria (Lane et al., 1986). Ficoll molecules mimic the bacterial cell wall polysaccharides (Inman, 1975), therefore NP-Ficoll immunization is an established

experimental system to probe the MZ B cell specific response. In order to test the immunoglobulin class switch, changes in IgM and IgG3 serum levels were measured in the function of time. Total serum levels of IgM and IgG3 non immunized mice were measured as well as a baseline negative control. Control and mutant littermates were immunized with 50µg of NP-Ficoll (2.2.19). Blood samples were taken at day 0, 3rd, 7th, 14th, 21st and 28th. Concentration of total IgM and IgG3 in the serum was measured by ELISA (2.2.16). Levels of IgG and IgM were measured, respectively in 10 control and 9 mutant not immunized mice, and in 6 control and 4 mutant immunized mice. In order to measure the levels of IgM and IgG3 a standard curve was build using standard serum supplied with ELISA Quantitation Set (Bethyl). Serial dilution of control and experimental sera were prepared by diluting samples 1 : 1,000 – 1 : 80,000. Measurement of the IgM and IgG3 concentration was performed rigorously within the linear range of the standard curve in order to ensure the precision of the measurement.

Total IgM levels in non immunized mice was on average 30,7% lower in mutant mice than in controls (1041,865µg/ml and 721,98µg/ml respectively) while the level IgG3 was on average lower by 15,95% (1766.179µg/ml – control and 1484,452µg/ml - mutant (Fig 21 A). In contrast, 28 days after the immunization levels of IgM in control mice did not change (879,850µg/ml at day 0 versus 818.945µg/ml at day 28th), while the levels of IgG3 doubled, comparing to the day 0 (1455,128µg/ml at day 0 vs. 2955,066 µg/ml at the day 28th) (Fig. 21 B), indicating the ability of control MZ B cells to switch immunoglobulin class in response to the antigen challenge. Instead, Mll2 deficient, Mll2F/F/CD21-Cre MZ B cells did not appear capable of switching the immunoglobulin class, yet were still able to respond to the Ficoll antigen - 28 days after the immunization in the blood serum concentrations of IgM rose by 94,08% with respect to the day 0 (604,131 µg/ml at day 0 versus 1172,552 µg/ml at day 28th) while concentrations of IgG3 raised only by 36,59% (1204,702µg/ml at the day 0 versus 1645,519 µg/ml at the day 28th) (Fig 21 B).

Measurement of the levels of anti-NP IgM and IgG3 specific is in progress.

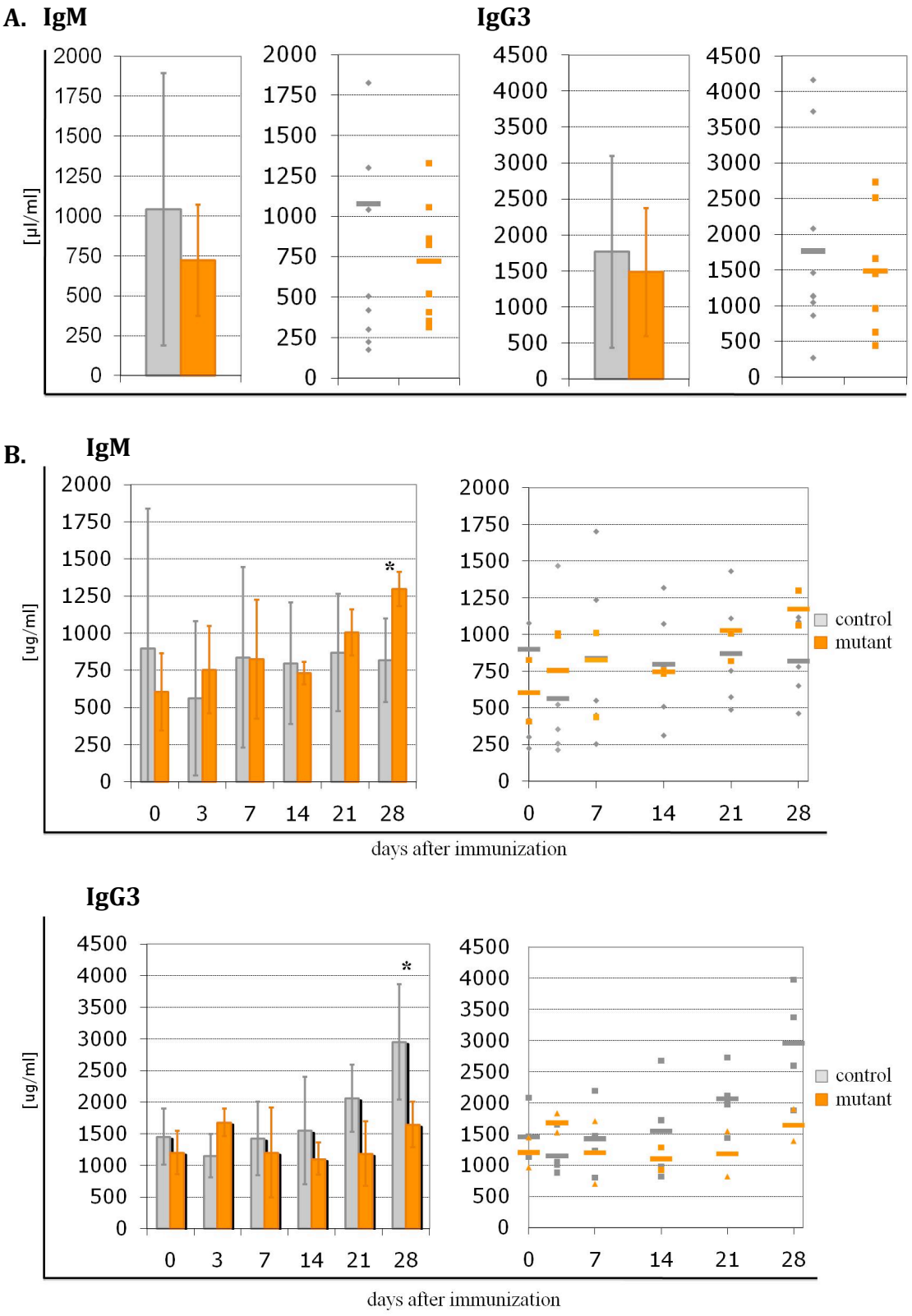

Figure 21. ELISA analysis of the IgM and IgG3 levels in blood serum of Mll2KO/F/CD21-Cre mice. A. Not immunized; **B.** Immunized with NP-Ficoll; Left panels - the average level of IgM or IgG3, Right panels – all analyzed samples; [µg/ml]; **control** - +/F/CD21-Cre (grey), **mutant** – Mll2KO/F/CD21-Cre and Mll2F/F/CD21- Cre (orange), * $p < 0,03$

3.4.2 Splenic B cell dynamics analysis - *in vitro* proliferation assay

In order to determine the viability and proliferation capacity of splenic B cells I performed an *in vitro* proliferation assay (2.2.18). In addition IL-4 treatment allowed a further characterization of proficiency in IgM to IgG1 immunoglobulin class switch.

Control and mutant splenic B cells were purified using CD19 MicroBeads (2.2.17.2) and stained with Carboxyfluorescein succinimidyl ester (CFSE). Next, cells were plated in duplicates at the concentration of 1mln cells/ml in B cell medium (2.1.1.8) containing LPS (20 μg/ml) and Il-4 (10 pg/μl). Cells were counted and analyzed daily by flow cytometry (2.2.17.1) for 4 consecutive days. Staining against CD19 and surface IgG1 was performed as indicated in the table below. Two control and two mutant sex matched littermates were used in this experiment.

After 4 days flow cytometry analysis showed in the mutant a higher percentage of surviving B cells (by 38,66%) than in controls (17,56% alive cells in control versus 24,35% alive cells in mutant) (Fig. 22 A). However analysis of CFSE positive, proliferating cells did not indicate higher proliferation rate *in vitro* (Fig. 22 B). This would suggest that Mll2 deficient CD19 positive cells might be characterized by higher viability. Interestingly progressively with the proliferation, scored by decreased fluorescence intensity of CFSE positive cells, 37,07% more of mutant cells switched class of immunoglobulin to IgG1 (Fig. 22 C) without however being activated more efficiently than control cells – percentage of mutant plasma cells was 14,32% lower that of control cells (Fig. 22 D). It is important to point out that this analysis was performed on the total $CD19^{high}$ splenic cell fraction, which consists in the vast majority of follicular B cells. Hence, on the basis of the flow cytometry analysis shown above, that did not indicate changes in follicular fraction upon Mll2 loss, (3.3.1 – 3.3.3) it is not surprising that Mll2 deficient cells did not show a proliferation impairment in this assay. Thus, in order to study

the dynamics of the MZ compartment upon Mll2 loss, it became necessary to label proliferating cells *in vivo*.

antibodies
IgG1 APC
CD19 Cy7PE
CD138

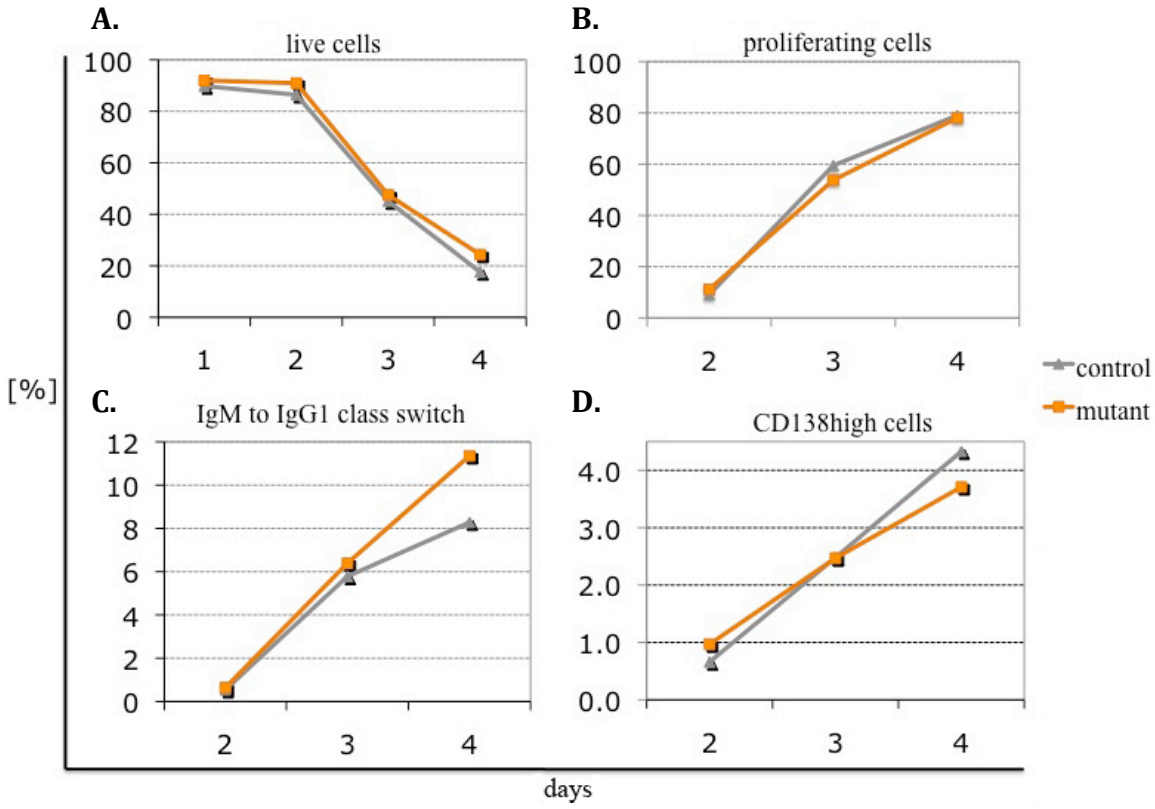

Figure 22. Flow cytometry analysis of *in vitro* proliferation assay. A. Average percentage of live cells; **B.** Average percentage of proliferating cells scored by CFSE decay; **C.** Average percentage of IgG1 positive cells (in function of CFSY decay); **D.** Average percentage of plasma cells ($CD19^{high}$ – $CD138^{high}$). Axis x – **[%]**, axis y – **days**; **gray** – control, **orange** – mutant; **control** - +/F/CD21, **mutant** – Mll2F/F/CD21

3.4.3 Marginal zone B cell compartment dynamics analysis – *in vivo* BrdU labeling

In order to understand the basis of the decreased marginal zone B cell population of Mll2KO/F/CD21-Cre line it is necessary to understand the dynamics of this population. It is important to determine if the MZ B cell compartment is reduced due to decreased number of the MZ B cell progenitors and/or rate of their proliferation, or rather due to increased cell death within MZ B cell compartment. Clarification of this issue would indicate the role of Mll2 in the B cell specification - if Mll2 is involved in the commitment to the marginal zone B cell lineage and activation of its transcriptional program or rather in the maintenance of it. For that reason I administrated 5-bromo-2-deoxyuridine (BrdU) to pairs of control-mutant Mll2KO/F/CD21-Cre animals. BrdU is a thymidine analogue and is thus incorporated into newly synthesised DNA. Using anti-BrdU antibodies it is possible to track replicating cells (Gratzner and Leif, 1981) and monitor the cycling dynamics of the labelled population by measuring the decay in the percentage of BrdU positive cells due to the progressive dilution of BrdU with subsequent rounds of cell division.

0,8mg/ml solution of BrdU, containing 5% of Glucose was administered in the drinking water for 4 weeks to sex matched control and mutant littermates (2.2.20). It was observed that animals do not drink water containing BrdU and eventually die due to dehydration. Therefore to avoid it and encourage animals to drink, 5% of Glucose was added to the BrdU solution[2]. BrdU labelled cells were assessed by flow cytometry (2.2.17.1) on the 7th, 14th and 28th day of BrdU administration. In total 10 control and 8 mutant mice were used in the experiment.

After 28 days of BrdU treatment all cells were BrdU positive, both in mutant and control mice (Fig. 23 A). However, already after 7 days the percentage of marginal zone B cell

[2] Observation and suggestion kindly communicated by Dr. David Allman

(MZ) BrdU positive cells in mutant mice was 74,85% higher with respect to the control (24,85% of BrdU positive MZ B cells - mutant vs. 14,21% - control) (Fig. 23 A and B). Similarly the percentage of follicular B cells (Fo) and immature/transitional (Imm/Tr) was higher in the mutant by 49,14% (9,60% positive Fo B cells - mutant vs. 6,44% - control) and 22,06% (70,32% positive Immature/Transitional B cells – mutant vs. 57,31% - control) respectively (Fig. 23 A and B). This result indicates a higher turnover of B cells compartments, and in particular the MZ B cells, in the mutant. Yet, despite an increase by nearly 75% (at day 7) in the fraction of mutant MZ B BrdU positive cells, on the average the MZ population was reduced with respect to the control (Fig. 23 C). Though indicative, this experiment is however not fully conclusive, because the cohort of 5 control-mutant pairs turned out to include also 3 of the 5 pairs that presented a phenotype opposite to the one featured by the overwhelming majority of mutant mice (MZ B cell population greater in mutants than in controls). In these 3 couples mutant MZ B compartments were higher with respect to the control by 56,04%, 73,73% and 153,61%.

This short term pulse experiment revealed striking difference in the turnover rate of MZ B cell compartment between mutant and control animals suggesting the presence of a feedback loop that increases proliferation rate upon loss of Mll2. It is possible that the higher turnover of Mll2 deficient tries to compensate depleted part of the MZ B cells compartment. Preliminary flow cytometry results of staining with cleaved Caspase-3 (Casp3), an apoptosis marker (Nicholson et al., 1995), did not indicate higher cell death in mutant MZ B cell compartment. Together, it is suggestive that Mll2 plays an important role during MZ B cell maturation, however due to not sufficient amount of data of staining with cleaved Casp3 no final conclusion is possible.

In addition this experiment yielded information about the time of BrdU administration required for saturation with BrdU B cell subpopulation of interest. Currently, long term pulse-and-chase experiments are being conducted in which B cells saturated with BrdU (4 week of application) are followed for several months. By scoring the BrdU incorporation

decay I will obtain information about the rate of self replenishing of MZ population. The capacity to self replenish was attributed to MZ B cells in the experiment in which MZ B cell compartment was the only one to maintain its normal level despite the block of bone marrow efflux by RAG2 deletion (Hao and Rajewsky, 2001). Combined together short and long term BrdU pulse-and-chase experiments should shed light on the role of Mll2 in the marginal zone B cell lymphopoiesis.

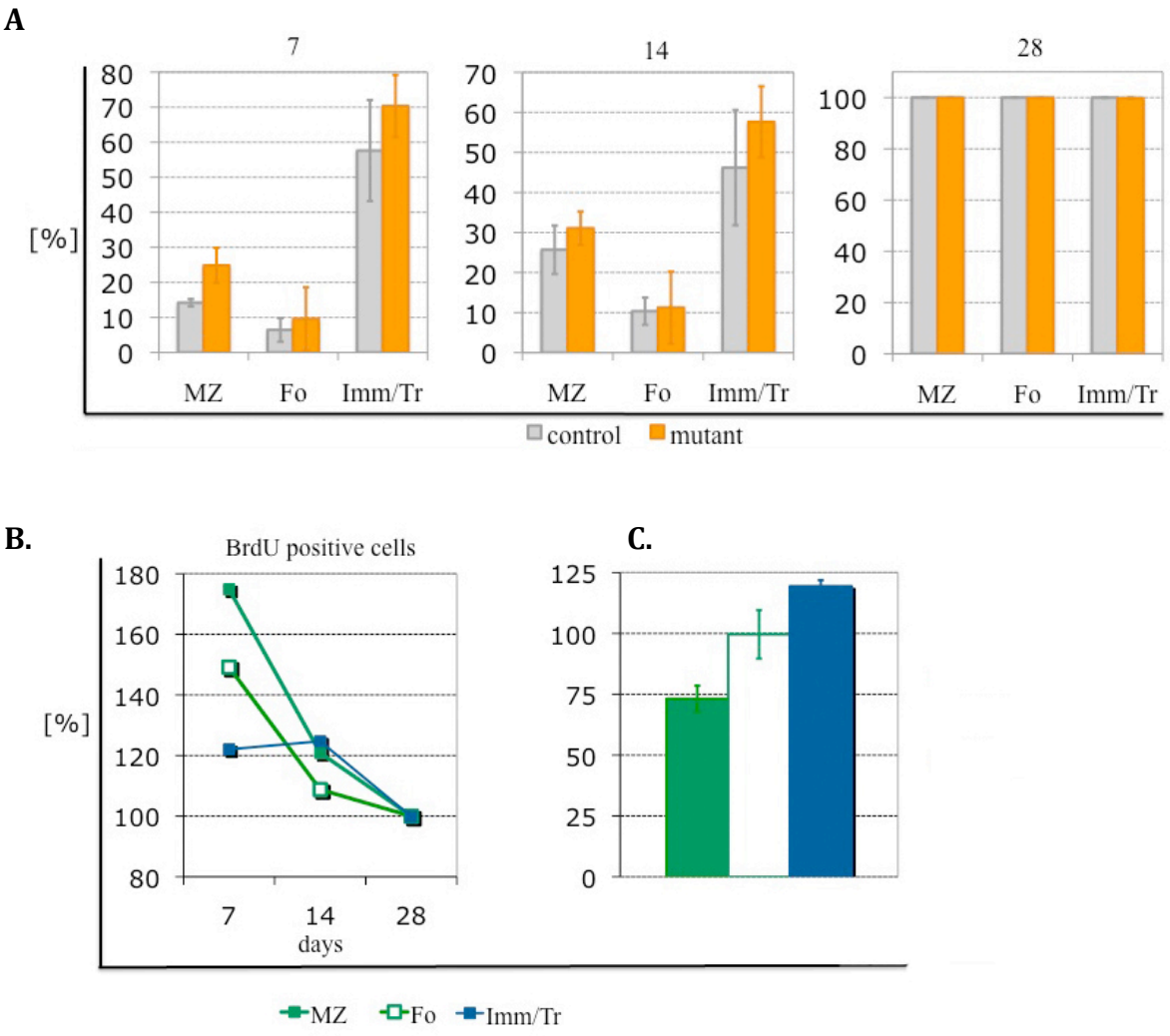

Figure 23. ***In vivo*** **BrdU labelling – flow cytometry analysis; A.** Average percentage of BrdU positive cells after 7,14,28 days of application; **gray** – control, **orange** – mutant; **B.** Average percentage of BrdU positive cells in mutant mice in respect to the control. The values of control mice are set to 100%. **C.** Average percentage of lymphocyte subsets of splenic B lymphocytes; **MZ** – marginal zone B cells (panel B and C – green), **Fo** – follicular B cells (panel B and C – white with green line), **Imm/Tr** – immature/transitional B cells (panel B and C – blue); **control** - +/F/CD21-Cre, **mutant** - Mll2F/F/CD21-Cre.

3.5 Molecular analysis of B lymphocytes from Mll2KO/F/CD21-Cre line

Mll2, a histone methyltransferase of lysine 4 of histone H3 (H3K4) is involved in the epigenetic regulation of development. In several recent studies on *Drosophila melanogaster* model of cancer Notch family was associated with epigenetic regulation of differentiation through histone methylation and demethylation (Ferres-Marco et al., 2006; Herz et al.). Previously, in a number of examples Notch family genes were demonstrated to control cell commitment into different lineages (Artavanis-Tsakonas et al., 1995; Artavanis-Tsakonas et al., 1999; de la Pompa et al., 1997; Tanigaki et al., 2001) including lymphopoiesis (Tanigaki and Honjo, 2007; Tanigaki et al., 2003). Moreover Notch2 was found to be essential in marginal zone B cell (MZ) specification (Saito et al., 2003; Tanigaki et al., 2002; Witt et al., 2003). Furthermore, several genes involved in Notch2 signaling were also shown to play a fundamental role in MZ development, such as Delta-like1 (Dll1) (Hozumi et al., 2004) – a Notch2 ligand, and Mastermind-like (Maml1) (Wu and Griffin, 2004; Wu et al., 2007), Lunatic and Manic Fringe (Lfng and Mfng) (Tan et al., 2009) – Notch2 coactivators. Hence I analyzed by qPCR the expression of these key MZ B cell regulators. I also checked the expression of Mll2 and Mll1 and of one of target genes of Notch, Hes1 (Fan et al., 2004). In addition, with a purpose of understanding the molecular profile of residual MZ B cells upon Mll2 depletion, I compared through cDNA microarrays the transcriptomes of control and mutant cells.

3.5.1 qPCR expression analysis of key regulator factors involved in marginal zone B cell specification

In order to elucidate the molecular basis for the reduction of the marginal zone (MZ) B cell compartment in Mll2 mutants, I analyzed by qPCR the expression of several genes that have been shown to be indispensable for MZ B cell development. Notch2, Maml1, Lfng and Mfng and Hes1 were all shown to be involved in the formation of the MZ B cells. Notch2 gene has been shown as the only one of Notch family to be preferentially expressed in the mature B cells. Its deletion leads to almost complete ablation of MZ B cell compartment and their CD1d^{high} precursors (Saito et al., 2003). Similarly, deletion any of following, Notch2 coactivator – Maml-1 or Notch2 ligand - Dll1, leads MZ B cells depletion (Hozumi et al., 2004; Wu et al., 2007). Lfng and Mfng were demonstrated to cooperatively enhance the Dll1-Notch2 interaction in promoting MZ B cell development (Tan et al., 2009). Hes 1 was chosen as one of the best know target of Notch. Additionally the level of Mll2 and Mll1 mRNA were controlled.

Splenic lymphocytes were isolated and stained for CD21, CD23 and CD19 markers in FACS buffer as indicated in the table below. This allowed to quantitize and FACS sort (2.2.17.1) marginal zone B cell (CD19^{high} - CD21^{high} - CD23^{low}) and follicular B cell (Fo) (CD19 ^{high} - CD21^{interm} - CD23^{high}) populations. cDNA was synthesized from 500ng (2.2.2) of total RNA (2.2.1.4) from cells of each compartment. qPCR analysis was performed with TaqMan probes (2.2.11). Levels of Mll2, Mll1, Notch2, Lfng, Mfng and Hes1 were normalized to the follicular B cells sample from the control mouse. qPCR reactions were performed separately for Mll2, Mll1, Notch2, Maml1 and Mfng, Lfng, Hes1 therefore are presented as two separated analysis (panels A and B of Figure 24 – respectively).

The analysis revealed similar levels of all analyzed genes of both MZ and Fo B cell compartments of control and mutant mice (Fig. 24 A and B). Moreover the level of Mll2 mRNA was still high, despite the very high degree of Cre-mediated deletion of the Mll2

gene previously detected by genomic qPCR (3.3.5) (Fig. 13 and further discussed in 3.5.2). It is important to point out the detected mRNA is transcript of frameshifted Mll2FC allele (Glaser et al., 2006).

On the basis of these results we can rule out that the reason for the selective decrease of the MZ subpopulation in Mll2 mutants is due to the downregulation of the known critical regulators of MZ cell fate. A second conclusion is that MZ B cells of control animals and the residual MZ B cells from the mutants appear to be similar, at least as far as the expression of these key regulators is concerned. This leads me to hypothesize, for the Mll2 deficient MZ cells that are still present in the spleen, a compensatory mechanism that has allowed them to develop nonetheless to acquire the mature marginal zone B fate. As qPCR results show, however, this compensatory mechanism does not involve the Mll1 gene, since its expression does not increase upon Mll2 depletion (Fig.24 A)

lymphoid organ	antibodies
spleen	CD21 FITC
	CD23 PE
	CD19 Cy7 PE

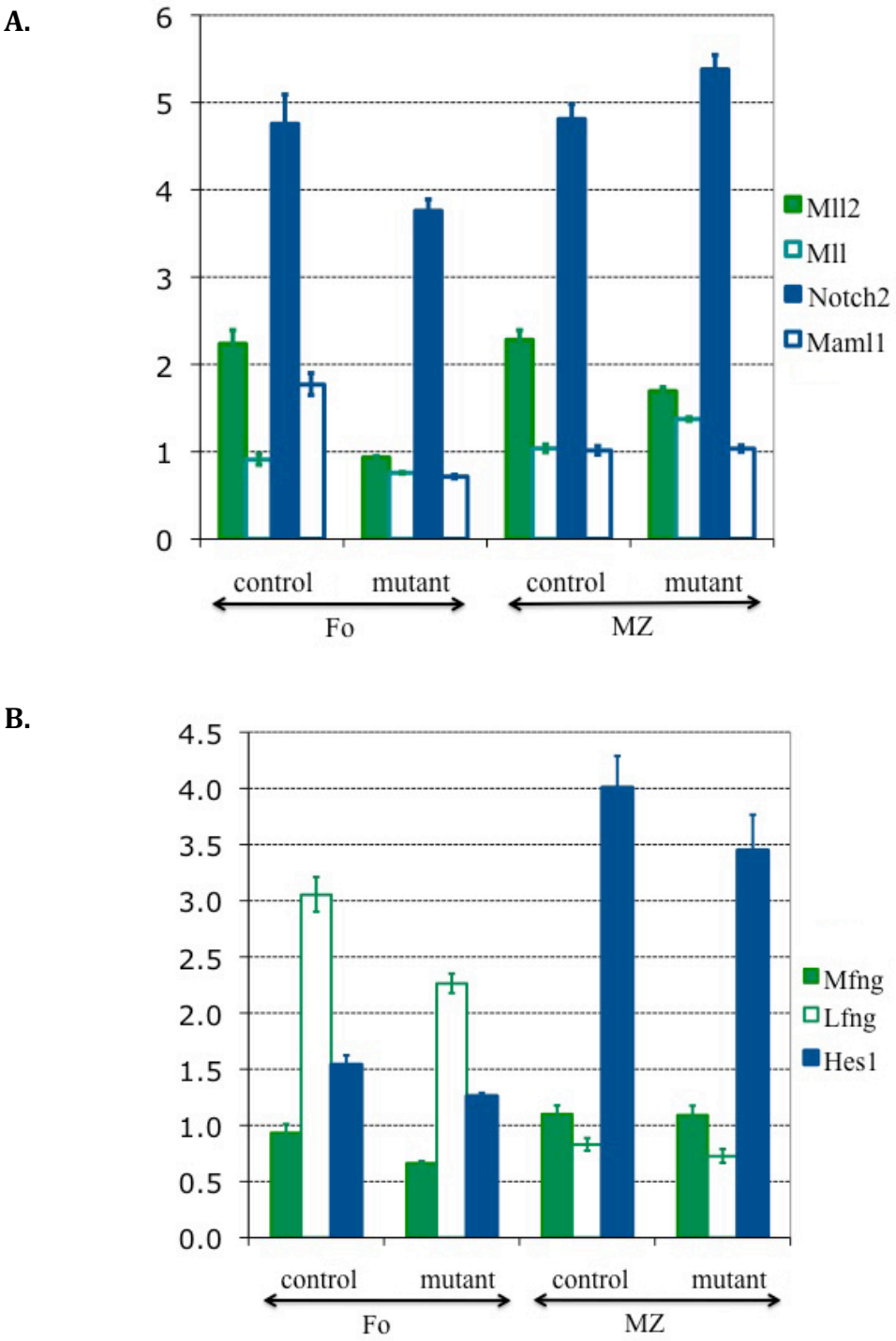

Figure 24. qPCR expression analysis of the Mll2, Mll1 and several Notch2 pathway genes in follicular and marginal zone B cells of control and mutant animals from Mll2KO/F/CD21-Cre line. A. qPCR expression analysis of Mll2 (green), Mll1 (white with green line), Notch2 (blue) and Maml1 (white with blue line); **B.** qPCR expression analysis of Mfng (green), Lfng (white with blue line) and Hes1 (blue); **MZ** – marginal zone B cell, **Fo** – follicular B cell; ; **control** - +/F/CD21-Cre mouse, **mutant** – Mll2KO/F/CD21-Cre mouse.

3.5.2 qPCR analysis of the Mll2 and Mll1 mRNA in FACS sorted lymphocytes

In order to analyze the level of Mll2 mRNA after CD21-Cre-mediated deletion as well as the expression of Mll1, upon Mll2 loss, in all, previously not analysed, B cell compartments I performed qPCR analysis of both genes. Despite the previous results (3.5.1; Fig. 24 A) it was possible that perhaps the mRNA of Mll1 is indeed upregulated in others than marginal zone and follicular B cell compartments.

In order to analyze the levels of Mll2 and Mll1 mRNA after Cre-mediated deletion total RNA was isolated from samples described previously (3.3.5). cDNA was synthesized from 500ng of total and qPCR analysis of Mll2 and Mll1 with TaqMan probes was performed. Levels of Mll2 and Mll1 mRNA were normalized to the Pre/Pro B sample from the control mouse. qPCR analysis showed that the level of Mll2 mRNA is still high in the IgM positive B, marginal zone B, follicular B and B1 cells where deletion occurs. Previous publication demonstrated the loss of Mll2 protein within 48h after Cre-mediated deletion (Glaser et al., 2009). Based on my previously discussed results (3.2.2 – 3.2.4, 3.5.2; Fig. 11 – 13, 20) proving genetic deletion of Mll2 gene upon CD21-Cre recombination, and on previously reported findings, it is possible that the frameshifted allele escapes nonsense mediated mRNA decay (Glaser et al., 2009 and personal communication). We can observe small increase in the Mll1 mRNA level in marginal zone B cells (Fig. 25), however based also on previous results (3.5.1; Fig. 24 A) it is not possible to conclude ultimately that upon Mll2 deletion, Mll1 becomes upregulated to fulfil a partially redundant function. The differences in the results 3.5.1 and 3.5.2 (Fig. 24 and 25) most probably result from the sum of such factors like discussed previously (3.1.2) partially mixed background of Mll2KO/F/CD21-Cre line and so individual differences between animals from different litters. It is clear however that loss of Mll2 does not cause a sticking upreguletion of Mll1,

hence it is possible that different H3K4 HMTs are involved in a potential compensatory mechanism.

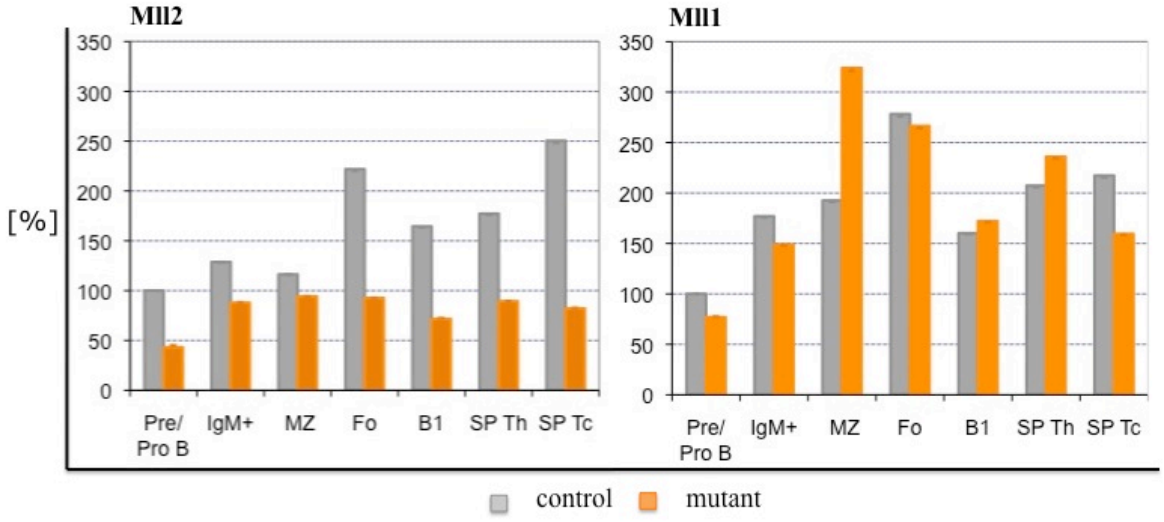

Figure 25. qPCR analysis of the Mll2 and Mll1 mRNA in in different B and T lymphocyte subsets Mll2KO/F/CD21-Cre line. Pre/Pro B – Pre/Pro B cell, **IgM+** - IgM positive B cell from bone marrow, **MZ** – marginal zone B cell, **Fo** – follicular B cell, **B1** – B1 B cell from peritoneal cavity, **SP Th** – spleenic T CD4+ cells, **SP Tc** – splenic T CD8+ cells; **control** - +/F/CD21-Cre mouse, **mutant** – Mll2KO/F/CD21-Cre mouse.

3.5.3 Microarray analysis of Mll2 deficient marginal zone B cell transcriptome

Previous analysis did not reveal any major difference in the expression of genes important for marginal zone B cell (MZ) differentiation upon Mll2 deletion (3.5.1 – 3.5.2 and Fig. 24 and 25). Therefore to gain further insight into the mechanisms of Mll2-dependent MZ cell homeostasis, I probed global alterations in gene expression through cDNA microarrays, profiling and comparing transcriptomes of Mll2 proficient and deficient sorted MZ B cells.

Splenic lymphocytes from two control and two mutant animals were isolated and stained for CD21, CD23 and CD19 markers in FACS buffer as indicated in the table below. That allowed FACS sorting (2.2.17.1) marginal zone B cell (CD19high - CD21high - $CD23^{low}$) population. cDNA was synthesized from 500ng (2.2.2) of total isolated RNA. RNA from one control – mutant pair was isolated using Tri Reagent (2.2.1.4) and purified with RNeasy® Plus Micro Kit according to the QIAGEN protocol supplied with the kit (protocol is further called "Q"). RNA from the second control – mutant pair was processed using RNeasy® Plus Micro Kit (protocol is further called "PM") Due to technical constraints, the two sets of samples were processed in two separate rounds with different RNA isolation kits. Hence, due to different RNA isolation method both control – mutant couples were analysed separately. Samples were hybridised to the GeneChip® Mouse Gene 1.0 ST Array (Affymetrix). This chip has arrayed 750,000 of 25bp long oligonucleotides that together compose a probe set of over 28,000 genes and so enables whole-genome gene level expression analysis.

Background were corrected with Robust Multi-array Average (RMA) (Bolstad et al., 2003). Next the data were normalized with Quantile normalization and in order to estimate the mean value of each probeset, data were summarized with median polish (Irizarry et al., 2003). Data were imported and analyzed with Partek GS 6.5 (Partek, 2008). To assess the significance of the differences between the two gene lists (control versus mutants) a two-way ANOVA (analysis of variance) was performed. Factors taken onto account in the two-way ANOVA test were protocol and genotype. To exclude the fraction of variation attributable to the difference in protocol, two gene lists were created. List A contains genes that vary between two genotypes (control vs. mutant) and list B contains genes that vary between two protocols (Q vs. PM). P values ($p < 0,05$) from both lists were adjusted for the false discovery rate (FDR) > 0,05. Finally, to avoid all genes whose difference in expression was only attributable to the difference between protocols, a final list of genes was created subtracting list B from list A (A – B). cDNA synthesis and biotinylation as

well as hybridization and statistical analysis, was performed by Affymetrix Microarray Unit of Cogentech on the IFOM-IEO-Campus, Milan (Italy) according to the indications of Affymetrix.

Principal component analysis (PCA) of 3 different principal components of variability (PC) indicates 75,1% of difference between control and mutant samples. Principal component 1 (PC1) – protocol (Q vs. PM) explains 48,9% of variability between samples. Interestingly about 25% of the difference is consistent between PC2 (26,2%) and PC3 (24,9%) which demonstrates that MZ B cells lacking Mll2 are distinct from control cells (Fig. 26). Principal component analysis (PCA) transforms a number of possibly correlated variables into a smaller number of uncorrelated variables - principal components (PC). The first principal component accounts for as much of the variability in the data as possible, and each succeeding component accounts for as much of the remaining variability as possible. PCA provides information if two samples are different.

Partially the 25% of difference can be explained comparing transcriptomes of Mll2 proficient and deficient marginal zone B cells. Doing so I have found the list of 42 genes aberrantly expressed with a fold change higher than 1,5 and a corrected p value < 0.05. Among 42 genes 33 were down regulated in mutant samples in comparison to the control (fold change: 1,5 – 2,8) and 9 were up regulated (fold change: 1,5 – 2,1). Genes are listed in the Table 1. Unfortunately, differences between control and mutant MZ B cells in analyzed samples are masked by the differences in protocols used for RNA isolation, therefore interpretation became very complex and requires more samples that would clarify it. Heatmap visualization of the microarray analysis is presented on the Figure 27.

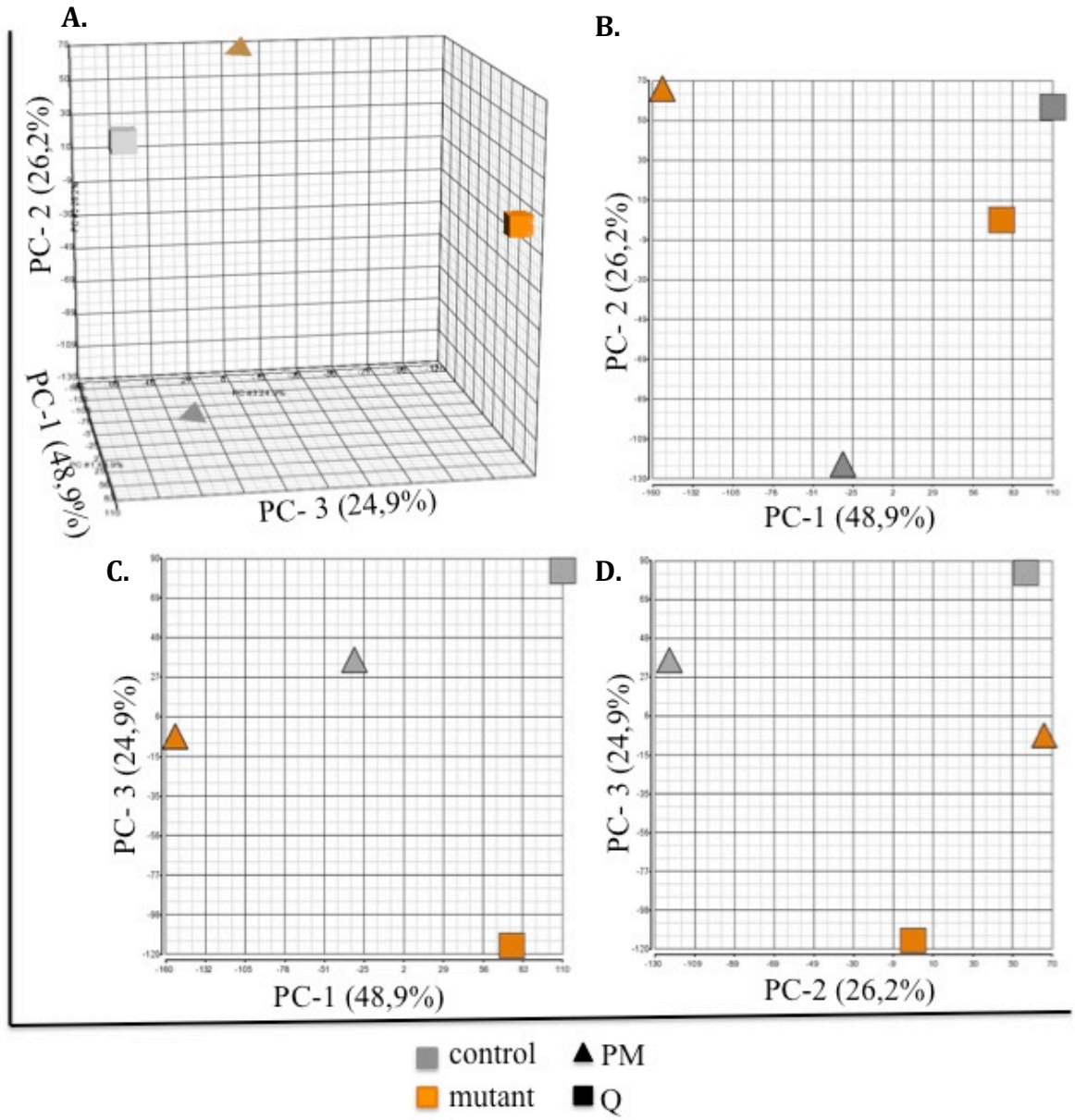

Figure 26. Microarray analysis of Mll2KO/F/CD21- Cre marginal zone B cells transcriptome - Principal Component Analysis (PCA). A. 3D visualization of plotted together PC1 – axes Z, PC2 – axes Y, PC3 – axes X**; B.** 2D visualization of plotted together PC1 – axes X, PC2 – axes Y; **C.** 2D visualization of plotted together PC2 – axes X, PC3 – axes Y; **D.** 2D visualization of plotted together PC2 – axes X, PC3 – axes Y; **gray** – control, **orange** – mutant; **triangle** – protocol PM, **square** – protocol Q; **control** - +/F/CD21-Cre mouse, **mutant** – Mll2KO/F/CD21-Cre mouse.

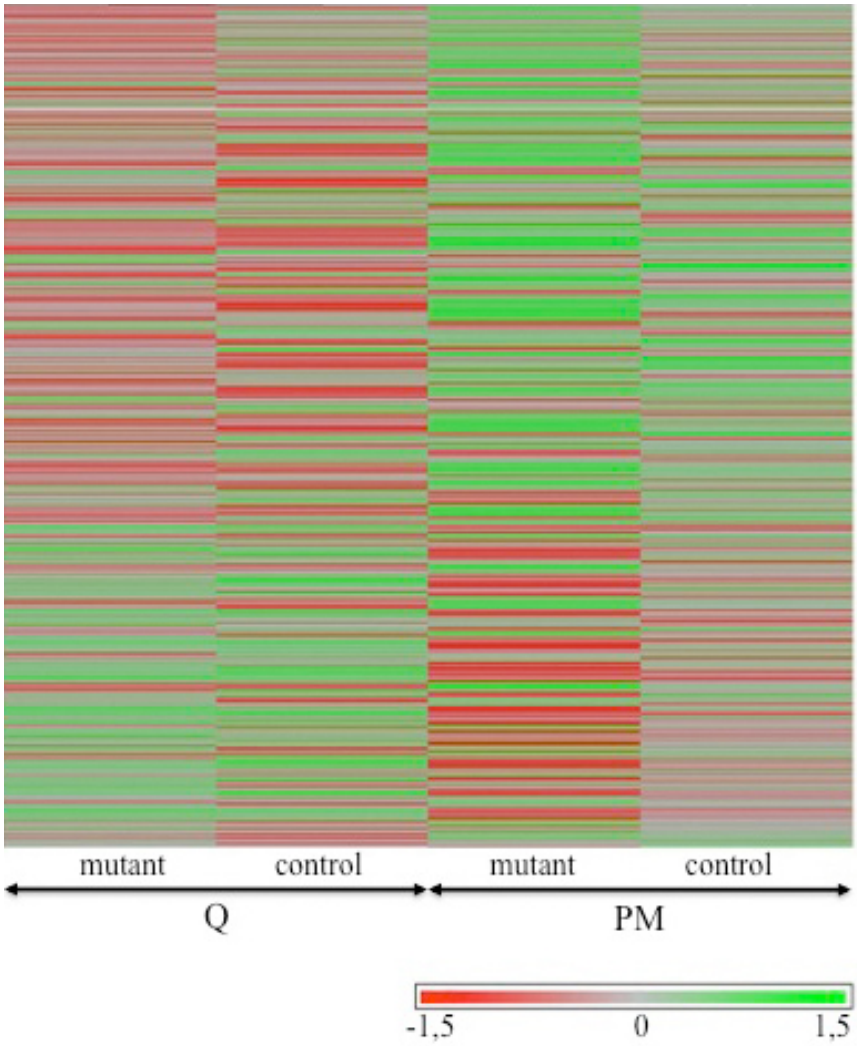

Figure 27. Microarray analysis of Mll2KO/F/CD21- Cre marginal zone B cells transcriptome – heatmap visualization. Fold change -1,5 – 1,5; **red** – downregulation mutant versus control, **gray** – no change, **green** – upregulation muatn versus control; **Q** – Qiagen protocol, **PM** - RNeasy® Plus Micro Kit protocol; **control** - +/F/CD21-Cre mouse, **mutant** – Mll2KO/F/CD21-Cre mouse.

Probeset ID	Gene symbol	RefSeq	p value	Fold change
10358928	Cacna1e	NM_009782	0.0359215	-2.87146
10402665	Cdc42bpb	NM_183016	0.0313497	-2.28411
10464251	Atrnl1	NM_181415	0.015538	-2.23516
10528090	Rundc3b	NM_198620	0.0121782	-2.1874
10402020	Eml5	NM_001081191	0.0133498	-2.08309
10353272	Stau2	NM_025303	0.036835	-2.07509
10583952	Ncapd3	NM_178113	0.0156119	-1.98492
10516393	Eif2c4	NM_153177	0.0252873	-1.97972
10376885	Snord49b	AF357373	0.0392474	-1.96823
10442250		---	0.0202034	-1.91526
10368647	Dse	NM_172508	0.0126036	-1.86656
10528880	Lmbr1	NM_020295	0.0145952	-1.86582
10463704	As3mt	NM_020577	0.0442185	-1.84325
10586967	EG639396	NM_001039251	0.00324593	-1.82935
10503251	2610301B20Rik	NM_026005	0.0316377	-1.82791
10362294	Arhgap18	NM_176837	0.0388939	-1.811
10582388		---	0.00877676	-1.76667
10492584		---	0.0094679	-1.7574
10564220	LOC100046764	XR_032907	0.033058	-1.73978
10441511			0.0470261	-1.72836
10453636	Svil	NM_153153	0.000142646	-1.71707
10369176	D630037F22Rik	NM_001033385	0.00277962	-1.67588
10504891	Tmeff1	NM_021436	0.04157	-1.6607
10392642	Abca5	NM_147219	0.0265	-1.65574
10397683	Ttc8	NM_198311	0.0169848	-1.64679
10407327	Emb	NM_010330	0.0374876	-1.63859
10409660	Gkap1	NM_019832	0.037364	-1.63629
10445293	Pla2g7	NM_013737	0.0435272	-1.61716
10598023		---	0.0483347	-1.6144
10571274	Gsr	NM_010344	0.0147039	-1.59544
10395684	Nubpl	NM_029760	0.0408717	-1.57881
10403466	Dip2c	NM_001081426	0.0471327	-1.56629
10386921	Zfp287	NM_133208	0.039646	-1.55015
10491960		---	0.0122894	1.5037
10488465	Zfp345	NM_001034900	0.0307611	1.51627
10597020	Fbxw14	NM_015793	0.0328633	1.52508
10404069	Hist1h1a	NM_030609	0.0125848	1.54402
10564565	EG665570	XR_033989	0.0434637	1.55646
10490203		---	0.0236234	1.58313
10424670	Hemt1	NM_010416	0.0157512	1.64361
10478523		---	0.0195483	1.80265
10404772	ENSMUSG00000074927	ENSMUST00000099561	0.0262096	2.16488

Table 1. **Microarray analysis of Mll2 deficient marginal zone B cell transcriptome**. Genes shown in the table differ between control and mutant samples (both up and downregulation) independently of the RNA isolation protocol and have fold change higher than 1,5, $p < 0,05$ corrected by FDR <0.05. Chip: GeneChip® Mouse Gene 1.0 ST Array (Affymetrix).

4. Discussion

4.1 Lymphopoiesis and H3K4 methylation mark

Such complex process as cell specification requires a tight regulation that controls switching between different transcriptional programs – silencing one and establishment and maintenance of another. Control of this reprogramming is, in a substantial part, epigenetic (Bernstein et al., 2007; Bhaumik et al., 2007) and consists of several different modifications among which covalent posttranslational modifications of histones seems to play the most important role as is the most plastic and dynamic (Su et al., 2004).

In present work I present the data supporting the importance of the H3K4 methyltransferase Mll2 in lymphopoiesis. Following previous results demonstrating requirement of Mll2 for the activation and timing of lineage-specific transcriptional programs (Andreu-Vieyra et al., 2010; Glaser et al., 2009; Lubitz et al., 2007), I propose Mll2 as a component of a B cell development regulatory system. Despite the extensive studies about the role of Mll2, due to the embryonic lethality of Mll2 ablation, all the work was focused at the early stages of development and very little was known about the function of this key epigenetic regulator in differentiating cell compartments of adult animals. Therefore applying conditional mutagenesis I investigated the role of Mll2 in mature B cell compartments. To this end I employed the Mll2 conditional knock-out mouse line (Glaser et al., 2006) generated according to the "knock-out first" strategy (Testa et al., 2004) via which Mll2 gene was targeted with a trap cassette (Testa et al., 2004; Testa et al., 2003) (Fig. 4). In order to knock out Mll2 specifically in mature B cells I selected the CD21-Cre3A mouse line that expresses Cre recombinase under the CD21 promoter established by inserting Cre gene into CD21/35 locus on a bacterial artificial chromosome (Kraus et al., 2004) (Fig. 5). Cre-mediated deletion follows the expression of

CD21, which takes place at the immature B to mature B cell transition (Kraus et al., 2004; Takahashi et al., 1997) (Fig. 6).

Previously, number of evidences proved a critical role of H3K4 methylation in B cell development and maturation. Pax5-dependent enrichment of H3K4me2 and H3K4me3 was found at the promoters and immediate downstream sequences of the nine Pax5 target genes (Schebesta et al., 2007). As Pax 5 has been proven to be essential for the development and identity of B cells (Horcher et al., 2001) we can expect that block of Pax5 regulation pathway leads to a developmental arrest, similarly to the arrest that occurs in case of deletion of Pax5 itself (Nutt et al., 1998; Nutt et al., 1997). To the advantage of this hypothesis operates the colocalization of H3K4me2 and H3K4me3 at the promoter of Rag1/2, one of Pax5 target genes (Schebesta et al., 2007), together with the numerously demonstrated indispensability of Rag1/2 for the B cell development (Matthews et al., 2007; Mombaerts et al., 1992; Oettinger et al., 1990; Shinkai et al., 1992). Consecutively with colocalization of H3K4me2 and H3K4me3 marks at the Rag1/2 promoters, the same epigenetic marks were found at the V(D)J clusters of immunoglobulin during their rearrangement. (Corcoran, 2005; Goldmit et al., 2005; Matthews et al., 2007; Morshead et al., 2003; Oettinger et al., 1990; Perkins et al., 2004). Interestingly so far none of the six known H3K4 methyltransferases was associated with the regulation of lymphopoiesis. However Mll2 was clearly proven to play a decisive role in the commitment to germ lineages and to be essential for the tightly timed establishment of lineage specific transcriptional programs (Andreu-Vieyra et al., 2010; Glaser et al., 2009). Moreover, Mll2 was demonstrated to be recruited in a lineage-specific manner during the establishment and maintenance of a transcriptional program in cells of the hematopoietic lineage (Demers et al., 2007). Hence I would like to discuss role of Mll2 as a putative lymphopoietic regulating factor that provides H3K4 methylation at the critical for lymphopoiesis loci.

4.2 Effect of the loss of Mll2 during B cell maturation

Mll2 was found to be expressed throughout B cell development in wild type animals (1.4; Fig. 1 and 2), thus suggesting that it may be implicated throughout entire lifespan of B cells. Conditional ablation of Mll2 at the stage of immature B into mature B cell transition allowed me to elucidate the role of Mll2 specifically in the mature B cell compartments (3.1.2, 3.2.2 – 3.2.4; Fig. 4, 11 - 13). Flow cytometry analysis at different stages of B cell development, did not reveal significant changes in most B cell populations. As expected bone (BM) marrow subpopulations of Pre and Pro B cells as well as splenic (SP) and bone marrow immature and transitional cells were not affected (Fig. 15 A, 16 A and 17 A). That is due to the specific occurrence of the Cre-mediated deletion along the CD21-Cre expression (Kraus et al., 2004), which takes place during B cell maturation in the spleen (Takahashi et al., 1997). Similarly most of the analyzed compartments of mature B cells were comparable between control and mutant animals. B1 and B2 lymphocytes from peritoneal cavity and spleen, germinal center B cells from mesenteric lymph nodes, Peyer's patches and spleen as well as T lymphocytes from thymus, spleen and mesenteric lymph nodes were not affected by loss of Mll2. All, small observed differences had weak statistical support ($p > 0,9$) (Fig. 15 – 17). In contrast, the splenic marginal zone B cell (MZ) compartment was found to be strongly reduced in mutants. Average size of MZ compartment in the 53 analyzed mutant animals was scored to 56,82% of a size in their sex matched littermates (Fig. 17 and 18). Importantly this reduction was consistent regardless of the surface markers used to define MZ B cell population (Fig. 18). Specifically, the size of the MZ population in mutants was reduced by 43,18%, 55,15% and 49,59% when defined by, respectively, the following combinations of markers as $CD21^{high}$ - $CD23^{low}$ - $CD19^{high}$ $CD1d^{high}$ - $CD23^{low}$ - $CD19^{high}$ and $CD38^{high}$ - $CD23^{low}$ - $CD19^{high}$ (3.3.2 – 3.3.3; Fig. 17 and 18). In addition, decreased size of the MZ B cell population was consistent with the reduction in total number of MZ B cells (3.3.1;). Total number of mutant MZ B

cells was lower by 28,13% in comparison to the control (p = 0,02) (Fig. 14 B). Furthermore the reduced size of the MZ compartment was confirmed by immunofluorescence analysis of the splenic sections in mutant mice. Taken together flow cytometry (3.3.1 – 3.3.3; Fig. 14 - 18) and immunofluorescence (3.3.4; Fig. 19) results confirmed strong reduction of marginal zone B cell population upon loss of Mll2. Moreover this reduction was limited to the MZ compartment (3.3.1 – 3.3.3). It is important also to highlight that all observation were independent of the allelic configuration (Fig. 4). Cohort of mice that lost both copies of Mll2 abruptly as opposed to mice that developed with only one copy of wild type Mll2 were not significantly different in terms of marginal zone B cell compartment. Comparable analysis of flow cytometry results of cohorts carrying one Mll2 KO allele and one Mll2F conditional allele (Mll2KO/F/CD21-Cre or Mll2KO/F/CD21-Cre) – 21 control-mutant pairs analyzed, or mice carrying both Mll2F alleles (Mll2F/F/CD21-Cre) - 32 pairs, demonstrated a similar reduction in the MZ subpopulation (Fig. 4, 8 and 17 A).

Interestingly testing the dynamics of the MZ compartment I found that the Mll2 deficient MZ B cells displayed higher rates of proliferation than control cells. Already after 7 days of BrdU administration, 74,85% more mutant MZ B cells were BrdU positive in comparison to control cells (3.4.3 Fig. 23). An increase in the proliferating fraction, however to lower extent, was also observed in mutant follicular and immature/transitional B cells. This suggests a higher turnover of splenic B cell populations upon loss of Mll2 and it is tempting to speculate that this may reflect the presence of a secreted stimulus promoting cell proliferation as part of a feed back loop triggered by the decrease in MZ B cells. The increased turnover was found to affect, however, also the Fo and Imm/Tr populations, which are not decreased in the mutants, suggesting that it may also reflect an additional effect of Mll2 ablation on the homeostasis of the proliferating pools that is independent of its role in the homeostasis of the mature B cell lineages. Furthermore, in an *in vitro* proliferation assay, in which the vast majority of B cells belong to the follicular

fraction, I did not detect increased proliferation upon Mll2 ablation (Fig. 22 A and B). Therefore in order to acquire conclusive evidence on the in vivo B cell dynamics upon loss of Mll2, particularly for the MZ B cell compartment, I am performing a complementary long term pulse-and-chase BrdU labelling experiment, that not only will assess the rate of turnover, but also by tracing cells for several months will demonstrate the self renewal capacity of Mll2 deficient MZ B cells.

Functional analysis of mutant MZ B cell compartment revealed their reduced capacity in mounting a response to an antigen stimulus. As mentioned above marginal zone B cells raise T-independent immunological response against blood borne antigens. When tested for their ability to respond to a specific, T-cell independent antigen – such as NP-Ficoll Mll2 deficient cells were able to respond to the antigen, but they were not capable of switching immunoglobulin class. In control animals, 28 days after immunization with NP-Ficoll, levels of IgM, remained the same whereas levels of IgG3 rose by 103,07% (3.5.1; Fig. 21 B), demonstrating the same the capacity of control animals to switch the class of secreted immunoglobulin from IgM to IgG3. In contrast, although mutant cells were still able to respond on the antigen challenge, they where not efficient in switching the immunoglobulin class. Thus, the concentration of IgM in the serum of mutant animals, after 28 days of immunization, was higher by 94,08% in comparison to its concentration at the day 0, while the concentration of IgG3 rose by only 36,59% (Fig. 21 B). On the other hand, after the *in vitro* IL-4 stimulation, 37,07% more mutant $CD19^{high}$ cells (in vast majority follicular B cells) switched the class of immunoglobulin from IgM to IgG1 (3.4.2; Fig. 22 C). Together, while Fo B cells show the capacity to switch the immunoglobulin class after IL-4 stimulation, MZ B cells were able to mount the primary response to the antigenic challenge, but they were not able to switch the immunoglobulin class. It is difficult however to compare two *in vivo* e *in vitro* experiments as they differ both in the approach and in the nature of the triggering stimulus. While this precludes a direct one to one comparison of the two sets of data, it is nevertheless possible to conclude that upon *in*

vivo immunization, Mll2 deficient MZ B cells are not efficient in switching the immunoglobulin repertoire. In turn, this suggests that Mll2 may be also required for the rearrangement of Ig loci and/or regulation of transcriptional factors involved in the process of the rearrangement of constant clusters of Igh, for example AID. This is even more plausible hypothesis if consider recently published link between loss of Mll3/Mll4-dependent H3K4 methylation and defects in Ig class switch recombination (CSR) (Daniel et al., 2010). It is possible that Mll2 as well is involved in CSR. What is more, it is possible that exist H3K4 HMT (or generally, epigenetic) and Ig class specificity. I would be exceptionally remarkable to find the pattern of specificity of histone methyltransferases catalyzing the methylation of H3K4 and switching to different Ig classes (also upon different stimuli). Furthermore, if this speculation would be confirmed, the HMTs (and putatively other epigenetic players) specificity would be very probable.

4.3 Role of Mll2 in the homeostasis of marginal zone B cell compartment

Marginal zone B cells are characterized by unique phenotypic and functional properties. They express high levels of CD19, CD220, CD21, CD1d, CD38, IgM, and low levels of CD23 and IgD. They are localized at the margin of splenic follicles, between white and red pulp (Martin and Kearney, 2002) (Fig. 19 A). Their localization exposes them at the constant stimulation with the antigens carried by the blood flow through the spleen, and indeed they are the first line of the humoral response raised against polysaccharides of cell wall of encapsulated bacteria (Lane et al., 1986). Similarly to the B1 cells, they are involved in the T-independent immunity of the organism (Garcia de Vinuesa et al., 1999; Martin et al., 2001), however their indirect participation in the T-dependent response was also suggested (Cinamon et al., 2008); (Ferguson et al., 2004). Similarly to the follicular B cells they arise from newly formed immature B cells that migrated from the bone marrow to the spleen. Several models have been proposed regarding the ontogeny of this highly

specialized B cell lineage. All of them agree that, similarly to the follicular B cells, MZ B cells develop through transitional stages of T1 and T2 cell that are characterized by high levels of the CD93 surface marker and are distinguishable among each other by the level of CD23 (T1 are $CD93^{high}$ - $CD23^{low}$ - $CD21^{neg\text{-}low}$ - IgM^{high} - $IgD^{neg\text{-}low}$ and T2 are $CD93^{high}$ - $CD23^{high}$ - $CD21^{low}$ - IgM^{high} IgD^{high}) (Srivastava et al., 2005). Allman and coworkers proposed a refinement of this model, according to which MZ B cells pass also through a transitional stage of T3 ($CD93^{high}$ – $CD23^{high}$ – $CD21^{low}$ – IgM^{low} - IgD^{high}) cells and/or can origin directly from follicular B cells (Allman et al., 2004; Srivastava et al., 2005). Furthermore, a very interesting characteristics of this population was described in 2001, when Rajewsky and coworkers, demonstrated, by blocking bone marrow efflux of B cell progenitors, that the only population that remained intact was the splenic marginal zone B cell compartment (Hao and Rajewsky, 2001), positing for this compartment a unique self renewal capacity. In order to understand the molecular mechanism that lies at the bottom of the reduction of MZ B cell compartment in Mll2 mutants, I explored in residual MZ cells the status of the molecular pathways known to be involved in the homeostasis of MZ cells. Expression analysis of several genes that have been shown to be essential for MZ B cell development did not reveal any changes at the mRNA level. Notch2, Maml1, Lfng and were all shown to be indispensable for the formation of MZ B cells (Hozumi et al., 2004; Saito et al., 2003; Tan et al., 2009; Wu et al., 2007). The Notch2 gene has been demonstrated as the only Notch family member to be preferentially expressed in mature B cells. Its deletion leads to almost complete ablation of MZ B cell compartment and their $CD1d^{high}$ precursors (Saito et al., 2003). Similarly, deletion of any of following, Notch2 coactivator – Maml1 or Notch2 ligand - Dll1, leads to MZ B cells depletion similar to the one observed in case of the deletion of Notch2 (Hozumi et al., 2004; Wu et al., 2007), while Lfng and Mfng were demonstrated to cooperatively enhance the Dll1-Notch2 interaction in promoting MZ B cell development (Tan et al., 2009). Unexpectedly upon loss of Mll2 none of the mentioned key regulators of the homeostasis of MZ B cell

compartments were aberrantly expressed (3.5.1; Fig. 24). Similarly, microarray analysis of the transcriptome of sorted MZ B cells did not reveal remarkable differences between Mll2 deficient and proficient cells (3.5.3; Fig. 26 and 27). Principal component analysis (PCA) of the microarray data indicated consistent differences between control and mutant samples, however it was impossible to make any final conclusions before performing additional analysis on more samples.

The lack of significant changes in gene expression between control and mutant samples is very indicative. Together, the qPCR and microarray data suggest that the residual 40% of MZ B cell population that is still present upon Mll2 loss is composed of cells that by and large do not differ from the control cells despite the ablation of Mll2. This apparent lack of differences is not complete as Mll2 deficient MZ B cells were proven to be impaired in their ability to change the transcriptional program as suggested by their strikingly ineffective immunoglobulin class switch (Fig. 21). The inability to alter gene expression programs upon loss of Mll2 can be conceptualized in the light of recent findings demonstrating that Mll2 is only transiently required at defines stages during gametogenesis and gastrulation (Andreu-Vieyra et al., 2010; Glaser et al., 2009; Lubitz et al., 2007). Thus loss of Mll2 leads to a pronounced decrease of the proliferative potential of embryonic stem cells and delays in the differentiation process (Lubitz et al., 2007). Similarly lack of Mll2 leads to both male and female infertility (Andreu-Vieyra et al., 2010; Glaser et al., 2009). Together, these data demonstrate that Mll2 is clearly involved in the activation of specific trascriptional programs during differentiation. The work I have presented adds to this emerging knowledge, by revealing that Mll2 is required not only during early developmental transitions but also in terminally differentiated cells. H3K4 methylation was demonstrated to be required for the correct V(D)J rearrangement and Igh assembly (Corcoran, 2005; Matthews et al., 2007; Morshead et al., 2003). In consequence aberrant expression of BCR would lead to abnormal signaling required for the follicular vs. marginal zone B cells transcriptional decision (Casola et al., 2004; Kraus et al., 2004),

what further could lead to the abnormal formation of marginal zone B cell compartment. This hypothesis is clearly in the accordance with the Allman's model of MZ B cell development (Allman et al., 2001; Allman et al., 2004). In fact, regardless of the pathway of the MZ B cell maturation, through a T3 transitional state intermediate or assuming their origin indirectly from the follicular compartment, I propose that upon loss of Mll2 a cell would no longer be able to establish a new transcriptional program of a characteristic of the marginal zone B lymphocyte. This would then lead to a strong decrease in the size of a MZ B cell compartment. In addition, variability in the expressivity observed between animals coming from different litters and which can be easily explained by the fact that maturation is a plastic process that includes stochastic differences between individual cells leads to further conclusions. As it is impossible to define the precise moment of CD21-Cre mediated deletion of Mll2 during maturation of B lymphocytes in the spleen, individual differences between cells, and not only between individual animals, could lead to variability in phenotype, depending on the relative percentage of MZ B cell progenitors that have undergone more precocious as opposed to more delayed Cre-mediated deletion in each individual animal (3.3.2 – 3.3.3; Fig. 15 - 18). If we now consider the converging lines of evidence pointing to the transitory role of Mll2 in the timed activation of trasncriptional programs, it appears then plausible that the numbers of residual MZ B cells I observed upon loss of Mll2, and their variable extents, may simply reflect the fact that in the progenitors of those cells Mll2 deletion took place after the narrow time window of requirement for Mll2. In this light impaired Igh class switch in Mll2 deficient cells could be considered as yet another manifestation of the same kind of transitory Mll2 requirement.

4.4 Lineage specificity of Mll2 histone methyltransferase

Upon CD21-Cre mediated Mll2 deletion the only B cell compartment that was affected was the marginal zone B cell population. It is still unclear if this lineage specific reduction

is due to a specifically timed requirement for Mll2 in the differentiation process – namely whether the MZ B cell compartment is the only population that is affected simply due to the timing of the CD21-Cre mediated deletion. The alternative scenario is that it is the particular biology of the MZ B cells that sensitizes this compartment for the loss of Mll2. This would implicate lineage specificity of a histone methyltransferases (HMT). This hypothesis should not be ignored due to several reasons. First, the presence of the 6 different mammalian HMT that methylate specifically H3K4 residue supports lineage and/or time specificity of HMT. Second, the exclusive involvement of MLL1 but not MLL2 in the development of leukaemia (Ayton and Cleary, 2001) indicates lack of complete redundancy in their function which is also proven by the embryonic lethality of the deletion of any of Mll1 through 3 (Glaser et al., 2006; Lee et al., 2006; Yu et al., 1995). Furthermore lineage-specific recruitment of Mll2 containing complex to the β-globin locus during terminal erythroid specification (Demers et al., 2007) suggests HMT specialization. Interestingly, authors of the work describing lineage specific recruitment of Mll2 do not agree with the hypothesis of tissue and/or time specificity of HMTs. According to Demers and her colleagues high degree of similarity between MLL1 and MLL2 and their activity within the same platform (Dou et al., 2006; Ruthenburg et al., 2007) excludes their specificity (Demers et al., 2007). However based on the same argumentation and recapitulating newest findings (Andreu-Vieyra et al., 2010; Glaser et al., 2009) and present work the lineage specificity of HMT should not be excluded.

On the other hand we cannot reject at least partial redundancy of H3K4 HMTs. It is possible that the presence of the residual MZ B cell population, as discussed above (4.3), could be explained by timing of the Cre-mediated deletion in the population of MZ B cell progenitors of individual animal. According to this hypothesis, progenitors of residual MZ B cells lost Mll2 after the window of time of its requirement, thus cells were able to differentiate into mature marginal zone B cells. However it is possible that the loss of Mll2

was compensated by one of 4 remaining H3K4 HMTs – based on my results, excluding Mll1 (3.5.1 – 3.5.2; Fig. 24 and 25).

Further analysis of dynamics and functionality of residual marginal zone B cell compartment should clarify the doubts about the role of Mll2. It would be valuable to examine subsets of transitional precursors of MZ B cells (Allman and Pillai, 2008) (Srivastava et al., 2005). Equally interesting would be comparison of the loss of Mll1 in context of the same experimental system. Exclusive implication of MLL1 but not MLL2 in various form of leukaemia (Ayton and Cleary, 2001) due to the intrinsic functional differences in the CXXC domain (Bach et al., 2009), and newly found link between MLL2 and solid tumours (Natarajan et al., 2010) implicates their different specificity. Hence it should not be excluded that loss of Mll1 would lead to different observations. In the context of involvement of Mll2 in the tightly timed establishment of lineage specific transcriptional reprogramming at both developmental and mature stage (Andreu-Vieyra et al., 2010; Glaser et al., 2009; Glaser et al., 2006) present results could suggest that Mll2 plays role also in the B lymphophoiesis and therefore we consider a candidacy of Mll2 as a putative lymphopoietic regulating factor.

List of figures and tables

Names and Abbreviations

ANOVA	analysis of variance
APS	Ammonium persulfate
BCR	B cell receptor
BM	bone marrow
BrdU	5-bromo-2-deoxyuridine
BSA	bovine serum albumin
CD	cluster of differentiation - system of identification based on cell surface molecules
CFSE	Carboxyfluorescein succinimidyl ester
CLP	common lymphoid progenitor
DAPI	4',6-diamidino-2-phenylindole
DEPC	Diethyl pyrocarbonate
DMSO	Dimethyl sulfoxide
DN	double negative T cells
DP	double positive T cells
DTT	Dithiothreitol
EDTA	Ethylene diamine tetraacetic acid
EGTA	Ethylene glycol tetraacetic acid
ELISA	Enzyme-linked immunosorbent assay
FACS	Fluorescence-activated cell sorting
FBS	Fetal bovine serum
FDR	false discovery rate
Fig.	Figure
Fo	follicular B cell
GC	germinal centre B cells

H	histone
HMT	histone methyltransferase
HSC	hematopoietic stem cell
Ig	immunoglobulin
IL	interleukin
Imm/Tr	Immature/transitional B cells
inetrm	intermediate
K	lysine
MACS	Magnetic-activated cell sorting
me1 (2, 3)	monomethylation, (di-, tri-)
MLL1	human mixed lineage leukemia 1 gene
MLL2	human mixed lineage leukemia 2 gene
Mll1	murine mixed lineage leukemia 1 gene
Mll2	murine mixed lineage leukemia 2 gene
MZ	marginal zone B cell
neg	negative
NP-Ficoll	4-Hydroxy-3-nitrophenylacetyl - Ficoll
OD	optical density
PBS	Phosphate buffered saline
PC	peritoneal cavity
PCA	principal component analysis
PCR	Polymerese chain reaction
PFA	Paraformaldehyde
PP	Peyer's patches
qPCR	Real Time PCR (quantitative PCR)
RT-PCR	Reverse Transcriptase PCR
SDS	Sodium dodecyl sulphate

SDS-PAGE	Sodium dodecyl sulfate - Polyacrylamide gel electrophoresis
SP	spleen
T	thymus
Tc	T cytotoxic cell
TEMED	Tetramethylethylenediamine
Th	T helper cell

References

1 Allman, D., Lindsley, R.C., DeMuth, W., Rudd, K., Shinton, S.A., and Hardy, R.R. (2001). Resolution of three nonproliferative immature splenic B cell subsets reveals multiple selection points during peripheral B cell maturation. J Immunol 167, 6834-6840.

2 Allman, D., and Pillai, S. (2008). Peripheral B cell subsets. Curr Opin Immunol 20, 149-157.

3 Allman, D., Srivastava, B., and Lindsley, R.C. (2004). Alternative routes to maturity: branch points and pathways for generating follicular and marginal zone B cells. Immunol Rev 197, 147-160.

4 Amano, M., Baumgarth, N., Dick, M.D., Brossay, L., Kronenberg, M., Herzenberg, L.A., and Strober, S. (1998). CD1 expression defines subsets of follicular and marginal zone B cells in the spleen: beta 2-microglobulin-dependent and independent forms. J Immunol 161, 1710-1717.

5 Andreu-Vieyra, C.V., Chen, R., Agno, J.E., Glaser, S., Anastassiadis, K., Stewart, A.F., and Matzuk, M.M. (2010). MLL2 is required in oocytes for bulk histone 3 lysine 4 trimethylation and transcriptional silencing. PLoS Biol 8.

6 Araki, Y., Wang, Z., Zang, C., Wood, W.H., 3rd, Schones, D., Cui, K., Roh, T.Y., Lhotsky, B., Wersto, R.P., Peng, W., et al. (2009). Genome-wide analysis of histone methylation reveals chromatin state-based regulation of gene transcription and function of memory CD8+ T cells. Immunity 30, 912-925.

7 Arney, K.L., and Fisher, A.G. (2004). Epigenetic aspects of differentiation. J Cell Sci 117, 4355-4363.

8 Artavanis-Tsakonas, S., Matsuno, K., and Fortini, M.E. (1995). Notch signaling. Science 268, 225-232.

9 Artavanis-Tsakonas, S., Rand, M.D., and Lake, R.J. (1999). Notch signaling: cell fate control and signal integration in development. Science 284, 770-776.

10 Ayton, P.M., and Cleary, M.L. (2001). Molecular mechanisms of leukemogenesis mediated by MLL fusion proteins. Oncogene 20, 5695-5707.

11 Bach, C., Mueller, D., Buhl, S., Garcia-Cuellar, M.P., and Slany, R.K. (2009). Alterations of the CxxC domain preclude oncogenic activation of mixed-lineage leukemia 2. Oncogene 28, 815-823.

12 Bannister, A.J., Schneider, R., Myers, F.A., Thorne, A.W., Crane-Robinson, C., and Kouzarides, T. (2005). Spatial distribution of di- and tri-methyl lysine 36 of histone H3 at active genes. J Biol Chem 280, 17732-17736.

13 Barr, M.L., and Bertram, E.G. (1949). A morphological distinction between neurones of the male and female, and the behaviour of the nucleolar satellite during accelerated nucleoprotein synthesis. Nature 163, 676.

14 Bauer, U.M., Daujat, S., Nielsen, S.J., Nightingale, K., and Kouzarides, T. (2002). Methylation at arginine 17 of histone H3 is linked to gene activation. EMBO Rep 3, 39-44.

15 Bentley, G.A., Lewit-Bentley, A., Finch, J.T., Podjarny, A.D., and Roth, M. (1984). Crystal structure of the nucleosome core particle at 16 A resolution. J Mol Biol 176, 55-75.

16 Berger, S.L., Kouzarides, T., Shiekhattar, R., and Shilatifard, A. (2009). An operational definition of epigenetics. Genes Dev 23, 781-783.

17 Bernstein, B.E., Kamal, M., Lindblad-Toh, K., Bekiranov, S., Bailey, D.K., Huebert, D.J., McMahon, S., Karlsson, E.K., Kulbokas, E.J., 3rd, Gingeras, T.R., et al. (2005). Genomic maps and comparative analysis of histone modifications in human and mouse. Cell 120, 169-181.

18 Bernstein, B.E., Meissner, A., and Lander, E.S. (2007). The mammalian epigenome. Cell 128, 669-681.

19 Bernstein, B.E., Mikkelsen, T.S., Xie, X., Kamal, M., Huebert, D.J., Cuff, J., Fry, B., Meissner, A., Wernig, M., Plath, K., et al. (2006). A bivalent chromatin structure marks key developmental genes in embryonic stem cells. Cell 125, 315-326.

20 Bhaumik, S.R., Smith, E., and Shilatifard, A. (2007). Covalent modifications of histones during development and disease pathogenesis. Nat Struct Mol Biol 14, 1008-1016.

21 Bird, A.P. (1986). CpG-rich islands and the function of DNA methylation. Nature 321, 209-213.

22 Birke, M., Schreiner, S., Garcia-Cuellar, M.P., Mahr, K., Titgemeyer, F., and Slany, R.K. (2002). The MT domain of the proto-oncoprotein MLL binds to CpG-containing DNA and discriminates against methylation. Nucleic Acids Res 30, 958-965.

23 Bolstad, B.M., Irizarry, R.A., Astrand, M., and Speed, T.P. (2003). A comparison of normalization methods for high density oligonucleotide array data based on variance and bias. Bioinformatics 19, 185-193.

24 Bolzer, A., Kreth, G., Solovei, I., Koehler, D., Saracoglu, K., Fauth, C., Muller, S., Eils, R., Cremer, C., Speicher, M.R., et al. (2005). Three-dimensional maps of all chromosomes in human male fibroblast nuclei and prometaphase rosettes. PLoS Biol 3, e157.

25 Briggs, S.D., Bryk, M., Strahl, B.D., Cheung, W.L., Davie, J.K., Dent, S.Y., Winston, F., and Allis, C.D. (2001). Histone H3 lysine 4 methylation is mediated by Set1 and required for cell growth and rDNA silencing in Saccharomyces cerevisiae. Genes Dev 15, 3286-3295.

26 Burgold, T., Spreafico, F., De Santa, F., Totaro, M.G., Prosperini, E., Natoli, G., and Testa, G. (2008). The histone H3 lysine 27-specific demethylase Jmjd3 is required for neural commitment. PLoS One 3, e3034.

27 Cairns, B.R. (2005). Chromatin remodeling complexes: strength in diversity, precision through specialization. Curr Opin Genet Dev 15, 185-190.

28 Cameron, E.E., Bachman, K.E., Myohanen, S., Herman, J.G., and Baylin, S.B. (1999). Synergy of demethylation and histone deacetylase inhibition in the re-expression of genes silenced in cancer. Nat Genet 21, 103-107.

29 Cao, R., Tsukada, Y., and Zhang, Y. (2005). Role of Bmi-1 and Ring1A in H2A ubiquitylation and Hox gene silencing. Mol Cell 20, 845-854.

30 Cariappa, A., Tang, M., Parng, C., Nebelitskiy, E., Carroll, M., Georgopoulos, K., and Pillai, S. (2001). The follicular versus marginal zone B lymphocyte cell fate decision is regulated by Aiolos, Btk, and CD21. Immunity 14, 603-615.

31 Cartwright, P., McLean, C., Sheppard, A., Rivett, D., Jones, K., and Dalton, S. (2005). LIF/STAT3 controls ES cell self-renewal and pluripotency by a Myc-dependent mechanism. Development 132, 885-896.

32 Casola, S., Otipoby, K.L., Alimzhanov, M., Humme, S., Uyttersprot, N., Kutok, J.L., Carroll, M.C., and Rajewsky, K. (2004). B cell receptor signal strength determines B cell fate. Nat Immunol 5, 317-327.

33 Chien, A., Edgar, D.B., and Trela, J.M. (1976). Deoxyribonucleic acid polymerase from the extreme thermophile Thermus aquaticus. J Bacteriol 127, 1550-1557.

34 Cinamon, G., Zachariah, M.A., Lam, O.M., Foss, F.W., Jr., and Cyster, J.G. (2008). Follicular shuttling of marginal zone B cells facilitates antigen transport. Nat Immunol 9, 54-62.

35 Cobaleda, C., Schebesta, A., Delogu, A., and Busslinger, M. (2007). Pax5: the guardian of B cell identity and function. Nat Immunol 8, 463-470.

36 Cohn, M. (2002). The immune system: a weapon of mass destruction invented by evolution to even the odds during the war of the DNAs. Immunol Rev 185, 24-38.

37 Cook, P.R. (2003). Nongenic transcription, gene regulation and action at a distance. J Cell Sci 116, 4483-4491.

38 Corcoran, A.E. (2005). Immunoglobulin locus silencing and allelic exclusion. Semin Immunol 17, 141-154.

39 Corcoran, A.E. (2010). The epigenetic role of non-coding RNA transcription and nuclear organization in immunoglobulin repertoire generation. Semin Immunol.

40 Cremer, T., Cremer, C., Schneider, T., Baumann, H., Hens, L., and Kirsch-Volders, M. (1982). Analysis of chromosome positions in the interphase nucleus of Chinese hamster cells by laser-UV-microirradiation experiments. Hum Genet 62, 201-209.

41 Cross, S.H., Meehan, R.R., Nan, X., and Bird, A. (1997). A component of the transcriptional repressor MeCP1 shares a motif with DNA methyltransferase and HRX proteins. Nat Genet 16, 256-259.

42 Cui, K., Zang, C., Roh, T.Y., Schones, D.E., Childs, R.W., Peng, W., and Zhao, K. (2009). Chromatin signatures in multipotent human hematopoietic stem cells indicate the fate of bivalent genes during differentiation. Cell Stem Cell 4, 80-93.

43 Daniel, J.A., Santos, M.A., Wang, Z., Zang, C., Schwab, K.R., Jankovic, M., Filsuf, D., Chen, H.T., Gazumyan, A., Yamane, A., et al. (2010). PTIP promotes chromatin changes critical for immunoglobulin class switch recombination. Science 329, 917-923.

44 de la Pompa, J.L., Wakeham, A., Correia, K.M., Samper, E., Brown, S., Aguilera, R.J., Nakano, T., Honjo, T., Mak, T.W., Rossant, J., et al. (1997). Conservation of the Notch signalling pathway in mammalian neurogenesis. Development 124, 1139-1148.

45 Demers, C., Chaturvedi, C.P., Ranish, J.A., Juban, G., Lai, P., Morle, F., Aebersold, R., Dilworth, F.J., Groudine, M., and Brand, M. (2007). Activator-mediated recruitment of the MLL2 methyltransferase complex to the beta-globin locus. Mol Cell 27, 573-584.

46 Denhardt, D.T. (1966). A membrane-filter technique for the detection of complementary DNA. Biochem Biophys Res Commun 23, 641-646.

47 Dillon, N., and Festenstein, R. (2002). Unravelling heterochromatin: competition between positive and negative factors regulates accessibility. Trends Genet 18, 252-258.

48 Dillon, S.C., Zhang, X., Trievel, R.C., and Cheng, X. (2005). The SET-domain protein superfamily: protein lysine methyltransferases. Genome Biol 6, 227.

49 Dou, Y., Milne, T.A., Ruthenburg, A.J., Lee, S., Lee, J.W., Verdine, G.L., Allis, C.D., and Roeder, R.G. (2006). Regulation of MLL1 H3K4 methyltransferase activity by its core components. Nat Struct Mol Biol 13, 713-719.

50 Edelman, G.M., and Poulik, M.D. (1961). Studies on structural units of the gamma-globulins. J Exp Med 113, 861-884.

51 Eden, A., Gaudet, F., Waghmare, A., and Jaenisch, R. (2003). Chromosomal instability and tumors promoted by DNA hypomethylation. Science 300, 455.

52 Emerling, B.M., Bonifas, J., Kratz, C.P., Donovan, S., Taylor, B.R., Green, E.D., Le Beau, M.M., and Shannon, K.M. (2002). MLL5, a homolog of Drosophila trithorax located within a segment of chromosome band 7q22 implicated in myeloid leukemia. Oncogene 21, 4849-4854.

53 Engvall, E., and Perlmann, P. (1971). Enzyme-linked immunosorbent assay (ELISA). Quantitative assay of immunoglobulin G. Immunochemistry 8, 871-874.

54 Era, T., Ogawa, M., Nishikawa, S., Okamoto, M., Honjo, T., Akagi, K., Miyazaki, J., and Yamamura, K. (1991). Differentiation of growth signal requirement of B lymphocyte precursor is directed by expression of immunoglobulin. EMBO J 10, 337-342.

55 Fan, X., Mikolaenko, I., Elhassan, I., Ni, X., Wang, Y., Ball, D., Brat, D.J., Perry, A., and Eberhart, C.G. (2004). Notch1 and notch2 have opposite effects on embryonal brain tumor growth. Cancer Res 64, 7787-7793.

56 Farthing, C.R., Ficz, G., Ng, R.K., Chan, C.F., Andrews, S., Dean, W., Hemberger, M., and Reik, W. (2008). Global mapping of DNA methylation in mouse promoters reveals epigenetic reprogramming of pluripotency genes. PLoS Genet 4, e1000116.

57 Feinberg, A.P., and Tycko, B. (2004). The history of cancer epigenetics. Nat Rev Cancer 4, 143-153.

58 Feinberg, A.P., and Vogelstein, B. (1983). A technique for radiolabeling DNA restriction endonuclease fragments to high specific activity. Anal Biochem 132, 6-13.

59 Feng, Q., Wang, H., Ng, H.H., Erdjument-Bromage, H., Tempst, P., Struhl, K., and Zhang, Y. (2002). Methylation of H3-lysine 79 is mediated by a new family of HMTases without a SET domain. Curr Biol 12, 1052-1058.

60 Ferguson, A.R., Youd, M.E., and Corley, R.B. (2004). Marginal zone B cells transport and deposit IgM-containing immune complexes onto follicular dendritic cells. Int Immunol 16, 1411-1422.

61 Ferreira, J., Paolella, G., Ramos, C., and Lamond, A.I. (1997). Spatial organization of large-scale chromatin domains in the nucleus: a magnified view of single chromosome territories. J Cell Biol 139, 1597-1610.

62 Ferres-Marco, D., Gutierrez-Garcia, I., Vallejo, D.M., Bolivar, J., Gutierrez-Avino, F.J., and Dominguez, M. (2006). Epigenetic silencers and Notch collaborate to promote malignant tumours by Rb silencing. Nature 439, 430-436.

63 FitzGerald, K.T., and Diaz, M.O. (1999). MLL2: A new mammalian member of the trx/MLL family of genes. Genomics 59, 187-192.

64 Fouse, S.D., Shen, Y., Pellegrini, M., Cole, S., Meissner, A., Van Neste, L., Jaenisch, R., and Fan, G. (2008). Promoter CpG methylation contributes to ES cell gene regulation in parallel with Oct4/Nanog, PcG complex, and histone H3 K4/K27 trimethylation. Cell Stem Cell 2, 160-169.

65 Gao, X., Tate, P., Hu, P., Tjian, R., Skarnes, W.C., and Wang, Z. (2008). ES cell pluripotency and germ-layer formation require the SWI/SNF chromatin remodeling component BAF250a. Proc Natl Acad Sci U S A 105, 6656-6661.

66 Garcia de Vinuesa, C., O'Leary, P., Sze, D.M., Toellner, K.M., and MacLennan, I.C. (1999). T-independent type 2 antigens induce B cell proliferation in multiple splenic sites, but exponential growth is confined to extrafollicular foci. Eur J Immunol 29, 1314-1323.

67 Glaser, S., Lubitz, S., Loveland, K.L., Ohbo, K., Robb, L., Schwenk, F., Seibler, J., Roellig, D., Kranz, A., Anastassiadis, K., et al. (2009). The histone 3 lysine 4 methyltransferase, Mll2, is only required briefly in development and spermatogenesis. Epigenetics Chromatin 2, 5.

68 Glaser, S., Schaft, J., Lubitz, S., Vintersten, K., van der Hoeven, F., Tufteland, K.R., Aasland, R., Anastassiadis, K., Ang, S.L., and Stewart, A.F. (2006). Multiple epigenetic maintenance factors implicated by the loss of Mll2 in mouse development. Development 133, 1423-1432.

69 Golderer, G., and Grobner, P. (1991). ADP-ribosylation of core histones and their acetylated subspecies. Biochem J 277 (Pt 3), 607-610.

70 Goldmit, M., Ji, Y., Skok, J., Roldan, E., Jung, S., Cedar, H., and Bergman, Y. (2005). Epigenetic ontogeny of the Igk locus during B cell development. Nat Immunol 6, 198-203.

71 Goll, M.G., and Bestor, T.H. (2005). Eukaryotic cytosine methyltransferases. Annu Rev Biochem 74, 481-514.

72 Gratzner, H.G., and Leif, R.C. (1981). An immunofluorescence method for monitoring DNA synthesis by flow cytometry. Cytometry 1, 385-393.

73 Gregory, T.R. (2001). Coincidence, coevolution, or causation? DNA content, cell size, and the C-value enigma. Biol Rev Camb Philos Soc 76, 65-101.

74 Gribnau, J., Diderich, K., Pruzina, S., Calzolari, R., and Fraser, P. (2000). Intergenic transcription and developmental remodeling of chromatin subdomains in the human beta-globin locus. Mol Cell 5, 377-386.

75 Guidos, C.J. (1996). Positive selection of CD4+ and CD8+ T cells. Curr Opin Immunol 8, 225-232.

76 Hagman, J., and Lukin, K. (2007). Hands-on regulation of B cell development by the transcription factor Pax5. Immunity 27, 8-10.

77 Hanna, J., Markoulaki, S., Schorderet, P., Carey, B.W., Beard, C., Wernig, M., Creyghton, M.P., Steine, E.J., Cassady, J.P., Foreman, R., et al. (2008). Direct reprogramming of terminally differentiated mature B lymphocytes to pluripotency. Cell 133, 250-264.

78 Hao, Z., and Rajewsky, K. (2001). Homeostasis of peripheral B cells in the absence of B cell influx from the bone marrow. J Exp Med 194, 1151-1164.

79 Hardy, R.R., Carmack, C.E., Shinton, S.A., Kemp, J.D., and Hayakawa, K. (1991). Resolution and characterization of pro-B and pre-pro-B cell stages in normal mouse bone marrow. J Exp Med 173, 1213-1225.

80 Havas, K., Whitehouse, I., and Owen-Hughes, T. (2001). ATP-dependent chromatin remodeling activities. Cell Mol Life Sci 58, 673-682.

81 Hayashi, S., Kunisada, T., Ogawa, M., Sudo, T., Kodama, H., Suda, T., and Nishikawa, S. (1990). Stepwise progression of B lineage differentiation supported by interleukin 7 and other stromal cell molecules. J Exp Med 171, 1683-1695.

82 Hendrich, B., and Bird, A. (1998). Identification and characterization of a family of mammalian methyl-CpG binding proteins. Mol Cell Biol 18, 6538-6547.

83 Hendzel, M.J., Wei, Y., Mancini, M.A., Van Hooser, A., Ranalli, T., Brinkley, B.R., Bazett-Jones, D.P., and Allis, C.D. (1997). Mitosis-specific phosphorylation of histone H3 initiates primarily within pericentromeric heterochromatin during G2

and spreads in an ordered fashion coincident with mitotic chromosome condensation. Chromosoma 106, 348-360.

84 Ho, L., Jothi, R., Ronan, J.L., Cui, K., Zhao, K., and Crabtree, G.R. (2009). An embryonic stem cell chromatin remodeling complex, esBAF, is an essential component of the core pluripotency transcriptional network. Proc Natl Acad Sci U S A 106, 5187-5191.

85 Ho, L., Ronan, J.L., Wu, J., Staahl, B.T., Chen, L., Kuo, A., Lessard, J., Nesvizhskii, A.I., Ranish, J., and Crabtree, G.R. (2009). An embryonic stem cell chromatin remodeling complex, esBAF, is essential for embryonic stem cell self-renewal and pluripotency. Proc Natl Acad Sci U S A 106, 5181-5186.

86 Hochedlinger, K., and Jaenisch, R. (2006). Nuclear reprogramming and pluripotency. Nature 441, 1061-1067.

87 Horcher, M., Souabni, A., and Busslinger, M. (2001). Pax5/BSAP maintains the identity of B cells in late B lymphopoiesis. Immunity 14, 779-790.

88 Hozumi, K., Negishi, N., Suzuki, D., Abe, N., Sotomaru, Y., Tamaoki, N., Mailhos, C., Ish-Horowicz, D., Habu, S., and Owen, M.J. (2004). Delta-like 1 is necessary for the generation of marginal zone B cells but not T cells in vivo. Nat Immunol 5, 638-644.

89 Illingworth, R., Kerr, A., Desousa, D., Jorgensen, H., Ellis, P., Stalker, J., Jackson, D., Clee, C., Plumb, R., Rogers, J., et al. (2008). A novel CpG island set identifies tissue-specific methylation at developmental gene loci. PLoS Biol 6, e22.

90 Im, H., Park, C., Feng, Q., Johnson, K.D., Kiekhaefer, C.M., Choi, K., Zhang, Y., and Bresnick, E.H. (2003). Dynamic regulation of histone H3 methylated at lysine 79 within a tissue-specific chromatin domain. J Biol Chem 278, 18346-18352.

91 Irizarry, R.A., Hobbs, B., Collin, F., Beazer-Barclay, Y.D., Antonellis, K.J., Scherf, U., and Speed, T.P. (2003). Exploration, normalization, and summaries of high density oligonucleotide array probe level data. Biostatistics 4, 249-264.

92 Iwase, S., Lan, F., Bayliss, P., de la Torre-Ubieta, L., Huarte, M., Qi, H.H., Whetstine, J.R., Bonni, A., Roberts, T.M., and Shi, Y. (2007). The X-linked mental retardation gene SMCX/JARID1C defines a family of histone H3 lysine 4 demethylases. Cell 128, 1077-1088.

93 Jaenisch, R., and Bird, A. (2003). Epigenetic regulation of gene expression: how the genome integrates intrinsic and environmental signals. Nat Genet 33 Suppl, 245-254.

94 Jenuwein, T., and Allis, C.D. (2001). Translating the histone code. Science 293, 1074-1080.

95 Jobst, K., Lakatos, A., and Horvath, A. (1991). Blocking of the amino groups of histone proteins by glucose. Histochem J 23, 107.

96 Johnston, C.M., Wood, A.L., Bolland, D.J., and Corcoran, A.E. (2006). Complete sequence assembly and characterization of the C57BL/6 mouse Ig heavy chain V region. J Immunol 176, 4221-4234.

97 Keohane, A.M., O'Neill L, P., Belyaev, N.D., Lavender, J.S., and Turner, B.M. (1996). X-Inactivation and histone H4 acetylation in embryonic stem cells. Dev Biol 180, 618-630.

98 Kim, S.H., McQueen, P.G., Lichtman, M.K., Shevach, E.M., Parada, L.A., and Misteli, T. (2004). Spatial genome organization during T-cell differentiation. Cytogenet Genome Res 105, 292-301.

99 Kim, T.H., Park, J.T., Lee, S.H., Chang, H.I. (1994). Possible Glycosylation of H1 Histone in murine Liver Nucleus. Korean Biochemistry Journal 27, 5.

100 Klose, R.J., and Zhang, Y. (2007). Regulation of histone methylation by demethylimination and demethylation. Nat Rev Mol Cell Biol 8, 307-318.

101 Kornberg, R.D. (1974). Chromatin structure: a repeating unit of histones and DNA. Science 184, 868-871.

102 Kornberg, R.D., and Lorch, Y. (1999). Twenty-five years of the nucleosome, fundamental particle of the eukaryote chromosome. Cell 98, 285-294.

103 Kornberg, R.D., and Thomas, J.O. (1974). Chromatin structure; oligomers of the histones. Science 184, 865-868.

104 Kourmouli, N., Jeppesen, P., Mahadevhaiah, S., Burgoyne, P., Wu, R., Gilbert, D.M., Bongiorni, S., Prantera, G., Fanti, L., Pimpinelli, S., et al. (2004). Heterochromatin and tri-methylated lysine 20 of histone H4 in animals. J Cell Sci 117, 2491-2501.

105 Kouzarides, T. (2002). Histone methylation in transcriptional control. Curr Opin Genet Dev 12, 198-209.

106 Kouzarides, T. (2007). Chromatin modifications and their function. Cell 128, 693-705.

107 Kraus, M., Alimzhanov, M.B., Rajewsky, N., and Rajewsky, K. (2004). Survival of resting mature B lymphocytes depends on BCR signaling via the Igalpha/beta heterodimer. Cell 117, 787-800.

108 Kumano, K., Chiba, S., Kunisato, A., Sata, M., Saito, T., Nakagami-Yamaguchi, E., Yamaguchi, T., Masuda, S., Shimizu, K., Takahashi, T., et al. (2003). Notch1 but not Notch2 is essential for generating hematopoietic stem cells from endothelial cells. Immunity 18, 699-711.

109 Lachner, M., O'Sullivan, R.J., and Jenuwein, T. (2003). An epigenetic road map for histone lysine methylation. J Cell Sci 116, 2117-2124.

110 Laemmli, U.K. (1970). Cleavage of structural proteins during the assembly of the head of bacteriophage T4. Nature 227, 680-685.

111 Lan, F., Nottke, A.C., and Shi, Y. (2008). Mechanisms involved in the regulation of histone lysine demethylases. Curr Opin Cell Biol 20, 316-325.

112 Lallemand, Y., Luria, V., Haffner-Krausz, R., and Lonai, P. (1998). Maternally expressed PGK-Cre transgene as a tool for early and uniform activation of the Cre site-specific recombinase. Transgenic Res 7, 105-112.

113 Lane, P.J., Gray, D., Oldfield, S., and MacLennan, I.C. (1986). Differences in the recruitment of virgin B cells into antibody responses to thymus-dependent and thymus-independent type-2 antigens. Eur J Immunol 16, 1569-1575.

114 Lang, J., Arnold, B., Hammerling, G., Harris, A.W., Korsmeyer, S., Russell, D., Strasser, A., and Nemazee, D. (1997). Enforced Bcl-2 expression inhibits antigen-mediated clonal elimination of peripheral B cells in an antigen dose-dependent manner and promotes receptor editing in autoreactive, immature B cells. J Exp Med 186, 1513-1522.

115 Lee, J.H., Hart, S.R., and Skalnik, D.G. (2004). Histone deacetylase activity is required for embryonic stem cell differentiation. Genesis 38, 32-38.

116 Lee, J.T., Strauss, W.M., Dausman, J.A., and Jaenisch, R. (1996). A 450 kb transgene displays properties of the mammalian X-inactivation center. Cell 86, 83-94.

117 Lee, S., Lee, D.K., Dou, Y., Lee, J., Lee, B., Kwak, E., Kong, Y.Y., Lee, S.K., Roeder, R.G., and Lee, J.W. (2006). Coactivator as a target gene specificity determinant for histone H3 lysine 4 methyltransferases. Proc Natl Acad Sci U S A 103, 15392-15397.

118 Levy-Wilson, B. (1983). Glycosylation, ADP-ribosylation, and methylation of Tetrahymena histones. Biochemistry 22, 484-489.

119 Li, E., Beard, C., and Jaenisch, R. (1993). Role for DNA methylation in genomic imprinting. Nature 366, 362-365.

120 Li, Y., McClintick, J., Zhong, L., Edenberg, H.J., Yoder, M.C., and Chan, R.J. (2005). Murine embryonic stem cell differentiation is promoted by SOCS-3 and inhibited by the zinc finger transcription factor Klf4. Blood 105, 635-637.

121 Lippman, Z., Gendrel, A.V., Black, M., Vaughn, M.W., Dedhia, N., McCombie, W.R., Lavine, K., Mittal, V., May, B., Kasschau, K.D., et al. (2004). Role of transposable elements in heterochromatin and epigenetic control. Nature 430, 471-476.

122 Loh, Y.H., Wu, Q., Chew, J.L., Vega, V.B., Zhang, W., Chen, X., Bourque, G., George, J., Leong, B., Liu, J., et al. (2006). The Oct4 and Nanog transcription network regulates pluripotency in mouse embryonic stem cells. Nat Genet 38, 431-440.

123 Lubitz, S., Glaser, S., Schaft, J., Stewart, A.F., and Anastassiadis, K. (2007). Increased apoptosis and skewed differentiation in mouse embryonic stem cells lacking the histone methyltransferase Mll2. Mol Biol Cell 18, 2356-2366.

124 Luger, K., Mader, A.W., Richmond, R.K., Sargent, D.F., and Richmond, T.J. (1997). Crystal structure of the nucleosome core particle at 2.8 A resolution. Nature 389, 251-260.

125 Lux, C.T., Yoshimoto, M., McGrath, K., Conway, S.J., Palis, J., and Yoder, M.C. (2008). All primitive and definitive hematopoietic progenitor cells emerging before E10 in the mouse embryo are products of the yolk sac. Blood 111, 3435-3438.

126 Lyon, M.F. (1961). Gene action in the X-chromosome of the mouse (Mus musculus L.). Nature 190, 372-373.

127 Madan, V., Madan, B., Brykczynska, U., Zilbermann, F., Hogeveen, K., Dohner, K., Dohner, H., Weber, O., Blum, C., Rodewald, H.R., et al. (2009). Impaired function of primitive hematopoietic cells in mice lacking the Mixed-Lineage-Leukemia homolog MLL5. Blood 113, 1444-1454.

128 Marshall, W.F. (2003). Gene expression and nuclear architecture during development and differentiation. Mech Dev 120, 1217-1230.

129 Martin, C., and Zhang, Y. (2005). The diverse functions of histone lysine methylation. Nat Rev Mol Cell Biol 6, 838-849.

130 Martin, F., and Kearney, J.F. (2002). Marginal-zone B cells. Nat Rev Immunol 2, 323-335.

131 Martin, F., Oliver, A.M., and Kearney, J.F. (2001). Marginal zone and B1 B cells unite in the early response against T-independent blood-borne particulate antigens. Immunity 14, 617-629.

132 Matthews, A.G., Kuo, A.J., Ramon-Maiques, S., Han, S., Champagne, K.S., Ivanov, D., Gallardo, M., Carney, D., Cheung, P., Ciccone, D.N., et al. (2007). RAG2 PHD finger couples histone H3 lysine 4 trimethylation with V(D)J recombination. Nature 450, 1106-1110.

133 McMahon, K.A., Hiew, S.Y., Hadjur, S., Veiga-Fernandes, H., Menzel, U., Price, A.J., Kioussis, D., Williams, O., and Brady, H.J. (2007). Mll has a critical role in fetal and adult hematopoietic stem cell self-renewal. Cell Stem Cell 1, 338-345.

134 Meissner, A., Mikkelsen, T.S., Gu, H., Wernig, M., Hanna, J., Sivachenko, A., Zhang, X., Bernstein, B.E., Nusbaum, C., Jaffe, D.B., et al. (2008). Genome-scale DNA methylation maps of pluripotent and differentiated cells. Nature 454, 766-770.

135 Meshorer, E., and Misteli, T. (2006). Chromatin in pluripotent embryonic stem cells and differentiation. Nat Rev Mol Cell Biol 7, 540-546.

136 Mikkelsen, T.S., Hanna, J., Zhang, X., Ku, M., Wernig, M., Schorderet, P., Bernstein, B.E., Jaenisch, R., Lander, E.S., and Meissner, A. (2008). Dissecting direct reprogramming through integrative genomic analysis. Nature 454, 49-55.

137 Mikkelsen, T.S., Ku, M., Jaffe, D.B., Issac, B., Lieberman, E., Giannoukos, G., Alvarez, P., Brockman, W., Kim, T.K., Koche, R.P., et al. (2007). Genome-wide maps of chromatin state in pluripotent and lineage-committed cells. Nature 448, 553-560.

138 Millar, C.B., Guy, J., Sansom, O.J., Selfridge, J., MacDougall, E., Hendrich, B., Keightley, P.D., Bishop, S.M., Clarke, A.R., and Bird, A. (2002). Enhanced CpG mutability and tumorigenesis in MBD4-deficient mice. Science 297, 403-405.

139 Miller, T., Krogan, N.J., Dover, J., Erdjument-Bromage, H., Tempst, P., Johnston, M., Greenblatt, J.F., and Shilatifard, A. (2001). COMPASS: a complex of proteins associated with a trithorax-related SET domain protein. Proc Natl Acad Sci U S A 98, 12902-12907.

140 Milne, T.A., Briggs, S.D., Brock, H.W., Martin, M.E., Gibbs, D., Allis, C.D., and Hess, J.L. (2002). MLL targets SET domain methyltransferase activity to Hox gene promoters. Mol Cell 10, 1107-1117.

141 Milne, T.A., Martin, M.E., Brock, H.W., Slany, R.K., and Hess, J.L. (2005). Leukemogenic MLL fusion proteins bind across a broad region of the Hox a9 locus, promoting transcription and multiple histone modifications. Cancer Res 65, 11367-11374.

142 Misteli, T. (2004). Spatial positioning; a new dimension in genome function. Cell 119, 153-156.

143 Mitsui, K., Tokuzawa, Y., Itoh, H., Segawa, K., Murakami, M., Takahashi, K., Maruyama, M., Maeda, M., and Yamanaka, S. (2003). The homeoprotein Nanog is required for maintenance of pluripotency in mouse epiblast and ES cells. Cell 113, 631-642.

144 Mohn, F., Weber, M., Rebhan, M., Roloff, T.C., Richter, J., Stadler, M.B., Bibel, M., and Schubeler, D. (2008). Lineage-specific polycomb targets and de novo DNA methylation define restriction and potential of neuronal progenitors. Mol Cell 30, 755-766.

145 Mombaerts, P., Iacomini, J., Johnson, R.S., Herrup, K., Tonegawa, S., and Papaioannou, V.E. (1992). RAG-1-deficient mice have no mature B and T lymphocytes. Cell 68, 869-877.

146 Morshead, K.B., Ciccone, D.N., Taverna, S.D., Allis, C.D., and Oettinger, M.A. (2003). Antigen receptor loci poised for V(D)J rearrangement are broadly associated with BRG1 and flanked by peaks of histone H3 dimethylated at lysine 4. Proc Natl Acad Sci U S A 100, 11577-11582.

147 Muller, J., Hart, C.M., Francis, N.J., Vargas, M.L., Sengupta, A., Wild, B., Miller, E.L., O'Connor, M.B., Kingston, R.E., and Simon, J.A. (2002). Histone methyltransferase activity of a Drosophila Polycomb group repressor complex. Cell 111, 197-208.

148 Nakayama, J., Rice, J.C., Strahl, B.D., Allis, C.D., and Grewal, S.I. (2001). Role of histone H3 lysine 9 methylation in epigenetic control of heterochromatin assembly. Science 292, 110-113.

149 Nakayama, T., and Takami, Y. (2001). Participation of histones and histone-modifying enzymes in cell functions through alterations in chromatin structure. J Biochem 129, 491-499.

150 Natarajan, T.G., Kallakury, B.V., Sheehan, C.E., Bartlett, M.B., Ganesan, N., Preet, A., Ross, J.S., and Fitzgerald, K.T. (2010). Epigenetic regulator MLL2 shows altered expression in cancer cell lines and tumors from human breast and colon. Cancer Cell Int 10, 13.

151 Nan, X., Meehan, R.R., and Bird, A. (1993). Dissection of the methyl-CpG binding domain from the chromosomal protein MeCP2. Nucleic Acids Res 21, 4886-4892.

152 Nan, X., Campoy, F.J., and Bird, A. (1997). MeCP2 is a transcriptional repressor with abundant binding sites in genomic chromatin. Cell 88, 471-481.

153 Ng, H.H., Robert, F., Young, R.A., and Struhl, K. (2003). Targeted recruitment of Set1 histone methylase by elongating Pol II provides a localized mark and memory of recent transcriptional activity. Mol Cell 11, 709-719.

154 Nichols, J., Zevnik, B., Anastassiadis, K., Niwa, H., Klewe-Nebenius, D., Chambers, I., Scholer, H., and Smith, A. (1998). Formation of pluripotent stem

cells in the mammalian embryo depends on the POU transcription factor Oct4. Cell 95, 379-391.

155 Nicholson, D.W., Ali, A., Thornberry, N.A., Vaillancourt, J.P., Ding, C.K., Gallant, M., Gareau, Y., Griffin, P.R., Labelle, M., Lazebnik, Y.A., et al. (1995). Identification and inhibition of the ICE/CED-3 protease necessary for mammalian apoptosis. Nature 376, 37-43.

156 Nishioka, K., Chuikov, S., Sarma, K., Erdjument-Bromage, H., Allis, C.D., Tempst, P., and Reinberg, D. (2002). Set9, a novel histone H3 methyltransferase that facilitates transcription by precluding histone tail modifications required for heterochromatin formation. Genes Dev 16, 479-489.

157 Niwa, H., Miyazaki, J., and Smith, A.G. (2000). Quantitative expression of Oct-3/4 defines differentiation, dedifferentiation or self-renewal of ES cells. Nat Genet 24, 372-376.

158 Nowak, S.J., and Corces, V.G. (2000). Phosphorylation of histone H3 correlates with transcriptionally active loci. Genes Dev 14, 3003-3013.

159 Nunez, C., Nishimoto, N., Gartland, G.L., Billips, L.G., Burrows, P.D., Kubagawa, H., and Cooper, M.D. (1996). B cells are generated throughout life in humans. J Immunol 156, 866-872.

160 Nutt, S.L., Urbanek, P., Rolink, A., and Busslinger, M. (1997). Essential functions of Pax5 (BSAP) in pro-B cell development: difference between fetal and adult B lymphopoiesis and reduced V-to-DJ recombination at the IgH locus. Genes Dev 11, 476-491.

161 Nutt, S.L., Morrison, A.M., Dorfler, P., Rolink, A., and Busslinger, M. (1998). Identification of BSAP (Pax-5) target genes in early B-cell development by loss- and gain-of-function experiments. EMBO J 17, 2319-2333.

162 Oettinger, M.A., Schatz, D.G., Gorka, C., and Baltimore, D. (1990). RAG-1 and RAG-2, adjacent genes that synergistically activate V(D)J recombination. Science 248, 1517-1523.

163 Okamura, M., Inagaki, T., Tanaka, T., and Sakai, J. (2010). Role of histone methylation and demethylation in adipogenesis and obesity. Organogenesis 6, 24-32.

164 Oliver, A.M., Martin, F., Gartland, G.L., Carter, R.H., and Kearney, J.F. (1997). Marginal zone B cells exhibit unique activation, proliferative and immunoglobulin secretory responses. Eur J Immunol 27, 2366-2374.

165 Oliver, A.M., Martin, F., and Kearney, J.F. (1997). Mouse CD38 is down-regulated on germinal center B cells and mature plasma cells. J Immunol 158, 1108-1115.

166 Orford, K., Kharchenko, P., Lai, W., Dao, M.C., Worhunsky, D.J., Ferro, A., Janzen, V., Park, P.J., and Scadden, D.T. (2008). Differential H3K4 methylation identifies developmentally poised hematopoietic genes. Dev Cell 14, 798-809.

167 Palis, J., and Yoder, M.C. (2001). Yolk-sac hematopoiesis: the first blood cells of mouse and man. Exp Hematol 29, 927-936.

168 Parada, L., and Misteli, T. (2002). Chromosome positioning in the interphase nucleus. Trends Cell Biol 12, 425-432.

169 Parada, L.A., McQueen, P.G., and Misteli, T. (2004). Tissue-specific spatial organization of genomes. Genome Biol 5, R44.

170 Pardue, M.L., and Gall, J.G. (1970). Chromosomal localization of mouse satellite DNA. Science 168, 1356-1358.

171 Partek, I. (2008). Partek© Discovery SuiteTM Revision 6.5. Partek Inc, St Louis, MO, USA.

172 Paul, W.E. (2003). Fundamental immunology, 5th edn (Philadelphia, Lippincott Williams & Wilkins).

173 Penny, G.D., Kay, G.F., Sheardown, S.A., Rastan, S., and Brockdorff, N. (1996). Requirement for Xist in X chromosome inactivation. Nature 379, 131-137.

174 Perkins, E.J., Kee, B.L., and Ramsden, D.A. (2004). Histone 3 lysine 4 methylation during the pre-B to immature B-cell transition. Nucleic Acids Res 32, 1942-1947.

175 Peters, A.H., O'Carroll, D., Scherthan, H., Mechtler, K., Sauer, S., Schofer, C., Weipoltshammer, K., Pagani, M., Lachner, M., Kohlmaier, A., et al. (2001). Loss of the Suv39h histone methyltransferases impairs mammalian heterochromatin and genome stability. Cell 107, 323-337.

176 Pirrotta, V. (1998). Polycombing the genome: PcG, trxG, and chromatin silencing. Cell 93, 333-336.

177 Plath, K., Fang, J., Mlynarczyk-Evans, S.K., Cao, R., Worringer, K.A., Wang, H., de la Cruz, C.C., Otte, A.P., Panning, B., and Zhang, Y. (2003). Role of histone H3 lysine 27 methylation in X inactivation. Science 300, 131-135.

178 Pokholok, D.K., Harbison, C.T., Levine, S., Cole, M., Hannett, N.M., Lee, T.I., Bell, G.W., Walker, K., Rolfe, P.A., Herbolsheimer, E., et al. (2005). Genome-wide map of nucleosome acetylation and methylation in yeast. Cell 122, 517-527.

179 Pui, J.C., Allman, D., Xu, L., DeRocco, S., Karnell, F.G., Bakkour, S., Lee, J.Y., Kadesch, T., Hardy, R.R., Aster, J.C., et al. (1999). Notch1 expression in early lymphopoiesis influences B versus T lineage determination. Immunity 11, 299-308.

180 Rea, S., Eisenhaber, F., O'Carroll, D., Strahl, B.D., Sun, Z.W., Schmid, M., Opravil, S., Mechtler, K., Ponting, C.P., Allis, C.D., et al. (2000). Regulation of chromatin structure by site-specific histone H3 methyltransferases. Nature 406, 593-599.

181 Reik, W. (2007). Stability and flexibility of epigenetic gene regulation in mammalian development. Nature 447, 425-432.

182 Reik, W., Santos, F., Mitsuya, K., Morgan, H., and Dean, W. (2003). Epigenetic asymmetry in the mammalian zygote and early embryo: relationship to lineage

commitment? Philos Trans R Soc Lond B Biol Sci 358, 1403-1409; discussion 1409.

183 Roark, J.H., Park, S.H., Jayawardena, J., Kavita, U., Shannon, M., and Bendelac, A. (1998). CD1.1 expression by mouse antigen-presenting cells and marginal zone B cells. J Immunol 160, 3121-3127.

184 Roth, T.L., Lubin, F.D., Sodhi, M., and Kleinman, J.E. (2009). Epigenetic mechanisms in schizophrenia. Biochim Biophys Acta 1790, 869-877.

185 Rumfelt, L.L., Zhou, Y., Rowley, B.M., Shinton, S.A., and Hardy, R.R. (2006). Lineage specification and plasticity in CD19- early B cell precursors. J Exp Med 203, 675-687.

186 Ruthenburg, A.J., Allis, C.D., and Wysocka, J. (2007). Methylation of lysine 4 on histone H3: intricacy of writing and reading a single epigenetic mark. Mol Cell 25, 15-30.

187 Sadoni, N., Langer, S., Fauth, C., Bernardi, G., Cremer, T., Turner, B.M., and Zink, D. (1999). Nuclear organization of mammalian genomes. Polar chromosome territories build up functionally distinct higher order compartments. J Cell Biol 146, 1211-1226.

188 Saiki, R.K., Scharf, S., Faloona, F., Mullis, K.B., Horn, G.T., Erlich, H.A., and Arnheim, N. (1985). Enzymatic amplification of beta-globin genomic sequences and restriction site analysis for diagnosis of sickle cell anemia. Science 230, 1350-1354.

189 Saito, T., Chiba, S., Ichikawa, M., Kunisato, A., Asai, T., Shimizu, K., Yamaguchi, T., Yamamoto, G., Seo, S., Kumano, K., et al. (2003). Notch2 is preferentially expressed in mature B cells and indispensable for marginal zone B lineage development. Immunity 18, 675-685.

190 Sambrook, J., Fritsch, EF, Maniatis, T (1989). Molecular cloning: A Laboratory Manual. Cold Spring Harbor Laboratory Press, New York.

191 Santos, F., Hendrich, B., Reik, W., and Dean, W. (2002). Dynamic reprogramming of DNA methylation in the early mouse embryo. Dev Biol 241, 172-182.

192 Santos-Rosa, H., Schneider, R., Bannister, A.J., Sherriff, J., Bernstein, B.E., Emre, N.C., Schreiber, S.L., Mellor, J., and Kouzarides, T. (2002). Active genes are tri-methylated at K4 of histone H3. Nature 419, 407-411.

193 Schebesta, A., McManus, S., Salvagiotto, G., Delogu, A., Busslinger, G.A., and Busslinger, M. (2007). Transcription factor Pax5 activates the chromatin of key genes involved in B cell signaling, adhesion, migration, and immune function. Immunity 27, 49-63.

194 Schotta, G., Lachner, M., Sarma, K., Ebert, A., Sengupta, R., Reuter, G., Reinberg, D., and Jenuwein, T. (2004). A silencing pathway to induce H3-K9 and H4-K20 trimethylation at constitutive heterochromatin. Genes Dev 18, 1251-1262.

195 Schotta, G., Sengupta, R., Kubicek, S., Malin, S., Kauer, M., Callen, E., Celeste, A., Pagani, M., Opravil, S., De La Rosa-Velazquez, I.A., et al. (2008). A chromatin-wide transition to H4K20 monomethylation impairs genome integrity and programmed DNA rearrangements in the mouse. Genes Dev 22, 2048-2061.

196 Schroeder, T., Meier-Stiegen, F., Schwanbeck, R., Eilken, H., Nishikawa, S., Hasler, R., Schreiber, S., Bornkamm, G.W., and Just, U. (2006). Activated Notch1 alters differentiation of embryonic stem cells into mesodermal cell lineages at multiple stages of development. Mech Dev 123, 570-579.

197 Sebastian, S., Sreenivas, P., Sambasivan, R., Cheedipudi, S., Kandalla, P., Pavlath, G.K., and Dhawan, J. (2009). MLL5, a trithorax homolog, indirectly regulates H3K4 methylation, represses cyclin A2 expression, and promotes myogenic differentiation. Proc Natl Acad Sci U S A 106, 4719-4724.

198 Shahbazian, M.D., and Grunstein, M. (2007). Functions of site-specific histone acetylation and deacetylation. Annu Rev Biochem 76, 75-100.

199 Shi, Y., Lan, F., Matson, C., Mulligan, P., Whetstine, J.R., Cole, P.A., and Casero, R.A. (2004). Histone demethylation mediated by the nuclear amine oxidase homolog LSD1. Cell 119, 941-953.

200 Shiio, Y., and Eisenman, R.N. (2003). Histone sumoylation is associated with transcriptional repression. Proc Natl Acad Sci U S A 100, 13225-13230.

201 Shilatifard, A. (2006). Chromatin modifications by methylation and ubiquitination: implications in the regulation of gene expression. Annu Rev Biochem 75, 243-269.

202 Shinkai, Y., Rathbun, G., Lam, K.P., Oltz, E.M., Stewart, V., Mendelsohn, M., Charron, J., Datta, M., Young, F., Stall, A.M., et al. (1992). RAG-2-deficient mice lack mature lymphocytes owing to inability to initiate V(D)J rearrangement. Cell 68, 855-867.

203 Sims, R.J., 3rd, and Reinberg, D. (2006). Histone H3 Lys 4 methylation: caught in a bind? Genes Dev 20, 2779-2786.

204 Slotkin, R.K., and Martienssen, R. (2007). Transposable elements and the epigenetic regulation of the genome. Nat Rev Genet 8, 272-285.

205 Southern, E.M. (1975). Detection of specific sequences among DNA fragments separated by gel electrophoresis. J Mol Biol 98, 503-517.

206 Srivastava, B., Quinn, W.J., 3rd, Hazard, K., Erikson, J., and Allman, D. (2005). Characterization of marginal zone B cell precursors. J Exp Med 202, 1225-1234.

207 Stier, S., Cheng, T., Dombkowski, D., Carlesso, N., and Scadden, D.T. (2002). Notch1 activation increases hematopoietic stem cell self-renewal in vivo and favors lymphoid over myeloid lineage outcome. Blood 99, 2369-2378.

208 Strahl, B.D., and Allis, C.D. (2000). The language of covalent histone modifications. Nature 403, 41-45.

209 Struhl, K. (1999). Fundamentally different logic of gene regulation in eukaryotes and prokaryotes. Cell 98, 1-4.

210 Su, R.C., Brown, K.E., Saaber, S., Fisher, A.G., Merkenschlager, M., and Smale, S.T. (2004). Dynamic assembly of silent chromatin during thymocyte maturation. Nat Genet 36, 502-506.

211 Sudo, T., Ito, M., Ogawa, Y., Iizuka, M., Kodama, H., Kunisada, T., Hayashi, S., Ogawa, M., Sakai, K., and Nishikawa, S. (1989). Interleukin 7 production and function in stromal cell-dependent B cell development. J Exp Med 170, 333-338.

212 Sweet, M.T., Jones, K., and Allis, C.D. (1996). Phosphorylation of linker histone is associated with transcriptional activation in a normally silent nucleus. J Cell Biol 135, 1219-1228.

213 Takahashi, K., Kozono, Y., Waldschmidt, T.J., Berthiaume, D., Quigg, R.J., Baron, A., and Holers, V.M. (1997). Mouse complement receptors type 1 (CR1;CD35) and type 2 (CR2;CD21): expression on normal B cell subpopulations and decreased levels during the development of autoimmunity in MRL/lpr mice. J Immunol 159, 1557-1569.

214 Takahashi, K., and Yamanaka, S. (2006). Induction of pluripotent stem cells from mouse embryonic and adult fibroblast cultures by defined factors. Cell 126, 663-676.

215 Tan, J.B., Xu, K., Cretegny, K., Visan, I., Yuan, J.S., Egan, S.E., and Guidos, C.J. (2009). Lunatic and manic fringe cooperatively enhance marginal zone B cell precursor competition for delta-like 1 in splenic endothelial niches. Immunity 30, 254-263.

216 Tanigaki, K., Han, H., Yamamoto, N., Tashiro, K., Ikegawa, M., Kuroda, K., Suzuki, A., Nakano, T., and Honjo, T. (2002). Notch-RBP-J signaling is involved in cell fate determination of marginal zone B cells. Nat Immunol 3, 443-450.

217 Tanigaki, K., and Honjo, T. (2007). Regulation of lymphocyte development by Notch signaling. Nat Immunol 8, 451-456.

218 Tanigaki, K., Kuroda, K., Han, H., and Honjo, T. (2003). Regulation of B cell development by Notch/RBP-J signaling. Semin Immunol 15, 113-119.

219 Tanigaki, K., Nogaki, F., Takahashi, J., Tashiro, K., Kurooka, H., and Honjo, T. (2001). Notch1 and Notch3 instructively restrict bFGF-responsive multipotent neural progenitor cells to an astroglial fate. Neuron 29, 45-55.

220 Tariq, M., and Paszkowski, J. (2004). DNA and histone methylation in plants. Trends Genet 20, 244-251.

221 Terranova, R., Agherbi, H., Boned, A., Meresse, S., and Djabali, M. (2006). Histone and DNA methylation defects at Hox genes in mice expressing a SET domain-truncated form of Mll. Proc Natl Acad Sci U S A 103, 6629-6634.

222 Testa, G., Schaft, J., van der Hoeven, F., Glaser, S., Anastassiadis, K., Zhang, Y., Hermann, T., Stremmel, W., and Stewart, A.F. (2004). A reliable lacZ expression reporter cassette for multipurpose, knockout-first alleles. Genesis 38, 151-158.

223 Testa, G., Zhang, Y., Vintersten, K., Benes, V., Pijnappel, W.W., Chambers, I., Smith, A.J., Smith, A.G., and Stewart, A.F. (2003). Engineering the mouse genome with bacterial artificial chromosomes to create multipurpose alleles. Nat Biotechnol 21, 443-447.

224 Thevenin, C., Nutt, S.L., and Busslinger, M. (1998). Early function of Pax5 (BSAP) before the pre-B cell receptor stage of B lymphopoiesis. J Exp Med 188, 735-744.

225 Tschiersch, B., Hofmann, A., Krauss, V., Dorn, R., Korge, G., and Reuter, G. (1994). The protein encoded by the Drosophila position-effect variegation suppressor gene Su(var)3-9 combines domains of antagonistic regulators of homeotic gene complexes. EMBO J 13, 3822-3831.

226 Usachenko, S.I., Bavykin, S.G., Gavin, I.M., and Bradbury, E.M. (1994). Rearrangement of the histone H2A C-terminal domain in the nucleosome. Proc Natl Acad Sci U S A 91, 6845-6849.

227 van Dijk, K., Marley, K.E., Jeong, B.R., Xu, J., Hesson, J., Cerny, R.L., Waterborg, J.H., and Cerutti, H. (2005). Monomethyl histone H3 lysine 4 as an epigenetic mark for silenced euchromatin in Chlamydomonas. Plant Cell 17, 2439-2453.

228 Wang, Y., Wysocka, J., Sayegh, J., Lee, Y.H., Perlin, J.R., Leonelli, L., Sonbuchner, L.S., McDonald, C.H., Cook, R.G., Dou, Y., et al. (2004). Human PAD4 regulates histone arginine methylation levels via demethylimination. Science 306, 279-283.

229 Wei, Y., Mizzen, C.A., Cook, R.G., Gorovsky, M.A., and Allis, C.D. (1998). Phosphorylation of histone H3 at serine 10 is correlated with chromosome condensation during mitosis and meiosis in Tetrahymena. Proc Natl Acad Sci U S A 95, 7480-7484.

230 Weintraub, H., and Groudine, M. (1976). Chromosomal subunits in active genes have an altered conformation. Science 193, 848-856.

231 Witt, C.M., Won, W.J., Hurez, V., and Klug, C.A. (2003). Notch2 haploinsufficiency results in diminished B1 B cells and a severe reduction in marginal zone B cells. J Immunol 171, 2783-2788.

232 Wolffe, A.P., and Hayes, J.J. (1999). Chromatin disruption and modification. Nucleic Acids Res 27, 711-720.

233 Workman, J.L., and Kingston, R.E. (1998). Alteration of nucleosome structure as a mechanism of transcriptional regulation. Annu Rev Biochem 67, 545-579.

234 Wu, L., and Griffin, J.D. (2004). Modulation of Notch signaling by mastermind-like (MAML) transcriptional co-activators and their involvement in tumorigenesis. Semin Cancer Biol 14, 348-356.

235 Wu, L., Maillard, I., Nakamura, M., Pear, W.S., and Griffin, J.D. (2007). The transcriptional coactivator Maml1 is required for Notch2-mediated marginal zone B-cell development. Blood 110, 3618-3623.

236 Yokota, T., Kouro, T., Hirose, J., Igarashi, H., Garrett, K.P., Gregory, S.C., Sakaguchi, N., Owen, J.J., and Kincade, P.W. (2003). Unique properties of fetal lymphoid progenitors identified according to RAG1 gene expression. Immunity 19, 365-375.

237 Yokoyama, A., Wang, Z., Wysocka, J., Sanyal, M., Aufiero, D.J., Kitabayashi, I., Herr, W., and Cleary, M.L. (2004). Leukemia proto-oncoprotein MLL forms a SET1-like histone methyltransferase complex with menin to regulate Hox gene expression. Mol Cell Biol 24, 5639-5649.

238 Yu, B.D., Hess, J.L., Horning, S.E., Brown, G.A., and Korsmeyer, S.J. (1995). Altered Hox expression and segmental identity in Mll-mutant mice. Nature 378, 505-508.

239 Zhang, Y. (2003). Transcriptional regulation by histone ubiquitination and deubiquitination. Genes Dev 17, 2733-2740.

240 Zhang, Y., and Reinberg, D. (2001). Transcription regulation by histone methylation: interplay between different covalent modifications of the core histone tails. Genes Dev 15, 2343-2360.